PLATELET DERIVED GROWTH FACTOR AND ITS RECEPTORS IN THE DEVELOPING RAT CENTRAL NERVOUS SYSTEM

Nigel Patrick Pringle

Thesis submitted to the University of London for the degree of Doctor of Philosophy in Cell Biology

Department of Biology (Medawar Building),
University College London.

1992

ABSTRACT

In the mature rat optic nerve there are several types of postmitotic glial cells including oligodendrocytes and type-1 astrocytes. Type-1 astrocytes develop from one type of precursor cell, while oligodendrocytes develop from a different progenitor cell known as an O-2A progenitor. O-2A progenitor cells can be stimulated to divide *in vitro* by mitogens secreted by cultured cortical (type-1-like) astrocytes or by purified platelet-derived growth factor (PDGF). By northern blotting I show that cultured cortical astrocytes synthesize the A chain of PDGF. Its time course of appearance in the brain and its distribution in the optic nerve suggest that type-1 astrocytes might be a source of PDGF-A *in vivo*, and that PDGF-A is probably important for O-2A progenitor proliferation during development.

O-2A progenitors express the α-subunit of the PDGF receptor PDGF-αR. To visualize these cells and other cells in the CNS that might express PDGF-αR, I performed *in situ* hybridization using a probe specific to PDGF-αR. During late embryonic and early postnatal neurogenesis, the spatiotemporal distribution of PDGF-αR$^+$ cells, together with ^{125}I-PDGF binding studies on subsets of glial cells *in vitro*, suggests that PDGF-αR may be expressed preferentially by cells of the O-2A lineage and might, therefore, be a useful marker for studying the development of this lineage from its earliest origins in the ventricular zones of the developing brain and spinal cord. By *in situ* hybridization I showed that, in the E14 spinal cord, PDGF-αR is expressed in the basal ventricular zone in two longitudinal columns, one each side of the central canal. These columns are initially comprised of only two cells in the cross-sectional plane, but the PDGF-αR cells appear subsequently to multiply and disseminate throughout the spinal cord. In the brain, PDGF-αR$^+$ cells seem to arise in a specialized germinal zone beneath the foramen of Monro, in the ventral half of the developing diencephalon. These results lead me to propose that the earliest oligodendrocyte precursors are generated in very restricted regions of the ventricular zones of the developing brain and spinal cord during a brief window of time around E14.

CONTENTS Page

FIGURES

TABLES

ACKNOWLEDGMENTS

I am indebted to Bill Richardson for his advice, encouragement and enthusiasm during the last few years, and also for his constructive criticisms of this thesis.

I would like to thank all the members of the Biology department with whom I've had the pleasure of working with over the last few years. In particular, I am grateful to Andy, Richard, George, Heather, Barbara, Julia, Caroline, Hussein, Wei Ping, Winfried, Colin, Mike and Linda; A special thank you to Ellen for her kind gift of the purified O-2A progenitor cells; Hardeep for cutting the optic nerve sections (shown in figure 22); Dr. C. Heldin for his gift of ^{125}I-PDGF; Rocky for reading my initial drafts and finally Louise for putting up with me in her office.

Also I'd like to thank some very special people for their much valued friendship over the years Sarah, Rob, Ally, Steve and Christine; and all their kids, Alice, Annie, John, Lucy, Martha, Paul and Rosie.

Finally, I wish to dedicate this thesis to my parents Dennis and Doreen Pringle.

ABBREVIATIONS.

aFGF	-acidic fibroblast growth factor
AMP	-ampicillin
bFGF	-basic fibroblast growth factor
BL	-*bandeiraea simplicifolia* B_4-lectin
BMP-2A	-bone morphogenic protein-2A
BMP-3	-bone morphogenic protein-3
boss	-bride of sevenless
BSA	-bovine serum albumin
BS	-Bottenstein and Sato's defined medium
C.elegans	-caenorhabditis elegans
CNS	-central nervous system
DEPC	-diethylpyrocarbonate
DMEM	-Dulbecco's modified Eagles medium
DMSO	-dimethylsulphoxide
DTT	-dithiothreitol
E.Coli	-*Escherichia coli*
EDTA	-ethylenediaminetetraacetic acid disodium salt
EGF	-epidermal growth factor
E	-embryonic
FCS	-foetal calf serum
FITC	-fluorescein-iso-thio-cyanate
G	-gravity
g	-gram
GC	-galactocerebroside
GFAP	-glial fibrillary acidic protein
IGF-I	-insulin-like growth factor-I

IGF-II	-insulin-like growth factor-II
Int-2	-inte.gration tumour-2
hst	-human stomach cancer/kaposi's sarcoma
KS	-Kaposi's sarcoma/human stomach cancer
FGF-5	-fibroblast growth factor-5
FGF-6	-fibroblast growth factor-6
KGF	-keratinocyte growth factor
LB	-luria broth
2ME	-2-ß-mercaptoethanol
MEMH	-HEPES buffered minimal essential medium
MOPS	-3(N-Morpholino) propanesulphonic acid monosodium salt
MIS	-mullerian Inhibiting substance
NCS	-newborn calf serum
OLB	-oligolabelling buffer
P	-postnatal
PBS	-phosphate buffered saline
PDGF-A	-platelet derived growth factor-A
PDGF-B	-platelet derived growth factor-B
PDGF-αR	-platelet derived growth factor receptor alpha
PDGF-ßR	-platelet derived growth factor receptor beta
Ph	-patch mouse mutant
Ran-2	-rat neural antigen-2
sev	-*sevenless*
Sl	-steel mouse mutant
SS-DNA	-salmon sperm DNA
SSV	-simian sarcoma virus
TET	-tetracycline

TGF-α	-transforming growth factor-α
TGF-ß1-6	-transforming growth factor-ß's
tRNA	-transfer RNA
VEGF	-vascular endothelial cell growth factor
W	-dominant-white spotting mouse mutant
XTC-MIF	-*Xenopus* tissue culture mesoderm inducing factor

CHAPTER 1

INTRODUCTION

A single cell, the fertilized egg, is capable of giving rise to the hundreds of different cell types that make the mature organism. During amphibian development this egg cell subdivides by repeated mitosis into many smaller cells (blastomeres), without any change in mass. At the 16-cell stage a cavity, called the blastocoel, forms inside this cellular mass. The cells forming the exterior of the embryo have become organised into an epithelial cell layer, and the embryo is now called a blastula. Gastrulation now occurs, transforming the simple hollow ball of cells into a multi-layered structure with a central gut tube and bilateral symmetry. Subsequently the embryo develops into a mature organism containing many highly specialised non-dividing cells such as muscle cells, nerve cells and red blood cells. These specialised cells descend from a population of less specialised proliferating "progenitor" cells by a process of change known as differentiation. What are the factors that determine whether a given progenitor cell should divide or differentiate, and what dictates its differentiation pathway? This is one of the questions that my thesis addresses and with which the first part of my introduction is concerned.

Cell-autonomous differentiation in *Caenorhabditis elegans*

Cellular development occurs as a series of choices between alternative cell fates. According to early theories of development these choices were made in a strict hierarchy, eg. it was thought that a cell would develop into either a mesodermal or ectodermal cell before deciding what type of mesodermal or ectodermal cell to become. The lineage of the cells of the nematode, *Caenorhabditis elegans* (*C.elegans*) suggests otherwise (Sulston and Horvitz, 1977; Sulston *et al.*, 1983). Lineage studies of *C.elegans* revealed that the somatic structures of the animal develop by invariant cell lineage with the exception of the germ-line cells. Each type of differentiated cell

(i.e. neuronal, muscular, gonadal) originates from many branches of the lineage tree and from several founder cells. Muscle cells (mesodermal) and neural cells (ectodermal) can even be produced as sisters in the final division of a precursor cell. What, then, determines the path that a cell takes when it differentiates?

Using a microlaser beam, individual nematode cells can be killed without damage to their neighbouring cells. In some cases the neighbouring cells persist in their normal course of development and only the progeny of the ablated cell(s) are missing (Sulston and White, 1980). These results imply a strict cell-autonomous process of differentiation. Cell-autonomous processes also operate in chordates. For example, isolated cells or groups of cells from Ascidian embryos can differentiate normally *in vitro*, as though they were still part of the intact embryo (Reverberi and Minganti, 1946; reviewed in Slack, 1983).

Cell-cell interactive differentiation in *Caenorhabditis elegans*

In many cases the differentiation pathway followed by a cell is not determined by cell-autonomous mechanisms, but depends on cues from nearby cells. One such example in *C.elegans* involves the fate of two somatic gonadal cells, designated Z1.ppp and Z4.aaa. During normal development one of these cells becomes the anchor cell and the other becomes the ventral uterine precursor cell. The decision occurs randomly during normal development, either cell being capable of adopting one fate or the other (Kimble and Hirsh, 1979). Laser ablation of all the gonadal cells except Z1.ppp *or* Z4.aaa has shown that the remaining cell will differentiate into the anchor cell (Kimble, 1981). This suggests that the anchor cell fate is the default pathway for Z1.ppp or Z4.aaa. However if all the gonadal cells except Z1.ppp *and* Z4.aaa are ablated then one of these cells will become the anchor cell, the other will become the ventral uterine precursor (Seydoux and Greenwald, 1989). The

implication is that the presumptive anchor cell sends a signal that is received by the presumptive ventral uterine precursor cell thereby influencing the fate of that cell.

The anchor cell-ventral uterine precursor cell decision is controlled by the activity of a gene, *lin*-12. Analysis of *C. elegans* mutants lacking *lin*-12 activity has shown that Z1.ppp and Z4.aaa now both become anchor cells. In mutants having elevated *lin*-12 activity both cells become ventral uterine precursor cells (Greenwald, 1985; Greenwald and Seydoux, 1990). Genetic mosaic analysis showed that *lin*-12 had to be expressed in either Z1.ppp or Z4.aaa in order for either of these cells to become the ventral uterine precursor cell (Seydoux and Greenwald, 1989).

The predicted *lin*-12 gene product is that of a transmembrane protein with large extracellular and intracellular regions, which contain a variety of peptide motifs including an epidermal growth factor (EGF)-like motif (Greenwald, 1985). The *lin*-12 gene product is thought to act as a receptor for the anchor cell to ventral uterine precursor signal.

The anchor cell subsequently directs the development of the vulva (Sternberg and Horvitz, 1986). During normal development, the anchor cell induces the six nearest underlying hypodermal precursor cells to form a vulva. If the anchor cell is killed, then these hypodermal precursor cells, instead of following a vulval lineage, give rise to normal hypodermal cells and no vulva is formed. If the six hypodermal precursor cells nearest the anchor cell are destroyed then adjacent hypodermal precursor cells will adopt a vulval fate in their place. The anchor cell is so important for vulval differentiation that if all the gonadal cells except the anchor cell are killed, then the vulva will still be formed. The anchor cell probably ensures the correct development of the vulva at the right time and the right place by production of an inducing factor(s), shown schematically in figure 1.

Figure 1. Schematic view of the larval *C.elegans* gonad and ventral hypodermis, depicting the relationship between the anchor cell (AC) of the gonad and the vulval precursor cells (VPC'S) in the ventral hypodermis.

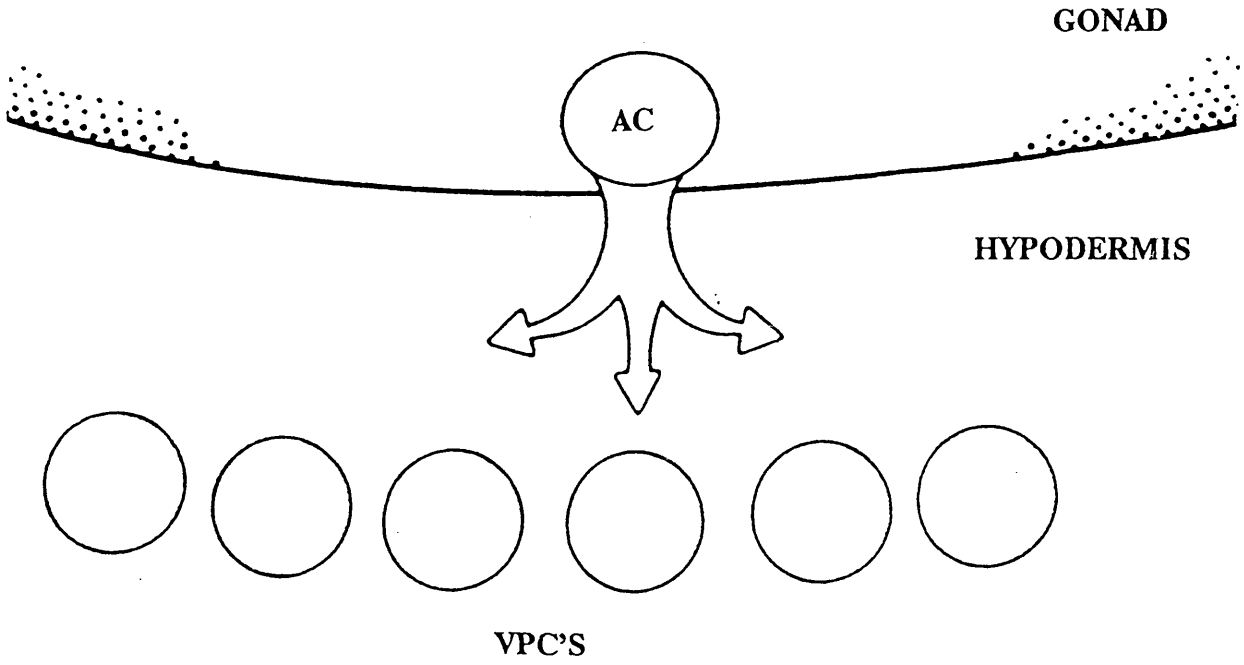

The anchor cell (AC), located in the gonad, produces a signal(s) (arrows) which interacts with the six nearest underlying vulval precursor cells (VPC'S) in the hypodermis and influences them to differentiate and form a vulva.

Genetic mutations in *Drosophila* eye development implicate specific ligands and receptors responsible for specifying cell fate

Probably the best understood example of cell-interactive development in invertebrates is the compound eye of *Drosophila*. The compound eye of *Drosophila* is composed of a crystalline array of identical units called ommatidia. Each ommatidium consists of 20 cells including eight photoreceptor cells that can be identified both morphologically and functionally (Hardie, 1984). The eight photoreceptor cells (R1-R8) comprise three functional classes: R1-R6 are grouped into one class containing the same rhodopsin photopigment and having axonal projections to the same second order neurons, R7 and R8 belong to two separate classes each containing different rhodopsin photopigments with unique neural projections to different second order neurons (Hardie, 1984; Melamed and Trujilzo-cenoz, 1975). Other cells of the ommatidia are: 4 cone cells located on top of the photoreceptor cell cluster that secrete the liquid-filled pseudocone, 2 primary pigment cells located in the distal portion of the ommatidia that secret the corneal lens, and 6 secondary pigment cells that are shared between two or three ommatidia and serve to isolate individual clusters. Cell precursors integrate into the ommatidial cluster in a precise temporal sequence. Except for R8 (the founder cell of each cluster) and R7, all other cells are added in pairs. The order of formation of the inner 12 cell ommatidial unit is: R8 followed by R2 and R5, followed by R3 and R4 followed by R1 and R6, followed by R7, followed by anterior and posterior cone cells and finally equatorial and polar cone cells (see Figure 2)

Both R7 and R8 photoreceptor cells respond to ultraviolet (UV) light. Harris *et al.* (1976) screened for mutant flies that did not respond to UV light and found three such mutants. In one mutant, the R7 photoreceptor cell was missing from each ommatidium, thus the mutant was called *sevenless (sev)*. In the ommatidia of *sev*

Figure 2. Schematic Diagram of *Drosophila* eye Ommatidium.

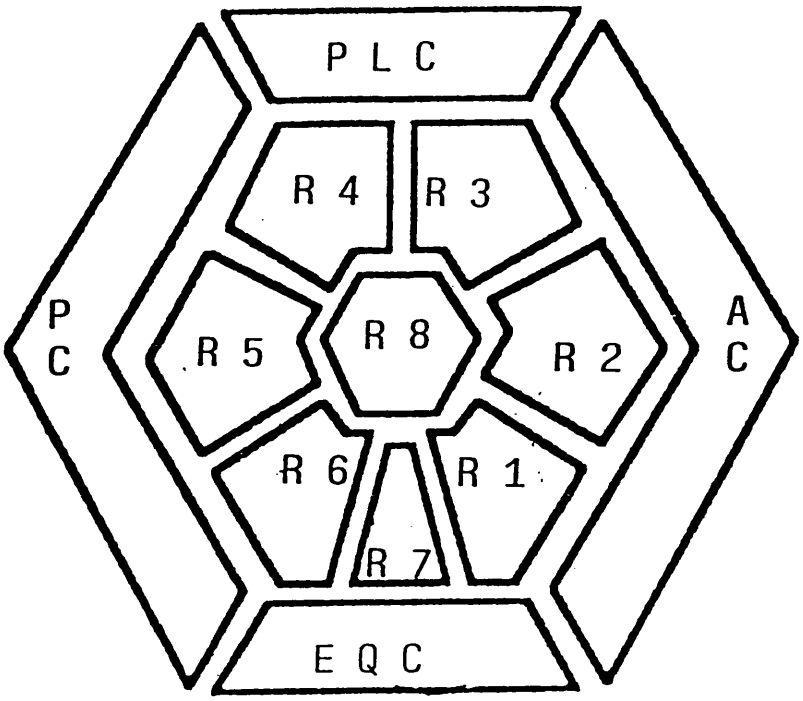

KEY:

R	Rod photoreceptor cells (1-8)
PLC	Polar cone cell
EQC	Equatorial cone cell
AC	Anterior cone cell
PC	Posterior cone cell

Order of formation:

1. R8
2. R2 + R5
3. R3 + R4
4. R1 + R6
5. R7
6. AC + PC
7. PLC + EQC

mutants, a non-photoreceptor cell occupies the position of the R7 photoreceptor (between R1, R6 and R8). This non-photoreceptor cell does not produce an axon or express nerve cell specific antigens (such as photopigments) normally expressed by the R7 precursor. This cell eventually becomes a functional cone cell and takes the position of the equatorial cone cell, but it retains contact with R1, R6 and R8 (contacts normally made only by the R7 photoreceptor cell). The generation of genetically mosaic eyes, where in some ommatidia both *sev*$^{+}$ and *sev*$^{-}$ cells are present, excludes the possibility that cell lineage could play a role in the determination of the different cell types in the ommatidia. Only in ommatidia where the cell in the R7 position was *sev*$^{+}$ did a normal R7 cell develop (Lawrence and Green, 1979). This suggests that the product of the *sev* gene is important for determining the fate of the R7 precursor cell, the product of the *sev* gene enabling the R7 cell to differentiate normally.

The *sev* gene has been cloned (Hafen *et al.*, 1987; Banerjee *et al.*, 1987a) and contains two putative transmembrane sequences and a cytoplasmic C-terminal domain. This C-terminal domain has close similarity to the tyrosine kinase domains found in some oncogene products and growth factor receptors (Simon *et al.*, 1989). The *sev* gene product is thought to be a receptor that is responsible for differentiation of the presumptive R7 cell.

The localisation of the *sev* protein has led to conflicting ideas regarding its expression. Banerjee *et al.* (1987b) carried out immunolocalisation studies by electron microscopy and found that all the photoreceptor cells and the surrounding cone cells expressed the *sev* protein. This finding led to the hypothesis that any cell could become R7, if present at the right place and time to respond to an environmental cue that specified that cell fate. Tomlinson *et al.* (1987), however, described differences in the staining of the different photoreceptor cells: R2, R5 and R8 are unstained while R7, R3 and R4 are stained only in those regions of these cells

that contact R8, specifically at the apices of the cells in microvilli. As R1 and R6 join the cluster, the low level of *sev* staining in these cells drops to background. The localised staining in R3 and R4 is interesting, since the development of these cells does not require the *sev* gene.

In another mutant, *bride of sevenless (boss)*, mosaic analysis indicates that the *boss* gene product must be present in R8 for R7 to develop (Reinke and Zipursky, 1988). This observation suggests that the *boss* gene may be the ligand for the *sev* protein. This evidence suggests that the fate of a cell can be determined by the presence of a specific receptor on the cell surface that responds to a factor or factors produced by a master or controlling cell (in this case the R8 cell).

Similarly, another *Drosophila* mutation *rough* also controls cell fate in the developing ommatidium. In *rough* mutations R3 and R4 do not differentiate (Saint *et al.*, 1988; Tomlinson *et al.*, 1988). Mosaic analysis showed that *rough* expression in R2 and R5 is necessary for the differentiation of R3 and R4 in the pre-cluster (Tomlinson *et al.*, 1988). The *rough* gene has been cloned and sequenced (Saint *et al.*, 1988; Tomlinson *et al.*, 1988). Its DNA sequence suggests that *rough* encodes a homeobox-containing protein. Such proteins have been shown to act as transcription factors (Bodner *et al.*, 1988; Ingraham *et al.*, 1988) by binding to DNA via the conserved homeodomain (Gehring, 1987; Scott and Carrol, 1987). Presumably in R2 and R5, the *rough* gene product controls the expression of another gene, the product of which is likely to be an extracellular signal that regulates the development of R3 and R4.

Another gene involved in *Drosophila* eye development known as *seven-up (svp)* has been isolated; its expression in R1, R3, R4 and R6 appears to be essential for the normal development of the 8 cell cluster (Miodzik *et al.*, 1990). In svp^- mutants, ommatidia precursor cells transform towards an R7 cell fate as judged by morphology and absence of pigment granules normally present in R1-R6. Sequencing of the *svp*

gene revealed it to be a steroid receptor gene containing both a DNA binding domain and a ligand binding domain (Miodzik *et al.*, 1990).

In summary, the decision to become the anchor cell or ventral uterine precursor cell, the development of the vulva of *C.elegans* and the ommatidia of *Drosophila*, appear to be controlled by the signals received from nearby cells. These signals act through specific receptors in or on their target cells and ultimately influence the fate of these cells.

Genetic mutants in vertebrates identify growth factors and their receptors as having important roles to play in normal development

Genetic analysis of vertebrate development is much less advanced than in invertebrates. Most studies of cell-cell interactions during vertebrate development must be studied *in vitro*. However, research into dominant-white spotting (*W*), Steel (*Sl*) and Patch (*Ph*) mouse mutants has yielded important information regarding cell-cell interactions necessary for normal mouse development.

Mice carrying mutations at the *W* locus are characterised by severe macrocytic anaemia and rarely survive long after birth. Defects at the *W* locus appear to affect the proliferation of cells during early embryogenesis and result in an intrinsic defect in the haematopoietic stem cell hierarchy (McCulloch *et al.*, 1964; Russell, 1949). The mouse mutant *W* has a deletion of the c-*kit* proto-oncogene that is tightly linked to the *W* locus (Chabot *et al.*, 1988). c-*kit* encodes a transmembrane protein tyrosine kinase that is structurally similar to the receptors for colony-stimulating factor-1 (CSF-1) and platelet derived growth factor receptor. (Yarden *et al.*, 1986; Qui *et al.*, 1988)

The growth factor for the c-*kit* receptor has been cloned (mast cell growth factor) and has been shown to map to the *Sl* locus (Anderson *et al.*, 1990; Copeland

et al., 1990; Huang *et al.*, 1990; Williams *et al.*, 1990; Zsebo *et al.*, 1990a; Zsebo *et al.*, 1990b). Mutations at the *Sl* locus, like *W*, are characterised by severe macrocytic anaemia with few homozygotes surviving until birth. Thus the normal development of macrophages from haemopoietic precursor cells appears to depend on the expression of the c-*kit* receptor and mast cell growth factor, deletion of either gene resulting in macrocytic anaemia.

Ph homozygote mouse mutants are embryonically lethal. The receptor for platelet derived growth factor alpha (PDGFαR) has been shown to be closely linked to the *Ph* locus (Stephenson *et al.*, 1990). PDGFαR expression appears to be essential for the normal development of a mouse, affecting the development of visceral endoderm, mesodermally derived structures and non-neuronal derivatives of cranial neural crest in *Ph* homozygous mice (Morris-Graham *et al.*, 1992; Schatteman *et al.*, 1992; Orr-Urtreger *et al.*, 1992).

These mouse mutants provide a direct demonstration that cell-cell signalling, mediated by diffusible growth factors and their receptors, is important for normal mammalian development.

Growth factors act through specific receptors. Receptor activation can affect both cell proliferation and differentiation

Growth factors are a large diverse group of proteins that effect cell proliferation and differentiation. They mediate their cellular responses on their target cells by binding to specific cell surface receptors on their target cells. Receptor activation triggers intracellular signals that ultimately lead to an altered pattern of gene expression. Growth factors can be organised into a limited number of gene families based on sequence homology. Some of these families are shown in Table 1. Growth factors are multi-functional, and can trigger a broad range of

Table 1. Some growth factor families.

Epidermal growth factor family	
Epidermal growth factor	EGF
Transforming growth factor-α	TGF-α
Transforming growth factor-ß superfamily	
Transforming growth factor-ß's	TGFß1-6
Activin-A	
also known as *Xenopus* tissue culture mesoderm inducing factor	XTC-MIF
Activin-AB	
Inhibin-A	
Inhibin-B	
Mullerian Inhibiting substance	MIS
Bone morphogenic protein-2A	BMP-2A
Bone morphogenic protein-3	BMP-3
Fibroblast growth factor family /heparin binding growth factors	
Acidic fibroblast growth factor	aFGF
Basic fibroblast growth factor	bFGF
Integration tumour-2	Int-2
Human stomach cancer/Kaposi's sarcoma	hst/KS
Fibroblast growth factor-5	FGF-5
Fibroblast growth factor-6	FGF-6
Keratinocyte growth factor	KGF
Platelet derived growth factor family	
Platelet derived growth factor A and B chains	PDGF-AA/ -AB/-BB
Vascular endothelial cell growth factor	VEGF
Insulin-like growth factor family	
Insulin	
Insulin-like growth factor-I	IGF-I
Insulin-like growth factor-II /somatomedin-C	IGF-II

cellular responses: cell division, extracellular matrix formation, cell motility, cell survival and the expression of differentiated characteristics (for reviews see; Burgess and Maciag, 1989; Rifkin and Moscatelli, 1989; Walicke, 1989 and Westermark and Heldin, 1989).

Growth factor receptors, characteristically, comprise an extracellular ligand binding domain, a transmembrane domain and an intracellular signalling domain. The intracellular signalling domains include protein-serine kinases, protein-tyrosine phosphatases or protein-tyrosine kinases. Growth factor receptors can also be grouped in families, defined by sequence and structural similarities. One family, designated as tyrosine kinase subclass III, includes the platelet derived growth factor receptors α and ß (PDGFαR and PDGFßR), colony stimulating factor 1 (CSF-1) and c-kit (for review see Ullrich and Schlessinger, 1990). Characteristics of this subclass of receptors are that they contain five immunoglobulin-like repeats in the extracellular domain and an interrupted tyrosine kinase domain (see figure 3). Ligand-induced activation of the kinase domain and its signalling potential is mediated by receptor dimerisation (for review see Schlessinger, 1988)

Many growth factors stimulate cell division during development of an organism and are sometimes specific to distinct tissue types. Basic fibroblast growth factor (bFGF) is a potent mitogen for mesodermal cells (Gospodarowicz *et al.*, 1987). Platelet derived growth factor (PDGF) is a potent mitogen for connective tissue cells, such as dermal and tendon fibroblasts, vascular smooth muscle, and chondrocytes (for review see Ross and Bowen-Pope, 1986) and can act as a chemotractant for connective tissue cells such as fibroblasts and smooth muscle cells. PDGF is also mitogenic for some glial cells of the CNS (for reviews see; Ross and Bowen-Pope., 1986; Raff, 1989; Richardson *et al.*, 1990). Transforming growth factor-ß1 (TGFß1), however, inhibits the proliferation of many cell types, including fibroblasts (Sporn *et*

Figure 3. Schematic representation of the protein structure of Tyrosine Kinase subclass III receptors.

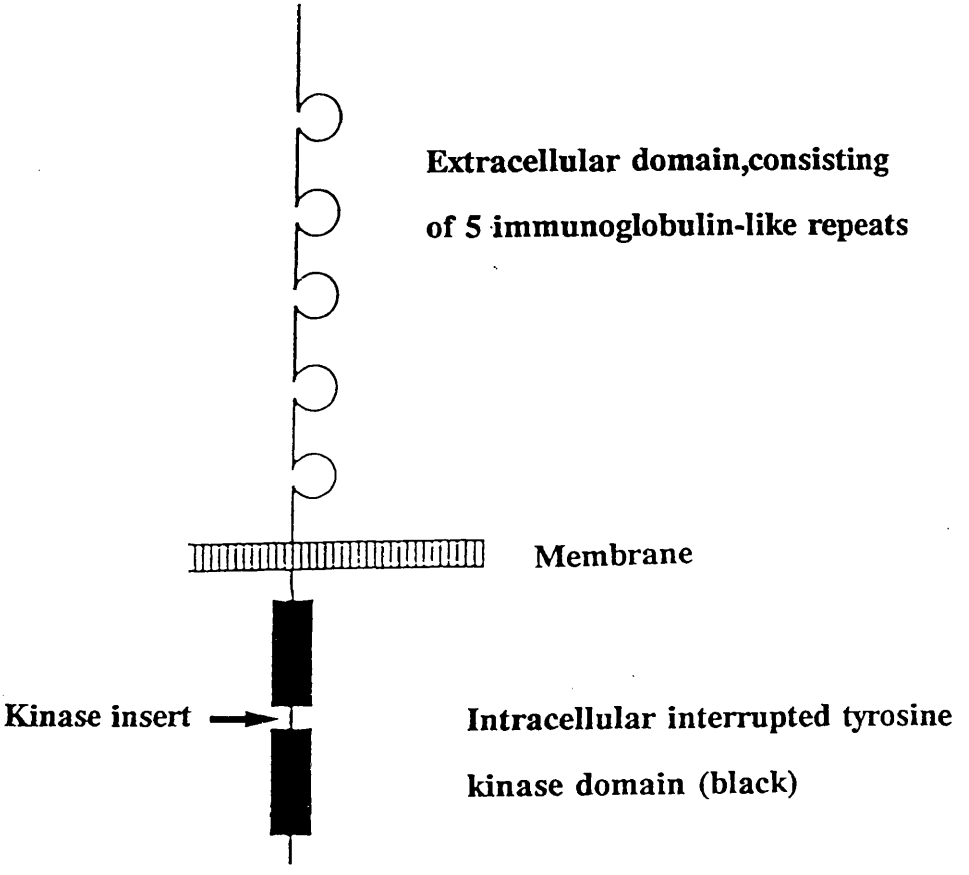

PDGFαR

PDGFßR

CSF-1-R

c-*kit*

al., 1986), but it can also stimulate growth of fibroblasts when they are cultured in soft agar suspensions (Roberts *et al.*, 1981).

Growth factors also regulate the differentiation of both primary and established cell lines. TGFß stimulates the differentiation of bronchial epithelial cells and inhibits the terminal differentiation of B cells and 3T3 adipocytes (Ignotz and Massagué, 1986; Sporn *et al.*, 1986). bFGF delays the differentiation of myoblasts (Gospodarowicz *et al.*, 1976; Clegg *et al.*, 1987) but stimulates differentiation or stabilises the differentiation of a wide variety of cell types, including chondrocytes, endothelial cells and a rat pheochromocytoma line (PC12) (reviewed in Gospodarowicz *et al.*, 1987). As described in this thesis PDGF stimulates the proliferation of the O-2A progenitor, a glial precursor cell, delaying their differentiation into oligodendrocytes *in vitro* (Richardson *et al.*, 1988).

Peptide growth factors can also regulate deposition and modification of the extra cellular matrix (ECM). TGFß can modify the ECM made by cells, by enhancing secretion of collagen and fibronectin (Ignotz and Massagué, 1986), increasing secretion of protease inhibitors and inhibiting secretion of cellular proteases (Laiho *et al.*, 1986). bFGF has been shown to effect ECM production in corneal and vascular endothelial cells, as well as chondrocytes. In these three cell types, bFGF promotes cell proliferation and stabilises their differentiated phenotype by modulating the synthesis and distribution of various ECM components such as collagen, fibronectin and proteoglycans (Gospodarowicz *et al.*, 1981; Tseng *et al.*, 1982). Using dishes coated with ECM produced by corneal endothelial cells exposed to bFGF, the ECM itself can support cell proliferation in the absence of bFGF in the growth medium (Gospodarowicz *et al.*, 1984). This suggests that bFGF binds to the ECM, providing an immobilized source of growth factor.

Growth factors may regulate embryonic morphogenesis by controlling cell movement, division and ECM production. Growth factor proteins and their

messenger RNAs (mRNA) are detected in the earliest stages of embryogenesis in both mammalian and non-mammalian organisms. PDGF mRNA transcript have been found in unfertilised eggs of both mouse and frog (Rappolee *et al.*, 1988; Mercola *et al.*, 1988). Similarly transcripts for TGFα and TGFß are expressed in pre-implantation mouse embryos (Rappolee *et al.*, 1988). Both FGF mRNA and FGF protein have been identified in frog oocytes and early embryos (Kimelman *et al.*, 1988; Slack and Isaacs, 1989). Embryonal carcinoma cell lines derived from mouse blastomeres secrete PDGF-like and FGF-like activities and express IGF-II transcripts (Heath and Isacke, 1984; Heath and Shi, 1986 and Rizzino and Bowen-Pope, 1985), suggesting that growth factors may influence the normal development of an embryo from its conception.

Growth factors induce mesoderm production in *Xenopus* embryos

Most of our understanding of the role of growth factors in mammalian developmental mechanisms has come from manipulating cells *in vitro*. For example bFGF, TGFβ2 and XTC-MIF (=Activin-A) have been shown to induce mesoderm like structures in isolated animal pole ectoderm (Slack *et al.*, 1987; Smith *et al.*,1988; Kimelman *et al.*,1988; Rosa *et al.*, 1988; Slack and Isaacs, 1989). In response to exposing isolated explants of ectoderm from the animal pole region of stage 8 *Xenopus* blastula to various concentrations of bFGF, mesoderm structures are formed. In control (untreated) explants the internal cells either become epidermal or remain undifferentiated. Explants which are treated with concentrations of bFGF, between 2-30 ng ml, are induced to form characteristic mesoderm structures such as mesenchyme, mesothelium, blood cells and occasional muscle cells. Higher concentrations of bFGF (30-120 ng/ml) give rise to significant blocks of muscle (Slack *et al.*, 1987). bFGF mRNA and protein are both present in early eggs and

embryos (Kimelman and Kirschner, 1987; Kimelman *et al.*, 1988; Slack and Isaacs, 1989); the protein appears to be present in quantities consistent with its proposed role as an inducing factor. However, FGF has not been directly shown to be localised to, or to be secreted, by endodermal tissue.

However, bFGF is not the only growth factor to show mesoderm inducing activity in *Xenopus* embryos, both TGFß-2 (Rosa *et al.*, 1988) and XTC-MIF (=Activin-A) (Smith, 1987; Smith *et al.*, 1988) also induce mesoderm formation. XTC-MIF has recently been shown to be the *Xenopus* homologue of mammalian Activin-A (Smith *et al.*, 1990; van den Eijnden-Van Raaij *et al.*, 1990).

Neither TGFß-1 or TGFß-2, nor XTC-MIF has been identified in early *Xenopus* embryos. However, a maternal RNA with significant homology to the TGFß family, *Vg*-1, is translated throughout embryogenesis (Dale *et al.*, 1989). Similarly a mRNA encoding TGFß-5 has recently been identified in *Xenopus* embryos (Kondaiah *et al.*, 1990)). Neither *Vg*-1 nor TGFß-5 has yet been directly demonstrated to function as a mesoderm inducer. Thus the role of TGFß-like molecules in the natural inductive process remains unclear.

Growth factor involvement in glial cell development

Growth factor involvement in the development and differentiation of the central nervous system is just beginning to be understood. Perhaps the best studied example is that of the differentiation of a rat glial precursor cell, the O-2A progenitor, into an oligodendrocyte (for reviews see Raff, 1989; Miller *et al.*,1989; Richardson *et al.*, 1990).

The majority of studies on the O-2A progenitor cell have focused on the rat optic nerve, where the first oligodendrocytes appear on the day of birth (Miller *et al.*, 1985). When dissociated embryonic optic nerve cells are cultured in defined medium,

the normal timing of oligodendrocyte development is disrupted; the O-2A progenitor cells stop dividing and differentiate within a day or two into oligodendrocytes, regardless of the age of the animal from which they were taken (Raff *et al.*, 1985). Normal timing can be restored by culturing embryonic optic nerve cells in medium conditioned by cortical astrocytes: now the O-2A progenitors continue to divide and first differentiate into oligodendrocytes on the *in vitro* equivalent of the day of birth (Raff *et al.*, 1985). Proliferation and differentiation into oligodendrocytes continues for several weeks in culture, just as *in vivo* (Noble and Murray, 1984; Raff *et al.*, 1985; Dubois-Dalcq, 1987). Thus cortical astrocytes provide a mitogen(s) which both stimulates O-2A progenitors to divide and prevents their premature differentiation in culture. The first chapter of my thesis deals with experiments that indicate that one of the factors produced by cortical astrocytes is a form of PDGF, and that PDGF is also present in the rat optic nerve *in vivo*.

Early development of the CNS

The early events of CNS development have been reviewed often (e.g. Boulder Committee, 1970; Jacobson, 1978). In most vertebrates studied, the CNS forms after gastrulation. The underlying mesoderm of the developing embryo induces the neural plate to invaginate, forming the neural tube. The apparently homogenous population of cells in the neural tube gives rise to the wide variety of neurons and glial cells found in the mature CNS. Before closure of the neural tube is complete, the rostral part of the tube forms three primary brain vesicles prosencephalon (forebrain), mesencephalon (midbrain) and rhombencephalon (hindbrain) (See figure 4). Subsequently, the prosencephalon sub-divides into two secondary brain vesicles, the telencephalon (develops into cerebral cortex), and a median part, the diencephalon (develops into epithalamus, thalamus and hypothalamus). At the same time the

rhombencephalon divides into the metencephalon (develops into cerebellum and pons) and the myelencephalon (develops into the medulla oblongata) (See figure 4). The optic system develops from a swelling of a region of the diencephalon which grows outwards towards the epithelium. This swelling gives rise to the optic stalk (which forms the optic nerve) and the optic vesicle (which forms the retina). The neuronal epithelium of the optic vesicle makes contact with the ectoderm covering the exterior of the head. This contact induces the ectoderm to invaginate to form a lens. At the same time, the outer part of the optic vesicle invaginates to form the optic cup, comprising of two layers of neural epithelium (see figure 5). The layer closest to the lens differentiates into neural retina, which contains the photoreceptor cells, several types of interneurons and ganglion neurons which relay visual stimuli through the optic nerve to the brain. The other layer differentiates into the retinal pigment epithelium which forms a dark enclosure for the photoreceptive system.

Tritiated thymidine incorporation studies which label mitotic cell nuclei have helped to describe the formation of the cerebral cortex and other regions of the brain, enabling a description of the neuronal development. The wall of the neural tube consists of a single layer of proliferating neuroepithelial cells. In the telencephalon, the cells divide rapidly and extend processes towards the pial (outer) surface to establish two zones: the ventricular zone containing the nuclei and the marginal zone containing the cell processes. Some nuclei migrate within their cell bodies towards the pial surface forming an intermediate zone and these cells will eventually differentiate into neurons. The cells of the ventricular zone continue to divide giving rise to postmitotic cells which migrate through the previously formed intermediate zone, passing the postmitotic cells already present before coming to rest, forming a laminar structure. Each new layer of postmitotic cells forms superior to the previous layer. In other regions of the brain such as the thalamus, this ordering of layers is reversed, with the most distal layer being formed first. Using tritiated

Figure 4. Diagram of the developing human brain and ventricular system.

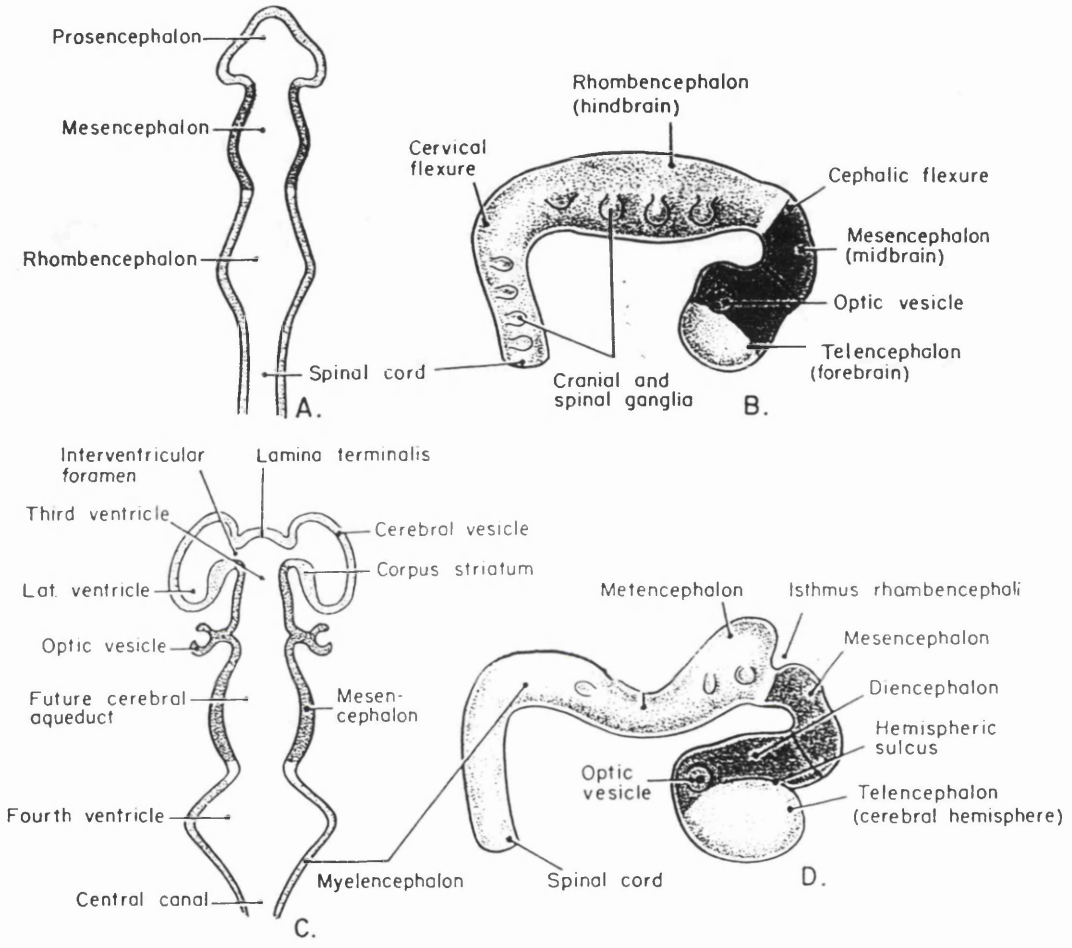

A and **B**:- The three brain vesicle of a 4-week human embryo.

C and **D**:- The five brain vesicle stage of a 6-week embryo

Diagram taken from Carpenter (1976).

Figure 5. Diagram of developing optic nerve and retina.

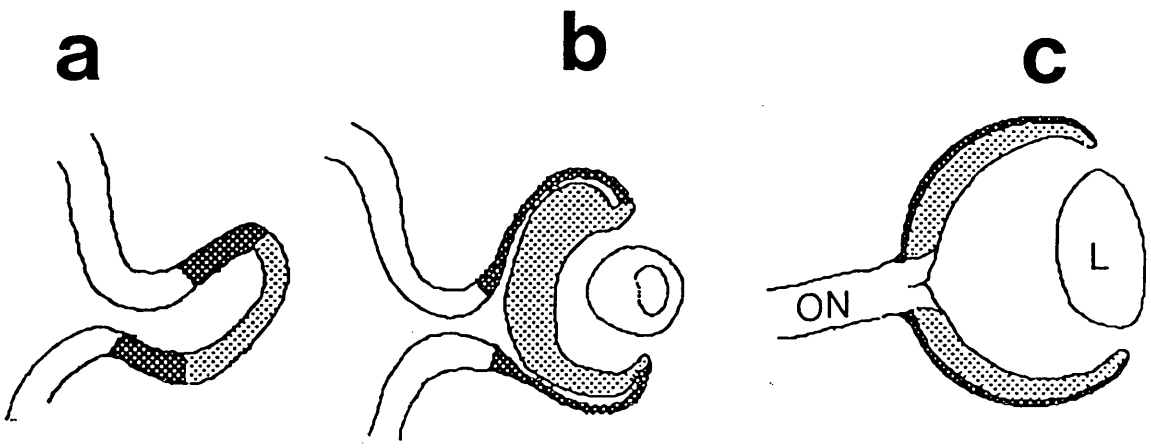

a. Shows the initial swelling of the diencephalon. The neural epithelium destined to become the retina is shown in light stipple. The region destined to become the pigmented epithelium is shown in dark stipple.

b. Shows the outer part of the optic vesicle invaginating to form the optic cup.

c. Shows the mature optic nerve (ON), retina and lens (L).

thymidine pulse labelling of DNA, cell division has been shown to be confined to the ventricular and subventricular zones. As neurons migrate out of this zone, they are post-mitotic. The time of final nuclear division of a cell is known as its birthday; neurons in a given area are usually born over a short well defined period.

Radial glial cells are the first glial cells to appear. These are elongated cells with cell bodies in the ventricular zone and processes spanning the neural tube from ventricular to pial surface. They have similar birthdays to the earliest neurons and seem to guide neurons to their final destinations (Rakic, 1972). Other glial cells arise from an area in the ventricular zone known as the subventricular (or subependymal) zone and are generated over an extended period, unlike neurons. Unfortunately these tritiated thymidine studies were unable to elucidate whether precursor cells capable of giving rise to both neurons and glial cell are present in the subventricular zone, or whether a separate glial precursor cell exists. Unlike neurons, glial cells do not stop dividing before they leave the ventricular zone and may divide several times after leaving the ventricular zones. This means that it is not generally possible to determine migration routes and final settling patterns of glial cells by pulse labelling, because the ^{3}H-thymidine is diluted at each cell division and soon becomes undetectable by autoradiography.

Cell lineage studies in the CNS

To answer questions about the origins, lineages and final settling patterns of both glial and neuronal cells other methods of studying these cells in the CNS have been devised. The question of cell lineage in the CNS has been addressed either by injecting individual cells with lineage markers (Holt *et al*, 1988) or by infecting individual cells with retroviral vectors (Turner and Cepko, 1987; Price and Thurlow, 1988; Luskin *et al.*, 1988). Both methods enable the progeny of a single progenitor cell to be specifically labelled. The retroviral vectors contain a reporter gene such

as the *E.coli* ß-galactosidase (*Lac-Z*) gene, the expression of which is readily detected histochemically or immunohistochemically. Infection of CNS cells before the end of cell differentiation allows the progeny of an individual infected cell to be traced after normal cellular differentiation is complete. In the rat retina, for example, infected precursor cells appear to be multipotential, giving rise to both neuronal and glial cells. Infected cell clones are found that contain most combinations of amacrine cells, bipolar cells, rod photoreceptors and Müller glial cells (Turner and Cepko, 1987).

In the mouse and rat cerebral cortex, retroviral studies indicate that by embryonic day 14 (E14; referring to days post-fertilization of the embryo), the glial and neuronal cell lineages have diverged (Price and Thurlow, 1988; Luskin *et al.*, 1988). All clones labelled after E14 consist entirely of either neurons or glial cells. Neuronal cells migrate outwards from the ventricular zone to become either pyramidal or non pyramidal. Thus when first labelled with retrovirus, these post-mitotic neuronal clones do not yet appear to be committed to their final phenotype. This apparently occurs at a later period of development, suggesting that neurons are born naive ("knowing" that they are neurons but not which type). However, similar studies by Parnavelas *et al.* (1991) suggest that clones consist of pyramidal or non pyramidal neurons only, and they do not see mixed clones. Also, catecholaminergic neurons of the brain stem make tyrosine hydroxylase (a differentiation marker enzyme) only two to three hours after birth (Specht *et al* 1981). These results suggest that neurons become committed to their final phenotype when they are born. These contrasting results make it unclear as to when or where neurons become committed to their final phenotype.

The development of O-2A progenitor cells in the CNS has been studied with antibodies that label these cells at different stages of their development (LeVine and Goldman, 1988a; LeVine and Goldman, 1988b; Reynolds and Wilkins 1988; Hardy

and Reynolds, 1991). These studies will be reviewed in more detail in the second chapter of my results where I investigate the possibility that the distribution of PDGF-α Receptor in the CNS, during late neurogenesis (after E16), may be restricted to cells of this lineage.

During early neurogenesis (prior to E16) PDGF-αR is transiently expressed in discrete regions of the ventricular zone. Individual PDGFαR$^+$ cells can be observed disseminating from a ventrally located zone in both the brain and spinal cord. These results are described in my third chapter of results, and have led me to propose that cells of the oligodendrocyte lineage arise from discrete regions of the ventricular zone over a short window of time, around E14.

CHAPTER 2

METHODS

Unless stated otherwise all chemicals and reagents were purchased from BDH Chemicals Limited and were of AnalaR grade wherever possible.

Restriction enzymes and molecular biological reagents were purchased from Pharmacia ltd.

Radio-nucleotides were purchased from Amersham International.

Specialized bacterial media components were obtained from Difco Laboratories Ltd, Detroit, Michigan, USA.

Most of the molecular techniques described are taken from Sambrook *et al,* (1989).

BACTERIOLOGY

Bacterial strains

For general cloning and sub-cloning of recombinant plasmids *Escherichia coli (E.coli)* strains LE392 [F^-,*hsd*R514 (r_k^-,m_k^+),*sup*E44, *sup*F58, *lac*Y1 or ∆(*lac*IZY)6, *gal*K2, *gal*T22, *met*B1, *trp*R55, λ^-] (Murray, 1977) and DH5 [F^-, *rec*A1, *end*A1, *gyr*A96, *thi*-1, *hsd*R17, (r_k^-, m_k^-), *sup*E44, *rel*A1 ,λ^-] (Hanahan,1985) were used.

Growth Media and agar plates

Bacteria were grown in Luria Broth (LB) containing 10 g bacto-tryptone, 5 g yeast extract and 10 g NaCl per litre, or on LB-agar plates (LB + 30 g bacto-agar/litre). Solutions were sterilized by autoclaving at 15 lb/sq.in. for 20 minutes and were stored at room temperature. When appropriate Ampicillin (AMP, final concentration 40μg/ml) or Tetracycline (TET, final concentration 12.5 μg/ml) was added to LB media or LB agar (antibiotics were added after the LB media or LB

agar had been sterilized and allowed to cool below 55°C. Agar was poured into 10 cm diameter Petri dishes (Falcon) and allowed to set at room temp. Plates were stored at 4°C and were air dried at 37°C for 1 hour prior to use.

All strains of *E.coli* were grown at 37°C. Liquid cultures were continuously agitated in a rotating environmental shaker.

Preparation of Competent Bacteria.

a) Calcium chloride method.

This was a modification of the method described by Mandel and Higa (1970). 200 ml of LB medium was inoculated with 500 μl of an overnight bacterial culture, either LE392 or DH5, and shaken at 37°C until the culture reached an absorbance at 550 nm (A_{550}) of between 0.2-0.4. The bacteria were pelleted at 3000 x G for 30 minutes, resuspended in 20 ml of ice cold 100 mM $CaCl_2$ and incubated on ice for 20 minutes. Then bacteria were pelleted as before, resuspended in 1 ml ice-cold 100 mM $CaCl_2$ and stored at 4°C for between 12-24 hours, before being used for transformations.

b) Rubidium chloride method.

This protocol was used to produce frozen stocks of competent bacteria and was adapted from Hanahan (1983). 200 ml of LB medium was inoculated with 500 μl of an overnight culture of DH5 cells and shaken at 37°C until the A_{550} was between 0.2-0.4. The bacteria were incubated on ice for 5 minutes and pelleted at 6,000 x G for 10 minutes at 4°C. Bacteria were resuspended in 40 ml of ice cold buffer, containing 300 mM potassium acetate, 100 mM rubidium chloride, 10 mM calcium chloride, 50 mM manganese chloride and 15% v/v glycerol (pH to 5.8 with acetic acid), and incubated on ice for 5 minutes. The bacteria were repelleted and

resuspended in 5 ml of ice cold buffer, containing 10 mM 3(N-Morpholino) propanesulphonic acid monosodium salt (MOPS), 75 mM calcium chloride, 10 mM rubidium chloride 15% v/v glycerol (pH to 6.5 with KOH) and incubated on ice for 15 minutes before storing at -70°C until required.

Transformation of bacteria with plasmid DNA

Between 50-100 ng of DNA and 100 μl of competent bacteria were used per transformation. Bacteria and DNA were mixed and incubated on ice for 10 minutes then heat shocked at 37°C for 5 minutes. Bacteria were incubated in LB at 37°C for 15 minutes before pelleting at 6000 x G for 10 minutes. Bacteria were resuspended in LB and spread onto LB-agar plates containing AMP or TET and incubated at 37°C overnight. Plasmid pUC-8 was transformed, at a known concentration, to check the transformation efficiency (this was usually found to be between 5 x 10^7 and 2 x 10^8 transformants/μg of plasmid DNA added).

NUCLEIC ACIDS

Phenol and chloroform extractions

Samples to be extracted were made 0.5 M with NaCl and equal volumes of UNC-phenol [containing 500 g phenol (melted at 65°C), 250 ml 1 M Tris-HCl (pH 7.5), 28 ml m-cresol, 1.1 ml 2-ß-mercaptoethanol(2-ME), 555 mg δ-hydroxyquinoline] and chloroform [containing 4% v/v iso-amyl alcohol] were added. Solutions were vigorously shaken and centrifuged at 10,000 x G for 10 minutes at 20°C. The upper aqueous phase was removed and re-extracted with an equal volume of chloroform, centrifuged as before and the upper aqueous phase collected.

Ethanol precipitation of DNA/RNA

All samples were made 0.5 M with NaCl before precipitating the DNA or RNA with 95% ethanol (kept at -20°C). Samples were incubated on dry-ice for 15 minutes or placed at -20°C for at least 1 hour before pelleting the DNA or RNA at 10,000 x G for 15 minutes at 4°C. The pellet was washed with 70% alcohol and air-dried, before dissolving in a suitable buffer. Samples containing less than 10 μg of DNA or RNA were precipitated with 25 μg of yeast transfer-RNA (tRNA) added to act as a carrier. For DNA 2x the original sample volume of 95% ethanol was added and for RNA 2.5x the original sample volume was added.

Restriction digests of DNA

DNA was digested at 37°C for a minimum of 1 hour, using appropriate enzymes and buffers. Four different salt concentrations were used:- 0, 50, 100, 150 mM NaCl all in 10 mM Tris-HCl, 10 mM $MgCl_2$ and 1 mM Dithiothreitol (DTT). For the enzyme *SmaI*, 20 mM KCl was substituted for NaCl.

As a general rule no more than 2 μg of DNA was digested in a 25 μl reaction volume

Electrophoresis of Nucleic Acids

Agarose gels were run as described in Sambrook *et al.*, (1989). Nucleic acid samples were electrophoresed through 0.8-2.0% agarose melted in Tris-acetate buffer (TAE); a 50x stock contains:- 242 g Tris-base, 57 ml glacial acetic acid and 100 ml

0.5 M Ethylenediaminetetraacetic acid disodium salt (EDTA, pH 8.0) per litre. DNA samples had loading buffer (10x stock contains 0.25% w/v bromophenol blue, 0.25% w/v xylene cyanol and 25% w/v Ficoll-400) added prior to their being electrophoresed in horizontal submarine gels. Gels were stained with ethidium bromide (5 μg/ml in TAE) for 5 minutes, and DNA bands were visualized using an Ultra-violet (U.V) transilluminator. Photographs were taken using Polaroid type 665 or type 667 film.

Purification of DNA fragments

The protocol was based on Vogelstein (1979). DNA fragments of below 6 kilobases (kb) were extracted with powdered glass from either high or low melting point agar gels run in TAE. Powdered Flint glass, 325 mesh, was a gift from Dr. R. Krumlauf. 1 ml of the glass was suspended in 2 ml of H_2O, stirred well and allowed to settle for 1 hour. The supernatant was centrifuged at 6,000 x G for 10 minutes and the pellet resuspended in 2 ml of H_2O and 2 ml of concentrated Nitric acid. This was boiled for 5 minutes and then centrifuged. The clean glass was resuspended in H_2O and the pH measured. This process was repeated until the pH reached 7. The glass milk was stored at 4°C as a 50:50 v/v solution in H_2O containing 0.01% Sodium azide (NaN_3).

DNA bands were stained with ethidium bromide and relevant band(s) were excised and the volume estimated. 2x the volume of 90% w/v NaIodide containing 0.5% w/v Na_2SO_3 was added. This was incubated at 37°C for 15 minutes, until the gel had dissolved. Approximately 1 μl of glass slurry per μg of DNA to be recovered was added, and this solution was incubated on ice for 1 hour with occasional gentle mixing. DNA bound to the glass powder was pelleted by centrifuging for 5 seconds

at 6000 x G and the glass pellet was washed at least 3x in wash buffer at -20°C (50% v/v ethanol in 0.1 M NaCl, 10 mM Tris-HCl (pH 7.5), 1 mM EDTA). Finally the glass pellet was resuspended in a suitable volume (eg. 10 μl) elution buffer at 37°C for 15 minutes. The glass was removed by centrifuging at 11,000 x G for 5 minutes and the supernatant containing the extracted DNA was removed and stored for future use.

Ligation of DNA

Ligation reactions usually contained ~50 ng of vector DNA and a 4-fold molar excess of the fragment to be inserted. In the case of blunt end ligations this molar ratio was raised to 10 x. Ligations were incubated at 14°C for at least 6 hours with 1 unit per reaction of T4 ligase in ligase buffer. 10x stock contained: 500 mM Tris-HCl (pH 7.5), 100 mM $MgCl_2$, 100 mM DTT, 10 mM Spermidine, 10 mM Adenosine Tri-Phosphate (ATP) and 1 mg/ml Bovine Serum Albumin (BSA). Competent bacteria were transformed with the ligation products and were grown on agar plates, containing either AMP or TET at 37°C overnight.

Screening of bacterial colonies

Two methods were used depending on the number of colonies to be tested. If there were few colonies they were screened by small scale plasmid preparations, in cases where there were numerous colonies they were screened using the colony lift hybridization protocol.

a. Small scale Plasmid preparation.

Individual colonies from transformed bacteria were grown overnight at 37°C. 1.5 ml was removed and the bacteria pelleted at 11,000 x G for 2 min. The pellet was resuspended in 100 μl of 50 mM Tris-HCl, pH 8.0; 10 mM EDTA; 50 mM Glucose and incubated at 20°C for 5 minutes before adding 200 μl of 0.2 M NaOH; 1% w/v SDS and placing on ice for 10 min. 150 μl of 3 M Potassium acetate; 2 M Acetic acid, pH 4.5 was added and the samples were incubated on ice for a further 5 min, the solution was spun at 11,000 x G for 5 min, the supernatant removed and centrifuged again for a further 5 min. Plasmid DNA was then precipitated by addition of 1 ml of 95% ethanol.

b. Colony lift hybridization protocol.

This protocol is an adaptation of Southern blotting (Sambrook *et al.*, 1989). A sheet of Gene Screen Plus paper (New England Nuclear) was placed on the bacterial colonies growing on agar plates for 2 minutes and gently removed. The blot was then incubated for 5 minutes, colony side uppermost, on 3MM filter paper (Whatman Ltd) soaked in 10% w/v SDS, then transferred onto 3MM paper soaked in 1.5 M NaCl, 0.5 M NaOH for 5 minutes and finally onto 3MM paper soaked in 1.5 M NaCl, 50 mM Tris-HCl (pH 8.0) for a further 5 min. The blot was then baked at 80°C for 2 hours then washed in 50 mM NaOH for 5 minutes and followed by 2 washes in 1.5 M NaCl, 50 mM Tris-HCl (pH 8.0). The blot was incubated for 1 hours at 50°C in 10 ml of hybridization buffer which contains 1 ml of 100x Denhardts solution (2% w/v Ficoll-400, 2% w/v polyvinylpyrolodone and 2% w/v BSA), 0.5 ml of freshly boiled salmon sperm DNA (5 mg/ml) and 3 ml of 20x Sodium Citrate

buffer (SSC; 20x stock contains 3 M NaCl and 0.3 M NaCitrate, pH 7.5). ^{32}P labelled cDNA probes were then added to the blot plus hybridization mixture and incubated at 50 ° C overnight. Blots were washed in 2x SSC with 1% w/v SDS for 30 minutes at 65 ° C before wrapping in Saranwrap and exposing to pre-sensitized Kodak X-OMat X Ray film. Exposure times varied from 1 hour to overnight. Any positive clones were selected and grown individually for further characterization.

Large scale plasmid preparations

Plasmid DNA was prepared as described in the Promega Biological Research Products catalogue 1989. 250 ml of LB containing antibiotics (AMP or TET) was inoculated with 500 μl of an overnight culture of bacteria and grown overnight at 37 ° C with constant agitation. The bacteria were pelleted at 6,000 x G for 15 minutes at 4 ° C and resuspended in 6 ml of 25 mM Tris-HCl, pH 7.5; 10 mM EDTA; 15% w/v sucrose; 2 mg/ml lysozyme and incubated on ice for 20 minutes. Bacteria were lysed by adding 12 ml of 0.2 M NaOH; 1% w/v SDS, the solutions were gently mixed and incubated on ice for 10 minutes. 7.5 ml of 3 M sodium acetate (pH 4.6) was then added and the mixture incubated on ice for a further 10 minutes, before centrifuging at 10,000 x G for 15 minutes at 4 ° C. The supernatant was removed and 50 μl of RNaseA (10 mg/ml stock) added, this was incubated at 37 ° C for 20 minutes before extracting with phenol and chloroform and precipitating the DNA as previously described. The DNA pellet was dissolved in 1.6 ml of H_2O, to which was added 0.4 ml of 4 M NaCl and 2 ml of 13% w/v Polyethylene Glycol 6000 (PEG), the mixture was incubated on ice for 60 minutes and the plasmid DNA pelleted at 22,000 x G for 10 minutes. The DNA pellet was washed with 70% ethanol, air dried and dissolved in a suitable volume (eg. 100 μl) of 10 mM Tris-HCl, pH 7.5; 1 mM EDTA (TE).

The concentration of the DNA was estimated by reading the absorbance at A_{260}.

$$\text{Nucleic acid concentration(mg/ml)} = \frac{A_{260} \times \text{Epsilon} \times \text{Dilution factor}}{1000}$$

Epsilon is the extinction co-efficient for the absorbance of DNA at 260 nm. For double-stranded DNA at 20°C is 50 and for single stranded DNA or RNA is 40 (Sambrook *et al.*, 1989)

Oligo labelling of DNA probes

cDNA probes were labelled with ^{32}P to a specific activity of ~2 x 10^8 cpm/μg by random priming (Feinberg and Vogelstein, 1984). The labelling reaction was carried out at room temp by adding the following reagents in the stated order. H_2O to bring the final volume up to 50 μls, 10 μl of Oligo labelling buffer (OLB), 2 μl of BSA (DNase free), 10-50 ngs of cDNA to be labelled (boiled for 3 minutes and cooled to 37°C prior to use), 50 μCuries [^{32}P] dTTP and 2 units of *E.coli* DNA polymerase 1 (large fragment). The mixture was incubated at 20°C for between 4-18 hours, and the ^{32}P-labelled DNA was separated from unincorporated nucleotides by centrifugation through a sephadex G50 column at 500 x G for 30 seconds. The labelled double stranded DNA was denatured to single stranded DNA immediately prior to hybridization by addition of 50 μl of 10 N NaOH, immediately followed by 140 μl of 2 M Tris-HCl, pH.7.5 and 500 μl of 1 M HCl.

Oligolabelling buffer (OLB) was prepared by mixing solutions A:B:C in a ratio of 10:25:15.

Solution A: 1 ml of 1.25 M Tris-HCl, pH 7.5; 0.125 M $MgCl_2$ containing 18 μl 2-Mercaptoethanol (2-ME), 5 μl dATP, 5 μl dCTP and 5 μl dGTP (all triphosphates 0.1 M in TE, pH 7.5).

Solution B: 2 M Hepes pH 6.6

Solution C: $Pd(N)_6$ dissolved at 90 OD units per ml. This is the primer for the DNA polymerase and consists of 6 randomly coupled oligonucleotides.

The following cDNA probes were used in the Northern blot studies described in this thesis. The IGF-I probe used was a 530 bp *Pst*I-*Bam*HI fragment, containing the coding sequence of human IGF-I (Jansen *et al.*, 1983). The IGF-II probe was a 260 bp *Acc*I-*Pst*I fragment, containing the coding region of human IGF-II (Bell *et al.*, 1984). The PDGF-A chain probe was an ~800 bp *Rsa*I fragment containing the coding sequence of the human cDNA isolated by Betsholtz *et al.* (1986). The PDGF-B chain probe was an ~840 bp *Pst*I-*Avr*II fragment of plasmid pSM1 (Josephes *et al.*, 1984), containing the human c-*sis* coding sequence. The GFAP probe was an ~500 bp *Sac*I coding sequence fragment of plasmid G1 (Lewis *et al.*, 1984), which contains a mouse GFAP cDNA. The pyruvate kinase (PK) probe was an ~1600 bp *Pvu*II-*Apa*I fragment of plasmid pPK300 (Lonberg and Gilbert, 1983), which encodes chicken muscle PK. The actin probe used was a ~2000 bp *Pst*1 fragment of chicken ß-actin (Lawrence and Singer, 1985). The Platelet derived growth factor alpha receptor (PDGF-αR) probe used was an 870 bp *Eco*RI-*Pst*I fragment of rat PDGF-α receptor (Lee *et al.*, 1990) encoding the extracellular domain.

RNA extraction and analysis

Total cellular RNA was prepared from various tissues and cultured cells using lithium chloride-urea (Auffray and Rougeon, 1980). Total RNA extracted was enriched for poly(A) containing RNA by oligo(dT)-cellulose chromatography.

N.B. All glassware used was oven baked at 250°C for at least 4 hours, usually overnight. All solutions were Diethylpyrocarbonate (DEPC) treated prior to use (0.1% v/v DEPC was added, the solutions shaken and autoclaved, to destroy any remaining DEPC). Chemicals used were specifically set aside for RNA work only and rubber disposable gloves were worn at all stages of the protocol. Operations were carried out on ice, except poly(A) selection, which was carried out at room temp.

Tissue or cells were suspended in 6 M Urea and 3 M Lithium Chloride and homogenized using a Dounce homogenizer, approximately 10 ml of buffer was used per gram of tissue. The homogenate was incubated at 4°C overnight and then centrifuged at 10,000 x G for 30 minutes at 4°C. The pellet was resuspended in 5 ml of buffer containing 20 mM Tris-HCl (pH 7.5); 1 mM EDTA; 0.1% w/v SDS. This was phenol and chloroform extracted and the RNA precipitated as previously described. Total cellular RNA was pelleted at 10,000 x G and resuspended in 10 mM Tris-HCl, pH 7.5; 0.5 M NaCl. The A_{260} was measured and the final concentration of RNA was adjusted to less than 1 mg/ml. Poly (A) RNA was selected by oligo(dT)-cellulose chromatography. The total RNA recovered was run over a 2 ml oligo(dT) column at least 2x before washing the column extensively. The bound poly(A) RNA was eluted from the column in 10 mM Tris-HCl, pH 7.5. This poly(A) containing RNA was precipitated and air dried prior to dissolving in a suitable

volume of TE. The A_{260} was measured and samples were adjusted to a final concentration of 1 mg/ml and stored at -70°C until required.

Electrophoresis of RNA and Northern Blotting

RNA was electrophoresed and blotted as described by Sambrook *et al.*, (1989). 10-15 μg of Poly(A) RNA (determined by A_{260}) per track was incubated at 65°C for 3 minutes in MOPS buffer (10x stock: 42 g MOPS; 6.8 g NaAcetate; 3.8 g EDTA per litre, pH 7.0) containing 50% v/v formamide and 0.4 M formaldehyde. 1/10 of the sample volume of loading buffer (50% v/v glycerol, 1 mM EDTA, 0.4% w/v bromophenol blue [BPB] and 0.4% w/v xylene cyanol) was added and samples were electrophoresed at 75 volts in 1% agarose gels, (melted in 0.4 M formaldehyde in MOPS) until the BPB indicator dye had reached the bottom of the gel. RNA was transferred to Gene Screen Plus nitrocellulose paper (NEN, Dupont) by capillary blotting. After transfer the blot was washed in 10x SSC and then baked at 80°C for 2 hours. The remains of the gel were stained with ethidium bromide (5 μg/ml) in MOPS for 10 minutes and the remaining RNA visualized using a U.V. transilluminator. Positions of the 28s and 18s ribosomal RNA bands were noted. Blots were prehybridized for at least 1 hour in 6x SSC containing: 50% v/v Formamide; 0.4% v/v Denhardts; 10 mM EDTA, 1% w/v SDS, 0.1 mg/ml sonicated Salmon Sperm DNA (SS-DNA) and 5% w/v Dextran sulphate (Sodium salt). The ^{32}P-cDNA probe was denatured as previously described and added to this mixture. The hybridization mixture was incubated at 45°C for a minimum of 12 hours before washing the blots in 2x SSC, 1% w/v SDS at 65°C for 2 x 30 minutes periods (for higher stringency washes the blots were washed in 0.5x SSC at 65°C). Blots were exposed to pre-sensitized Kodak X-Omat film at -70°C with tungsten intensifying screens. Developing times varied from a few hours to three to four weeks.

***In Situ* hybridization.**

In situ hybridization was performed as described by Lawrence and Singer (1985), with minor modifications as described in the following protocol.

Optic nerves were dissected from neo-natal (embryonic day 17), Newborn (postnatal day 0), P7 or adult Wistar rats. Brains were dissected from rats at postnatal ages and whole heads and embryos were used for embryonic animals. To time the pregnancies, female rats were caged with males overnight and then removed: this was taken as day zero of the pregnancy. Embryos of approximately the right ages were then dated by the morphological criteria described by Long and Burlingame (1932), two to three animals from each litter were examined at each age.

Optic nerves were fixed for 2 hours in 4% w/v paraformaldehyde in phosphate buffered saline (PBS, contains per litre: 8 g NaCl; 0.2 g KCl; 0.1 g $CaCl_2$, 0.1 g MgCl; 1.15 g Na_2HPO_4; 0.2 g KH_2PO_4) followed by 2-3 hours incubation in 0.5 M sucrose in PBS. Whole embryos, heads and brains were fixed for 24 hours followed by 24 hours in 0.5 M sucrose in PBS. Tissues were immersed in OCT embedding compound and frozen rapidly in an aluminium foil boat floated on liquid N_2. Tissue was stored desiccated at -70°C until required.

Frozen sections were cut (10-15 μm nominal thickness) on a cryostat and were collected on freshly prepared poly-L-lysine-coated glass microscope slides. (RNase free glass microscope slides were soaked for 30 minutes in sterile poly-L-lysine at 50 μg/ml in H_2O, air dried and used within 1 week of preparation.)

Sections were dried for 2 hours at 20°C and fixed in 4% paraformaldehyde for 15 minutes. Basic proteins were removed by incubating in 0.2 M HCl for 30 minutes at 20°C and then in 2x SSC for 30 minutes at 70°C. Sections were then incubated in a 0.125 mg/ml solution of predigested pronase, for 20 minutes at 20°C.

The digestion was arrested by rinsing for 30 seconds in PBS containing 0.2% w/v glycine followed by several washes in PBS. At this point control sections were treated with RNase-A, 100 μg/ml in TE and 0.5 M NaCl, for 1 hour at 37°C. All sections were post-fixed in 4 paraformaldehyde in PBS for 15 minutes at 20°C, then acetylated for 10 minutes at 20°C in a freshly prepared solution of 25 mM acetic anhydride in 0.1 M triethanolamine (pH 8.0). Sections were washed briefly in PBS and dehydrated in a series of ascending concentrations of ethanol (1 minute each in 30, 60, 80, 95, 100% v/v ethanol/water). Slides were allowed to dry before prehybridizing with non-radioactive α-thio UTP at 500 nM (Bandtlow *et al.*, 1987), in hybridization buffer (containing 0.3 M NaCl; 10 mM Tris-HCl, pH 6.8; 5 mM EDTA; 0.02% w/v Ficoll 400; 0.02% w/v polyvinylpyrolidone (PVP); 0.02% w/v BSA (Sigma fraction V); 0.1 mg/ml yeast tRNA; 10 mM dithiothreitol (DTT); 50% deionized formamide. Incubation was for 4 hours at 50°C. Slides were then washed briefly in 2x SSC for 15 minutes and were dehydrated through an ascending series of ethanols, before air drying and hybridization with RNA probes for at least 18 hours at 50°C.

Preparation of ^{35}S-labelled RNA probes.

cDNA of interest was cloned into either pGEM1 or pGEM3 vectors (Promega Biotec). These vectors contain initiation sequences for bacterial RNA polymerases, SP6 and T7, located adjacent to the multi-site cloning region. Details of the cloning are as follows:-

A 681 bp *Sac*I-*Hind*III fragment encompassing most of the coding region of a human PDGF-A chain cDNA (Betsholtz *et al.*, 1986) was cloned into plasmid pGEM3.

A 839 bp *Pst*I-*Avr*II coding region fragment of a human PDGF-B chain cDNA (Josephs *et al.*, 1984) was subcloned into pGEM1 (Promega).

A 12,00 bp *Hind*III-Kpn*I* coding fragment of a mouse GFAP cDNA (Lewis *et al.*, 1984) was subcloned into pGEM3.

A 870 bp *EcoR*I-*Pst*I fragment of rat PDGF-α receptor, which contains the region encoding the extracellular domain of the receptor (Lee *et al.*, 1990), was subcloned into pGEM1.

Single-stranded RNA probes were generated by *in vitro* transcription as described by Cox *et al.*, (1986). Using bacteriophage T7 or SP6 RNA polymerases (obtained from Promega), α[^{35}S]-thiotriphosphate (1300 Ci/mM) (α[^{35}S]-UTP), and linear DNA templates, ^{35}S-labelled "sense" or "antisense" RNA run-off transcripts (2x 10^8 cpm/μg) were generated *in vitro*. Reaction conditions were as described by Promega, using 1 μg of linear plasmid DNA in a total reaction volume of 20 μl; containing 4 μl of 5x reaction buffer (200 mM Tris-HCl, pH 7.6; 30 mM $MgCl_2$; 10 mM spermidine; 50 mM NaCl), 2 μl of 100 mM DTT, 0.8 μl RNasin (Promega, 25 units/μl stock), 4 μl of ATP, GTP, CTP (stock solution contains all 3 ribonucleotides at 2.5 mM.), 2.4 μl of UTP (non-radioactive stock at 100 μM.), 5 μl of Uridine α[^{35}S]UTP. 20 units of SP6 or T7 polymerase were added per reaction which were incubated at 37 °C. After 30 minutes an additional 20 units of either SP6 or T7 was added and the reaction allowed to proceed for a further 30 minutes. After this time 1 unit of DNase I (Pharmacia, RNase free) was added and the reaction allowed to proceed for an additional 15 minutes. 3 M Sodium acetate was added to a final concentration of 0.3 M and the RNA transcripts were precipitated. Efficiency of incorporation of α-[^{35}S]UTP into the probe RNA was calculated by binding to

GF/C glass microfibre filters (Whatman). 0.5 μl of probe was added to 500 μl of 10% w/v NaH_2PO_4, 50 μl was applied to each GF/C filter. Half of the filters were washed in 500 ml of 10% w/v NaH_2PO_4 at 20°C for 2 minutes to remove unincorporated radioactivity. Filters were dried before immersing in Optiscint scintillation fluid (LKB Ltd.) and counted in a ß-counter. The incorporation efficiency was usually between ~30-50%.

The full length transcripts were reduced in size by limited alkaline hydrolysis, to an average size of 150 bp. The transcripts were resuspended in 50 μl of 10 mM DTT and 50 μl of 100 mM carbonate buffer pH 10.2 (Na_2CO_3:$NaHCO_3$, 6.5:3.5), and were incubated at 60°C for ***X*** minutes.

X minutes was determined by:- $\frac{Lo - Lf}{KLoLf}$

Where:-

Lo = Original transcript length in Kb.

Lf = Final transcript length in Kb.

K = 0.1

Alkaline digestion was halted by adding 100 μl of neutralisation buffer (0.2 Sodium acetate pH 6.0; 1% glacial acetic acid; 10 mM DTT). The digested probes were ethanol precipitated and the sizes of transcripts generated (both full length and digested) were estimated by comparison to DNA size markers on formaldehyde-containing agarose gels. (see Northern blotting). Probes were dissolved in 10 mM DTT, 50% Formamide to a final concentration of 1 ng/μl/kb (10x stock),and were stored at -20°C until required.

^{35}S-labelled probes were heated for 5 minutes at 80°C in hybridization buffer, chilled briefly on ice and 10-25 μl of this solution was applied to each slide, a siliconized glass coverslip was placed over the top. The slides were incubated in a humid chamber for 18-24 hours at 50°C. Coverslips were removed by submerging in hybridization buffer for 30 minutes at 50°C; sections were washed in the same buffer at 50°C for a further hour and then at 65°C for 30 minutes. Non specific ^{35}S-labelled probe binding was removed by digestion with RNase A (20 μg/ml) for 30 minutes at 37°C in 0.5 M NaCl in TE. Finally the slides were washed for 30 minutes at 45°C in 2x SSC, then 30 minutes at 45°C in 0.1x SSC. The sections were dehydrated through ascending concentrations of ethanol, containing 0.25 M ammonium acetate, and air dried. For autoradiography, the slides were coated with Ilford K5 nuclear emulsion, and exposed for between 1-4 weeks in the dark at 4°C. After developing in Kodak D-19 for 2 minutes, and fixing in 30% w/v Sodiumthiosulphate for 5 minutes, the sections were counter stained in 0.02% w/v toluidine blue, dehydrated in ethanol, cleared with xylene and mounted for examination by bright-field and dark-field microscopy.

In Situ hybridization of cultured cells lines was performed essentially as described above, but using much shorter incubation times: 10 minutes fixation steps in 4% w/v paraformaldehyde, 5 minutes extraction in 0.2 M HCl followed by 10 minutes in 2x SSC at 70°C, 5 minutes in pronase (40 μg/ml). Hybridization and initial washes (i.e. prior to RNase treatment) were at 37°C instead of 50°C and 65°C.

Cell counts in brain and optic nerve sections

The proportion of cells in the CNS that are PDGF-αR$^+$ was estimated from pairs of bright- and dark-field micrographs of lightly-stained sections of anterior

hypothalamus or optic nerves. Micrographs were printed at approximately 50x final magnification. PDGFαR$^+$ cells were counted in dark field, and the total number of cell nuclei in bright field. At least three pairs of micrographs from different sections of one animal were counted at each age. Approximately 500 total cells were counted in each section and the proportion of PDGF-αR$^+$ cells (mean percent ± standard deviation) tabulated (Table 2). These numbers are likely to be minimum estimates, as PDGF-αR$^+$ cells frequently occur in pairs and it is difficult to resolve these pairs under dark field illumination. Neither the density of PDGF-αR$^+$ cells nor total cell density varied significantly throughout the hypothalamus at each age, so the figures we obtained were not critically dependent on the precise region of hypothalamus examined. Nevertheless, the numbers in Table 2 are only approximate estimates, intended merely to illustrate how the PDGF-αR$^+$ cell population increases in the hypothalamic region during development. The estimates of cell numbers in optic nerve have a higher confidence level because counts were made at different positions along the length of the nerve in order to minimise systematic errors that might be caused by regional variations in cell density, which at any rate appeared to be insignificant after P2.

TISSUE CULTURE, IMMUNOFLUORESENCE AND ^{125}I-PDGF BINDING

Media and culture solutions

Foetal calf serum (FCS) and new born calf serum (NCS) were obtained from Gibco-BRL.

Dulbecco's modified Eagles medium (DMEM), and HEPES buffered minimal essential medium, (MEMH), 0.25% w/v trypsin (Difco 1:250) in Tris saline

(10 mM TRIS-HCl and 0.7% w/v NaCl pH 7.2) and 0.02% w/v versene (EDTA) in PBS were all obtained from the Imperial Cancer Research Fund, Clare Hall, London.

Specialist ingredients used for astrocyte and O-2A progenitor cell primary cultures were obtained from Sigma.

Sterile disposable tissue culture vessels were obtained from Falcon laboratories ltd.

Established Cell lines

A7-6-3. A rat cell line isolated from optic nerve cells growing on a monolayer of type-1 astrocytes, infected with a retrovirus carrying the large T gene of simian virus 40. From the resultant mixture of transformed cells, a series of clonal lines was derived, including A7-6-3. They were kindly provided by M. Dubois-Dalc.

C6. A rat glioma cell line derived from a chemically induced brain tumour (Benda *et al.*, 1968).

157 and 328. These are both human glioma cell lines isolated from autopsy material. They were kindly provided by Dr. M. Noble.

SIS-NRK. A simian sarcoma virus transformed normal rat kidney cell line, a kind gift from Dr. P. Stroobant.

Swiss 3T3. A mouse fibroblast cell line, obtained from ICRF.

L-cells. A mouse fibroblast cell line which produces colony stimulating factor 1 (CSF-1), a macrophage mitogen, was a kind gift from Dr. H. Stauss.

All these cell lines were adherent and were grown in Falcon 75 cm^2 flasks in DMEM medium containing 5% v/v NCS at 37°C in a 5% CO_2/95% air atmosphere. Cells were passaged by replacing the medium with 0.25% trypsin solution and incubating at 37°C until the cells had detached from the surface of the flask. Cells were pelleted at 1500 x G for 5 minutes, resuspended in fresh medium and plated out into new flasks. Cell stocks were kept frozen under liquid N_2 in 90% NCS/10% dimethylsulphoxide (DMSO). Conditioned medium from L-Cell cultures, which contains CSF-1, was removed and stored frozen before supplementing the medium used to grow macrophages.

Astrocyte and meningeal cultures

Cultures of type-1 astrocytes from neonatal rat cerebral cortex were established by a modification of the method of McCarthy and de Vellis (1980). Neonatal rat pups (~2 days old) were killed and the brain removed. The cerebral cortex was dissected out and the surrounding meninges was removed and cultured separately. The cortex and meninges were finely chopped (separately) and placed in 10 ml of DMEM containing 0.025% trypsin. After incubating at 37°C for 30 minutes, cells were pelleted at 1,500 x G for 10 minutes, resuspended in 4 ml DNase (40 μg/ml) and SBTI (0.52 mg/ml) and triturated for 20 cycles using a pasteur pipette. Cells were again pelleted at 1500 x G for 10 minutes then resuspended in DMEM + 10% FCS and plated out into 75 cm^2 flasks. The medium was changed after 24 hours and the cells were grown at 37°C until confluent. Meningeal cultures were passaged (1 flask to 4) and when these 4 flask had become confluent the medium

was replaced with 0.25% trypsin solution. When the cells had detached they were pelleted by centrifuging at 1,500 x G for 10 minutes and used to make RNA.

Confluent astrocyte cultures were vigorously agitated overnight at 37°C (180 revolutions/minute on a horizontal rotating platform), this process removes all the loosely adherent cells in the flask. Fresh medium containing cytosine arabinoside at 10^{-5} M was added, to preferentially kill rapidly dividing cells i.e. fibroblasts. After 24 hours the medium was removed and replaced with DMEM + 10% FCS only, and the cells grown for a further 48 hours. After this period the cells were passaged (1 flask into 4). Finally when cultures became confluent they were harvested for RNA preparation. To assess the purity of the culture some astrocytes were grown on coverslips and stained with antibodies against glial fibrillary acidic protein (GFAP), an astrocyte specific marker (Eng *et al.*, 1971). Cultures were routinely between 96-98% $GFAP^+$ (see immunofluorescence).

O-2A progenitor cultures

The cultures of purified brain O-2A progenitors used in the binding studies detailed in this thesis (see table 3) were kindly prepared for me by Dr. E. Collarini. A brief outline of the methods used by her follows:-

Purified O-2A progenitor cultures were established by a modification of a method developed by B. Barres and E. Collarini (Barres *et al.*, 1992; Collarini *et al.*, 1992). Cultures of cells from neonatal rat cerebral cortex were established as described above. Instead of agitating the cultures as above, they were trypsinized and the cell suspension depleted of astrocytes and macrophages by incubating on Petri-dishes coated with anti-RAN-2 antibody (Bartlett *et al.*, 1981). Oligodendrocytes were removed on dishes coated with anti-galactocerebroside (GC) (Raff *et al.*, 1978; Ranscht *et al.*, 1982). O-2A progenitors were positively selected on

dishes coated with antibody A2B5 (Eisenbarth *et al.*, 1979). O-2A progenitors were trypsinized from the A2B5 dishes and grown in 24-well dishes in our modification of Bottenstein and Sato's (BS) defined medium (Richardson et al., 1988), supplemented with 0.5% FCS, PDGF-AA and bFGF (Peprotech recombinant growth factors, 10 ng/ml each). O-2A progenitors were grown until confluent and used for ^{125}I-PDGF binding studies (see ^{125}I-PDGF binding studies). The final cultures were at least 96% A2B5^{+}GC^{-} O-2A progenitors (see immunofluorescence).

Microglial cell cultures

Cultures of microglial cells (the macrophages of the CNS) were established from rat brains by a modification of the method of Giulian and Baker (1986). Neonatal rat brains were dissected and the meninges removed. The brains were finely diced using scissors and enzymatically dissociated with papain (33 units/ml in MEM-H). The papain was activated with L-cysteine (0.3 mg/ml) and titrated to pH 7.0 before adding to the diced brain. Enzymatic dissociation was allowed to proceed at 37°C for 90 minutes. The papain was inactivated with 10 ml of MEM-H containing 100 μl of DNAse (4 mg/ml), 20 mg of Trypsin Inhibitor (obtained from Boehringer Mannheim which contains ovomucoid, a papain inhibitor) and 20 mg of BSA. The lumps were allowed to settle and the supernatant removed. 1 ml of inhibitor solution was added and the mixture was triturated until the lumps had broken up (approximately 10x). The cell suspension was filtered through a fine gauze and plated onto Petri dishes coated with IgM (to retain cells carrying Fc receptors) for 20 minutes at 20°C. Petri dishes were coated with IgM overnight at 4°C by incubating IgM at 2 mg/ml in Tris-HCL, pH 9.0. Dishes were washed 3x with MEM-H before applying the cell suspension. The adherent microglia were trypsinized from the dishes in Ca^{2+} and Mg^{2+} free DMEM, containing 0.25% trypsin, for 10 minutes

at 37°C and the cells pelleted at 1500 x G for 10 minutes. Microglia were grown in 24-well dishes in DMEM/FCS supplemented with 25% mouse L-cell conditioned medium (which contains CSF-1, a macrophage mitogen). When the cells were semi-confluent they were used for ^{125}I-PDGF binding studies as described below. The purity of the microglial cultures was assessed by staining with *Bandeiraea simplicifolia* B_4-lectin (BL) (Sigma), which labels microglia in the CNS (Chugani *et al.*, 1991). Cultures were greater than 98% BL^+.

Immunofluorescence

Astrocytes

Astrocytes grown on coverslips were fixed for 15 minutes in ethanol at -20°C and rehydrated by washing 5 x in MEMH. Cells were incubated in rabbit anti-GFAP (Eng *et al.*, 1971), diluted 1/100 in MEM + 10% NCS for 30 minutes at 20°C. Fluorescein-iso-thio-cyanate (FITC) conjugated goat anti-rabbit antibody (Amersham international) diluted 1/100 in MEM + 10% NCS, was added and the cells incubated and washed as before. Coverslips were mounted in glycerol containing 0.1% triethylenediamine to prevent fading and were examined using an Olympus inverted fluorescent microscope.

O-2A progenitor cultures

Cultures grown on coverslips were prefixed in 2% w/v paraformaldehyde in MEMH for 20 minutes at 20°C. The cells were then incubated in a mixture of mouse monoclonal antibodies A2B5 (IgM; Eisenbarth *et al.*, 1979) and anti-

galactocerebroside (Ig3; Raff *et al.*, 1978) both diluted 1/100, followed by a mixture of rhodamine-labelled rabbit anti-mouse-IgM and fluorescein-labelled rabbit anti-mouse-Ig3 class specific antibodies (Nordic) both diluted 1/100. Cells were washed and post-fixed in 4% w/v paraformaldehyde in PBS for 5 minutes before mounting for fluorescent microscopy as previously described.

Macrophages

Cultures grown on coverslips were incubated with FITC-labelled *Bandeiraea simplicifolia* B_4-lectin (BL) (Sigma), which labels microglia in the CNS (Chugani *et al.*, 1991), at 4°C for 4 hours. Cells were washed and post-fixed in 4% paraformaldehyde before mounting for fluorescent microscopy as previously described.

^{125}I-PDGF binding

^{125}I-labelled PDGF-AA and ^{125}I-labelled PDGF-BB homodimers were a kind gift from Dr.C.Heldin and had specific activities of ~27,000 cpm/ng. Cultures of cells grown in 24-well linbros were incubated for 24 hours in MEM containing 0.5% FCS (O-2A progenitors were grown in Satos, 0.5% FCS, supplemented with insulin at 50 ng/ml). Cultures were washed in MEMH before incubating with ^{125}I-PDGF-AA or ^{125}I-PDGF-BB at 33 ng/ml in MEMH containing 0.1% w/v BSA; with or without a 100-fold excess of unlabelled PDGF-AA or PDGF-BB. Samples were incubated for 6 hours at 4°C. Binding was terminated by washing 3 x in MEMH + 0.1% w/v BSA at 4°C. Cells were then lysed in PBS + 1% v/v Triton X-100 for 30 minutes at 20°C. Samples were counted on a γ-counter for 1 minute per sample.

CHAPTER 3

EXPRESSION OF PLATELET DERIVED GROWTH FACTOR AND INSULIN-LIKE GROWTH FACTORS IN THE RAT CNS AND CELL LINES.

INTRODUCTION

The rat optic nerve has been a popular and fruitful tissue for studies of gliogenesis in the CNS. Vertebrate optic nerves are comprised mainly of macroglial cells. Other cell types present are endothelial cells of the blood vessels and microglial cells (the macrophages of the CNS). The axons of retinal ganglion neurons pass through the nerve, but their cell bodies reside in the retina. In cultures of perinatal rat optic nerve cells, three types of postmitotic macroglial cells can be distinguished by their morphology and antigenic phenotype: Oligodendrocytes are process-bearing cells with small cell bodies, and express the ganglioside galactocerebroside (GC) on their surface (Raff *et al.*, 1978; Ranscht *et al.*, 1982). Type-1 astrocytes are flat cells that express glial fibrillary acidic protein (GFAP) and rat neural antigen-2 (Ran-2) (Bartlett *et al.*, 1981). Type-2 astrocytes appear as multi-processed cells expressing GFAP and A2B5 (Eisenbarth *et al.*, 1979). Type-1 astrocytes develop from one type of precursor cell (Raff *et al.*, 1984), while oligodendrocytes and type-2 astrocytes develop from a different, bipotential progenitor cell known as the O-2A progenitor which expresses A2B5, but not GC, Ran-2 or GFAP (Raff *et al.*, 1983). *In vivo* oligodendrocytes myelinate the axons in the nerve and type-1 astrocytes extend processes to the pial surface, to blood vessels (Miller *et al.*, 1989a) and, in some cases, to nodes of Ranvier (Suarez and Raff, 1989). Much less is known about type-2 astrocytes *in vivo*, largely because the antibodies that have helped to identify them in culture do not do so in tissue sections (Miller *et al.*, 1989a). Thus it is not certain what type-2 astrocytes look like in the intact CNS or even whether they exist *in vivo* (reviewed in Richardson *et al.*, 1990).

O-2A progenitors are thought to migrate into the optic nerve from germinal zones in the brain (Small *et al.*, 1987). Small numbers of O-2A progenitors are found in the nerve by E15. The O-2A progenitors proliferate for several weeks afterwards (Skoff *et al.*,1976). Some begin differentiating into oligodendrocytes starting on the

day of birth (Miller *et al.*, 1985), while others continue to divide. Thus O-2A progenitor cell proliferation and differentiation continue side-by-side in the optic nerve for several weeks after birth.

When dissociated embryonic optic nerve cells are cultured in defined medium, the normal timing of oligodendrocyte development *in vivo* is disrupted and the O-2A progenitor cells stop dividing prematurely and differentiate into oligodendrocytes within 48 hours (Raff *et al.*, 1985). Normal timing of oligodendrocyte differentiation is restored by a factor(s) secreted by cultured cortical astrocytes. When O-2A progenitor cells are cultured on a monolayer of cortical astrocytes or in astrocyte conditioned medium they continue to divide and first give rise to oligodendrocytes *in vitro* on a time schedule that is equivalent to the day of birth (Raff *et al.*, 1985). Proliferation and differentiation into oligodendrocytes continues for several weeks in culture, just as *in vivo* (Noble and Murray, 1984; Raff *et al.*, 1985; Dubois-Dalcq, 1987). Cortical astrocytes seem to provide a factor(s) that both stimulates O-2A progenitors to divide and prevents their premature differentiation into oligodendrocytes in culture. It was therefore important to identify and characterise this factor.

To investigate growth factor(s) produced by cortical astrocytes I looked for the presence of growth factor mRNA transcripts in poly(A)-containing mRNA isolated from primary cortical rat astrocytes (cortical astrocytes are thought to be equivalent to the type 1 astrocytes of the optic nerve; they have a similar flat morphology *in vitro*, and also express GFAP and Ran-2). I also examined poly(A) mRNA isolated from a variety of glial cell lines and rat brains of different ages for growth factor transcripts. I decided to screen for growth factors which had already been demonstrated to have an effect on glial cells *in vitro*. Three such growth factors were chosen, IGF-I, IGF-II and PDGF. McMorris *et al.* (1986) had shown that addition of insulin or IGF-I to primary cultures of rat cerebrum increased the numbers of oligodendrocytes forming in these cultures suggesting that IGF-I or insulin was

acting, either directly or indirectly on oligodendrocyte formation. IGF-II was included in the initial screen as it can also activate IGF-I receptors (Gammeltoft *et al.*, 1985). PDGF is frequently expressed at high levels in human gliomas (Eva *et al.*, 1982; Betsholtz *et al.*, 1986) suggesting a possible role for PDGF in the control of normal glial cell growth. PDGF consists of either a homodimer or a heterodimer of A-and/or B-chain polypeptides that are encoded by homologous but separate genes located on human chromosome 7 (Betsholtz *et al.*, 1986) and 22 (Dalia Favera *et al.*, 1982; Swan *et al.*, 1982). The majority of PDGF isolated from human platelets consists of heterodimers of A and B chains (Hammacher *et al.*, 1988), but homodimers can also form. For instance, PDGF isolated from porcine platelets resembles a homodimer of B chains (Stroobant and Waterfield, 1984), while some osteosarcomas and glioma cell lines secrete AA homodimers (Heldin *et al.*, 1986; Nistér *et al.*, 1988). Therefore I screened for both A-chain and B-chain transcripts.

The results of my investigations into determining the presence of IGF-I, IGF-II, PDGF-A and PDGF-B chain mRNAs in cortical astrocytes, glial cell lines and rat brain are presented in this chapter.

RESULTS

IGF-I mRNA is expressed in rat brain and cortical astrocytes.

I prepared poly(A)-containing RNA from rat brains of various ages, from embryonic day 15 (E15) to postnatal day 12 (P12). After separation on formaldehyde agarose gels I blotted the mRNAs onto nylon membrane and probed for transcripts encoding IGF-I using a human coding region IGF-I probe (Figure 6). I also reprobed the same blot for pyruvate kinase (PK) mRNA to control for sample loadings. At E15, major IGF-I transcripts of ~7.1 and 1.9 kb were present, as were minor transcripts at ~3.4 and 3.8 kb (Figure 6, denoted by arrows). The transcript visible between the ~3.8 and 7.1 kb transcripts coincides with the 28s ribosomal band, and probably represents non-specific hybridization to this. The ~7.1 kb transcript is only expressed at E15, and is not detectable at any other ages (Figure 6). The ~1.9 kb transcript is strongly expressed at E15, but by E17 has decreased in intensity, whilst the levels of PK remain roughly the same (Figure 6). Subsequently the levels of the ~1.9 kb transcript remain at roughly constant levels until P12 (Figure 6). The minor ~3.8 and 3.4 kb transcripts are faintly visible from E15 to P3, and just detectable at E12.

Poly(A)-containing mRNA was prepared from cultured rat cortical astrocytes and treated as above before probing for IGF-I transcripts. A single transcript of ~1.9 kb was visible in these cells (Figure 7). No transcripts were observed in any other glial cells lines tested except for primary meningeal cultures, which also contained a similar ~1.9 kb transcript.

IGF-II mRNA is expressed in rat brain.

Poly(A)-containing mRNA was prepared from rat brains of different ages from E15 to P3 and used for northern blot analyses with a ^{32}P-labelled human probe

specific to IGF-II. I also reprobed the same blot for pyruvate kinase (PK) mRNA to control for sample loadings. At E15 a major transcript of ~4 kb was present, as were minor transcripts at ~1.5 and 2 kb (Figure 8). The ~1.5 and 2 kb transcripts were not detectable by E17 (Figure 8). The ~4 kb transcript appeared to decrease in intensity from E15 to E17, and remained at roughly constant levels until at least P3 (Figure 8). A fourth transcript of ~2.7 kb was first detected at E17 and remained thereafter until P3 (Figure 8).

The northern blot shown in figure 7 was stripped and reprobed for IGF-II transcripts. I was unable to detect any IGF-II transcripts in cortical astrocyte mRNA. Subsequent reprobing of this northern with a probe for actin mRNA revealed a single transcript at ~2.2 kb (data not shown) indicating that mRNA was still bound to the blot.

Figure 6. Time course of appearance of IGF-I mRNAs in rat brain.

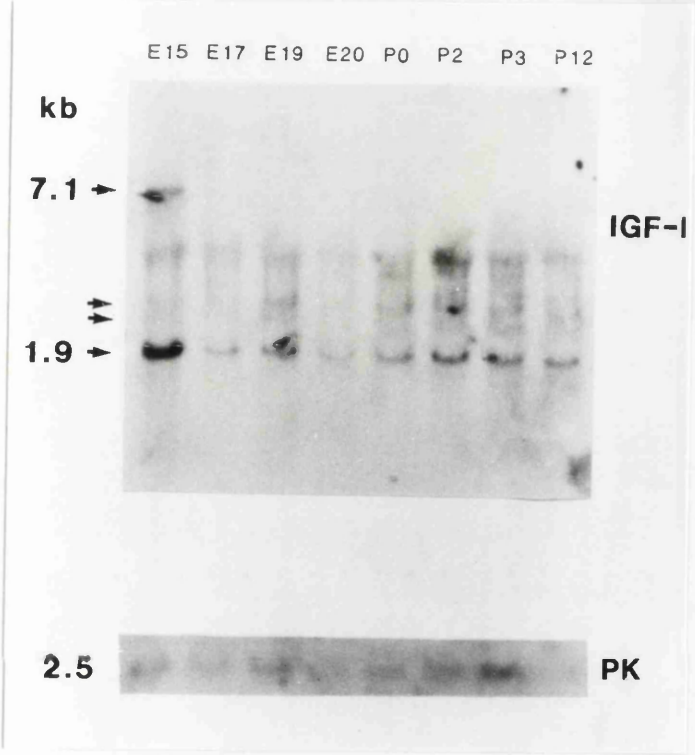

Poly(A)-containing RNA (10 μg/lane) from rat brains of various ages was electrophoresed on a 1% agarose gel containing formaldehyde, transferred to nylon membrane, hybridized with ^{32}P-labelled DNA probes specific for IGF-I. After autoradiographic exposure, the probe was removed by boiling, and the blot rehybridized with a probe specific for pyruvate kinase (PK) mRNA. mRNA transcripts of ~1.9, 3.4 and 3.8 kb are expressed from E15 until P12, whereas a ~7.1 kb transcript is only detected at E15. PK mRNA remains at roughly constant levels over the time period examined, and acts as a control for lane loadings.

Figure 7. IGF-I mRNA is expressed in cortical astrocytes.

Poly(A)-containing RNA (15 μg) isolated from cortical astrocytes was electrophoresed on a 1% agarose gel containing formaldehyde, transferred to nylon membrane and hybridized with ^{32}P-labelled probes specific for IGF-I. A single mRNA transcript of 1.9 kb was detected.

Figure 8. Time course of appearance of IGF-II mRNAs in rat brain.

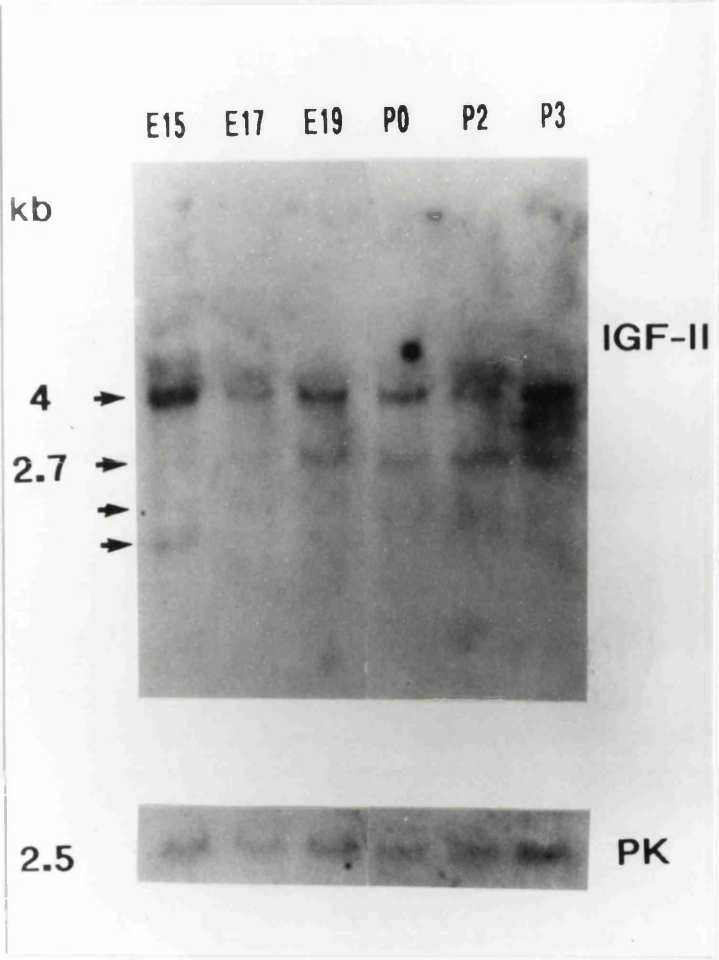

Poly(A)-containing RNA (10 μg/lane) from rat brains of various ages was electrophoresed on a 1% agarose gel containing formaldehyde, transferred to nylon membrane, hybridized with ^{32}P-labelled DNA probes specific for IGF-II. After autoradiographic exposure, the probe was removed by boiling, and the blot rehybridized with a probe specific for pyruvate kinase (PK) mRNA. mRNA transcripts of ~2.7, and 4 kb are expressed from E15 until P3, whereas transcripts of ~1.5 and 2 kb transcript are only detected at E15. PK mRNA remains at roughly constant levels over the time period examined, and acts as a control for lane loadings.

PDGF-A chain mRNA is expressed by cortical astrocytes *in vitro*

Poly(A)-containing mRNA was prepared from cultured rat cortical astrocytes and used for Northern blot analysis with ^{32}P-labelled DNA probes specific for PDGF-A or B chain. On the same blot, for comparison, I included equivalent quantities of poly(A) RNA from a variety of other rat and human cell types (meningeal cells, A7.6.3, C6, 157 and *sis*-nrk). The A chain probe, a human cDNA (isolated by Betsholtz *et al,*. 1986), hybridized with mRNA transcripts from all the cell types examined, including type-1 astrocytes and meningeal cells (Figure 9). The human glioma line 157 (lane 6) contains high levels of A chain mRNAs at ~1.9 kb, 2.3 kb, and 2.9 kb, as described for other human gliomas (Betsholtz *et al.*, 1986). A7-6-3, an SV40-large-T transformed rat CNS-derived cell line obtained from M. Dubois-Dalcq, and C6 (a rat glioma line, Benda *et al.*, 1968), both contain a single major PDGF-A chain transcript of ~1.9 kb, plus other minor species (lane 4 and 5). Primary rat cortical astrocytes (lane 3) and meningeal cells (lane 2) contain a similar ~1.9 kb transcript, present at levels comparable to that in A7-6-3. mRNA from 3 day old rat brain (lane 1) also contains a ~1.9 kb transcript, and additional transcripts similar in size to the 2.3 kb and 2.9 kb human transcripts. Astrocytes also contain very small amounts of a ~3.5 kb transcript that hybridized with the B chain probe, a fragment of the human B chain (c-*sis*) coding sequence (Josephs *et al.*, 1984). Trace amounts of an RNA of the same size may also have been present in A7-6-3 cells, but nothing could be detected in meningeal cells (Figure 9, lane 8). As a positive hybridization control for B chain I included RNA from the SSV-transformed rat cell line, sis-NRK (obtained from P.Stroobant, Ludwig Institute for Cancer Research, London). This cell line contains two very abundant transcripts at ~2 kb and 3 kb, and other less abundant transcripts (Figure 9, lane 7).

Figure 9. PDGF-A and B chain mRNAS in Various CNS-Derived cell Types

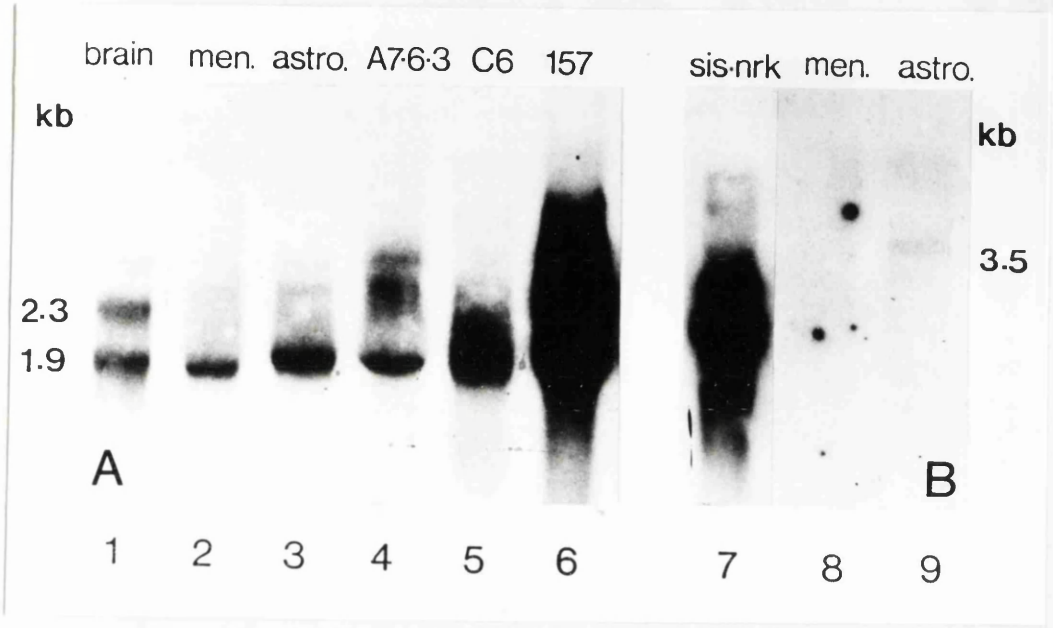

Poly(A)-containing RNA (15 μg/lane) was electrophoresed on a 1% agarose gel containing formaldehyde, transferred to nylon membrane, hybridized with ^{32}P-labelled DNA probes specific for PDGF-A or B chain, and autoradiographed. Left panel: A-chain probe. RNA from the following sources: Lane 1, P3 rat brain. Lane 2, cultures of primary meningeal cells from neonatal rat. Lane 3, cultures of primary astrocytes from neonatal rat cerebral cortex. Lane 4, A7-6-3 rat CNS cells. Lane 5, C6 rat glioma cells. Lane 6, 157 human glioma cells. Right panel: PDGF-B chain probe. Lane 7, SSV-transformed normal rat kidney cells. Lane 8, cultures of primary meningeal cells from neonatal rat. Lane 9, cultures of primary astrocytes from neonatal rat cerebral cortex. The exposure time of lane 7 was approximately one-fifth that of lanes 8 and 9.

Figure 10. Time Course of Appearance of PDGF-A Chain mRNAS in Rat Brain

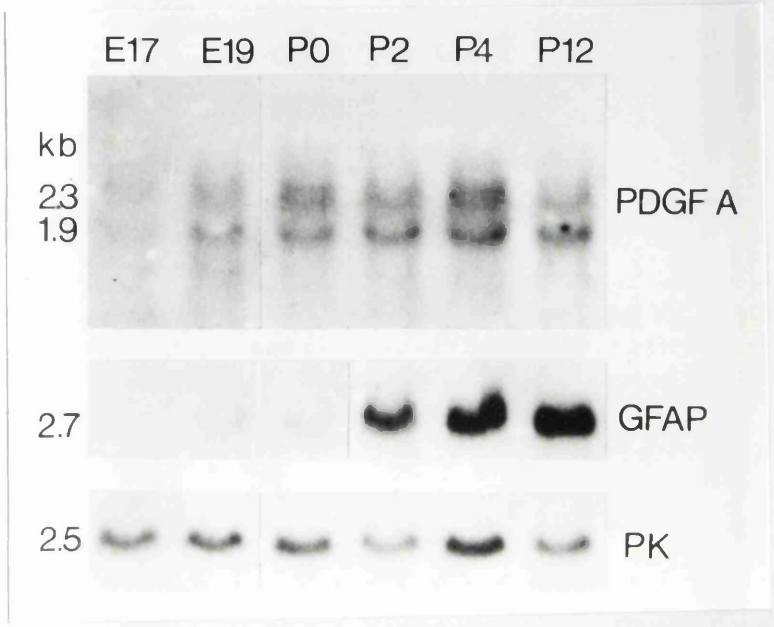

Poly(A)-containing RNA (10 μg/lane) from rat brains of various ages was electrophoresed on a 1% agarose gel containing formaldehyde, transferred to nylon membrane, hybridized with ^{32}P-labelled DNA probes specific for PDGF-A chain. After autoradiographic exposure, the probe was removed by boiling, and the blot rehybridized with a probe specific for glial acidic fibrillary protein (GFAP) mRNA, and then again with a probe for pyruvate kinase (PK) mRNA. PDGF-A chain mRNAs and GFAP mRNA both increase several fold between E17 and E19; PDGF-A chain mRNAs then remain at a fairly constant level to P12, whereas GFAP mRNA increases further between P0 and P12, probably reflecting the growth of astrocytes processes. PK mRNA remains at roughly constant levels over the time period examined, and acts as a control for lane loadings. PDGF-A chain mRNA levels remain constant up to 2 years of age (data not shown).

Figure 11. Time Course of Appearance of PDGF-B Chain mRNAS in Rat Brain

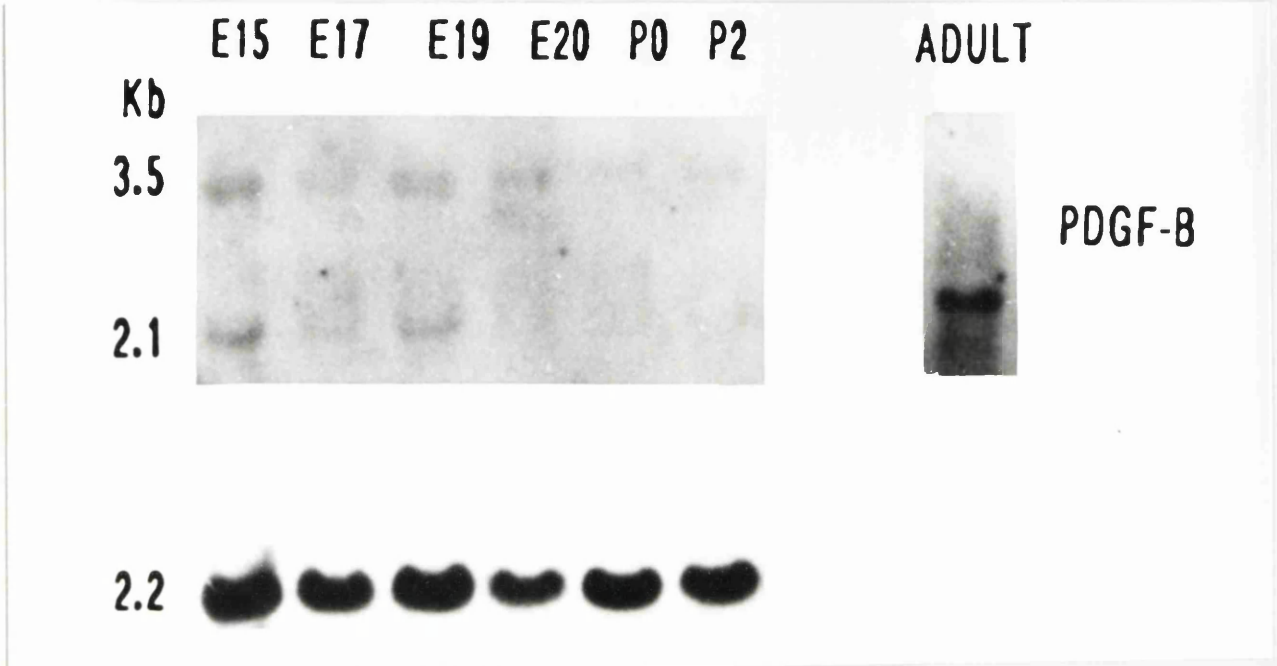

Poly(A)-containing RNA (10 μg/lane) from rat brains of various ages was electrophoresed on a 1% agarose gel containing formaldehyde, transferred to nylon membrane, hybridized with ^{32}P-labelled DNA probes specific for PDGF-B chain. After autoradiographic exposure, the probe was removed by boiling, and the blot rehybridized with a probe specific for actin mRNA. PDGF-B chain mRNAs transcripts decrease between E17 and P2, a single 2.1 kb transcript being seen in adult brain. Actin mRNA remains at roughly constant levels over the time period examined (not done in the adult) and acts as a control for lane loadings.

Developmental Regulation of PDGF-A Chain mRNA in Brain is consistent with its Synthesis by Type-1-like Astrocytes *In Vivo*

I prepared poly(A)-containing RNA from rat brains of various ages, from embryonic day 17 (E17) to 2 years. After separation on formaldehyde agarose gels I blotted the mRNAs onto nylon membrane and probed for transcripts encoding the PDGF-A chain (Figure 10). I also reprobed the same blot for pyruvate kinase mRNA to control for sample loadings, and for GFAP mRNA an astrocyte specific marker (Figure 10). PDGF-A chain transcripts of ~1.9 and 2.3 kb were present but barely detectable at E15 (data not shown) and E17 (Figure 10), but increased several-fold in amount between E17 and E19 (Figure 10), and thereafter remained at a fairly constant level up to postnatal day 12 (P12) (Figure 10) and even up to 2 years of age (data not shown). A single pyruvate kinase transcript of ~2.5 kb was present on the same blot at a roughly constant level at all ages, showing that similar amounts of RNA were loaded in each gel lane. The single ~2.7 kb GFAP transcript was first detected at E17 (at a longer exposure than is shown in Figure 2), but increased several-fold between E17 and E19, coinciding with the increase in PDGF-A chain MRNA, and then increased several-fold after birth. These observations are consistent with the idea that type-1 astrocytes are a source of PDGF-A chain mRNA in the brain (see discussion), although other cell types, notably neurons may contribute.

PDGF-B chain mRNA is developmentally regulated in rat brain.

I prepared poly(A)-containing RNA from rat brains of various ages, from embryonic day 17 (E17) to P2. After separation on formaldehyde agarose gels I

blotted the mRNAs onto nylon membrane and probed for transcripts encoding the PDGF-B chain (Figure 3). I also reprobed the same blot for actin mRNA to control for sample loadings. A second northern blot containing mRNA from a two year old adult animal was also probed for transcripts encoding the PDGF-B chain mRNA. Low levels of PDGF-B chain transcripts at ~3.5 kb and ~2.1 kb were detected in rat brain (Figure 11, panel A). Both the ~3.5 kb and ~2.1 kb mRNA transcripts decrease in levels postnatally (Figure 11, panel A), and in the adult only a single transcript at ~2.1 kb can be detected (Figure 11, panel B). The level of the PDGF-B chain transcript shown in figure 11, panel B, is not directly comparable with the transcripts shown in figure 11, panel A, as this figure is from a different northern blot, exposed for a longer interval of time (10 days compared to 6 days for figure 11, panel A). However, in both cases 10 μg of poly(A)-containing RNA was used for each northern blot, and the result suggests that an increase in the level of the ~2.1 kb transcript has occurred in the adult brain.

The expression of PDGF-B chain mRNA transcripts in rat brain, at ~2.1 kb and ~3.5 kb, appear to decrease in levels during late embryonic and early postnatal development. A single transcript of ~2.1 kb transcript is still visible in the adult.

Localization of PDGF mRNA *in vivo*

Before it can be concluded that IGF-I, IGF-II and PDGF play a role in oligodendrocyte formation in the rat optic nerve *in vivo*, it is necessary to demonstrate that these growth factors are present in the developing CNS. PDGF-B chain, IGF-I and IGF-II mRNAs appear to decrease during early postnatal development, whereas PDGF-A chain mRNA transcripts in the rat brain are developmentally up-regulated at approximately the same time as GFAP (an astrocyte specific marker) is up-regulated, consistent with the idea that PDGF-A chain may be

produced by astrocytes. Other workers in our laboratory and elsewhere had demonstrated that although insulin-like growth factors are important for oligodendrocyte development *in vitro*, they have little mitogenic effect on O-2A progenitor cells. PDGF, however, was shown to be mitogenic on O-2A progenitor cells *in vitro* (Pringle *et al.*, 1989; Richardson *et al.*, 1988; Raff *et al.*, 1988; Noble *et al.*, 1988). I therefore decided to concentrate on determining whether PDGF mRNA (rather than IGF-I or IGF-II) was expressed in the rat optic nerve *in vivo*. I therefore performed *in situ* hybridization, using ^{35}S-RNA probes specific to the A and B chain of PDGF.

I first confirmed the specificity of my probes for PDGF-A and B chains, by performing *in situ* hybridization on cell lines known to contain PDGF mRNA (Figure 12). Cell line sis-NRK (obtained from P.Stroobant, Ludwig Institute for Cancer Research, London) is a simian sarcoma virus (SSV)-transformed normal rat kidney cell line which expresses high levels of v-*sis* transcripts (Figure 9). v-*sis* is the viral homologue of c-*sis*, the cellular PDGF-B chain gene (Doolittle *et al.*, 1983; Waterfield *et al.*, 1983). As expected, I obtained a clear autoradiographic signal following *in situ* hybridization with ^{35}S-labelled single strand RNA probe complementary to the PDGF-B chain mRNA (antisense probe, Figure 12A), but not with a probe homologous to the mRNA (sense probe, Figure 12B). Cell line 157 (obtained from M.Noble, Ludwig Institute for Cancer Research, London) is a human glioma line which expresses high levels of PDGF-A chain mRNAs (Figure 9). As predicted, I obtained a positive *in situ* hybridization signal using the antisense A chain probe (Figure 12, panel C), but no significant signal over background with the sense A chain probe (Figure 12, panel D).

Cryosections (10μm nominal thickness) of rat optic nerves were prepared and subjected to *in situ* hybridization with the PDGF-A and B chain probes, Figure 13 shows the results obtained with P8 optic nerves; similar results were obtained with

newborn and adult nerves (not shown). Figure 13, panel A, shows a longitudinal section through the mid-region of a P8 nerve, stained with toluidine blue and photographed under bright field illumination. Figure 13, panel C, shows an autoradiograph of the same section viewed in dark field, following *in situ* hybridization with the PDGF-A chain antisense probe. Developed silver grains are distributed more or less uniformly over the entire optic nerve, with perhaps a narrow region of slightly higher density just beneath the surface of the nerve. Note the signal in the meningeal cell layer (Figure 13, panel C), which is absent in the section probed with GFAP (Figure 13, panel H). Pretreatment of the sections with ribonuclease A, before hybridization with the antisense probe, reduced the signal to near background levels (Figure 13, panel E). Hybridization with the A chain sense probe without prior ribonuclease treatment gave no signal over background (Figure 13, panel G). No signal was obtained with either antisense or sense probes for the PDGF-B chain (Figure 13, panels D and F).

All the sections illustrated in figure 2 were prepared and processed together under as similar conditions as possible, so the results demonstrate that PDGF-A chain mRNA is present in the developing optic nerve, and also suggest that PDGF-B chain mRNA is absent, or is present at very low levels in comparison with the A chain. I therefore conclude that the major form of PDGF in the rat optic nerve is probably a homodimer of PDGF-A chains (PDGF-AA). PDGF-like mitogenic activity has also been demonstrated in postnatal extracts of rat optic nerve (Raff *et al.*, 1988), which adds further support to my observations.

To compare the distribution of PDGF-A chain mRNA with the distribution of type 1 astrocytes in the P8 optic nerve (type 2 astrocytes have not yet started to develop at this age), I performed *in situ* hybridizations with a probe for mRNA encoding the astrocyte-specific intermediate filament protein (GFAP). The exposed silver grains were distributed uniformly over the optic nerve, except for the meninges

(Figure 13, panel H). Prior treatment with ribonuclease A abolished the signal, and the sense probe gave no signal (not shown). Thus the distribution of PDGF-A chain mRNA and GFAP mRNA within the nerve are similar, consistent with the idea that type 1 astrocytes in the rat optic nerve may be a source of PDGF in the optic nerve. Meningeal cells which appear to express PDGF-A chain mRNA *in vitro* (Figure 9, lane 8), and *in vivo* (Figure 13, panel C), may also contribute PDGF-AA to the periphery of the optic nerve. However, unlike cortical astrocytes, they do not appear to secrete PDGF constitutively *in vitro* (Richardson *et al.*, 1988), and thus their influence on oligodendrocyte formation is unclear.

Figure 12. Testing the Specificity of my *in situ* Hybridization Probes

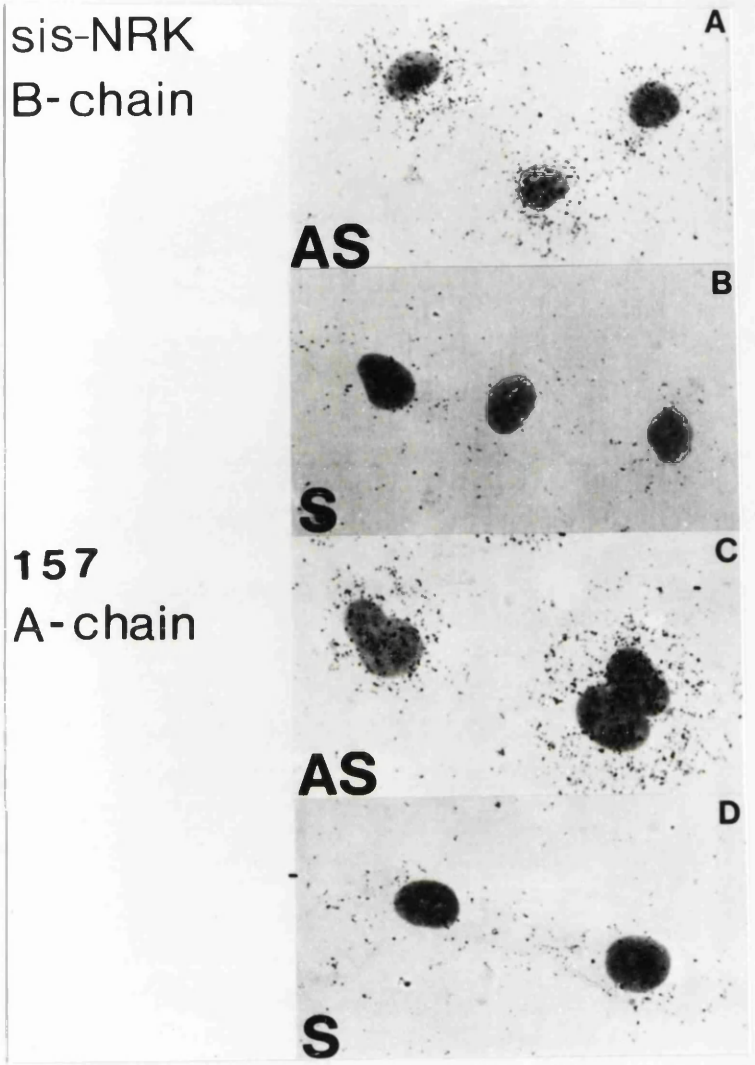

Cell lines *sis*-NRK (SSV-transformed rat kidney cells) and 157 (a human glioma line) were grown on glass coverslips and subjected to *in situ* hybridization and autoradiography, using ^{35}S-labelled single-stranded RNA probes. Sis-NRK cells (**A** and **B**) contain high levels of PDGF-B chain related transcripts, while 157 cells (**C** and **D**) contain high levels of PDGF-A chain mRNAs. *sis*-NRK cells gave a positive autoradiographic signal with the B chain antisense probe (**A**) but not with the B chain sense probe (**B**). 157 cells give a positive signal with the A chain antisense probe (**C**), but not with the A chain sense probe (**D**). The cells have been stained with toluidine blue to reveal their nuclei, and viewed by bright field microscopy.

Figure 13. Expression of PDGF mRNAs in P8 Rat Optic Nerves

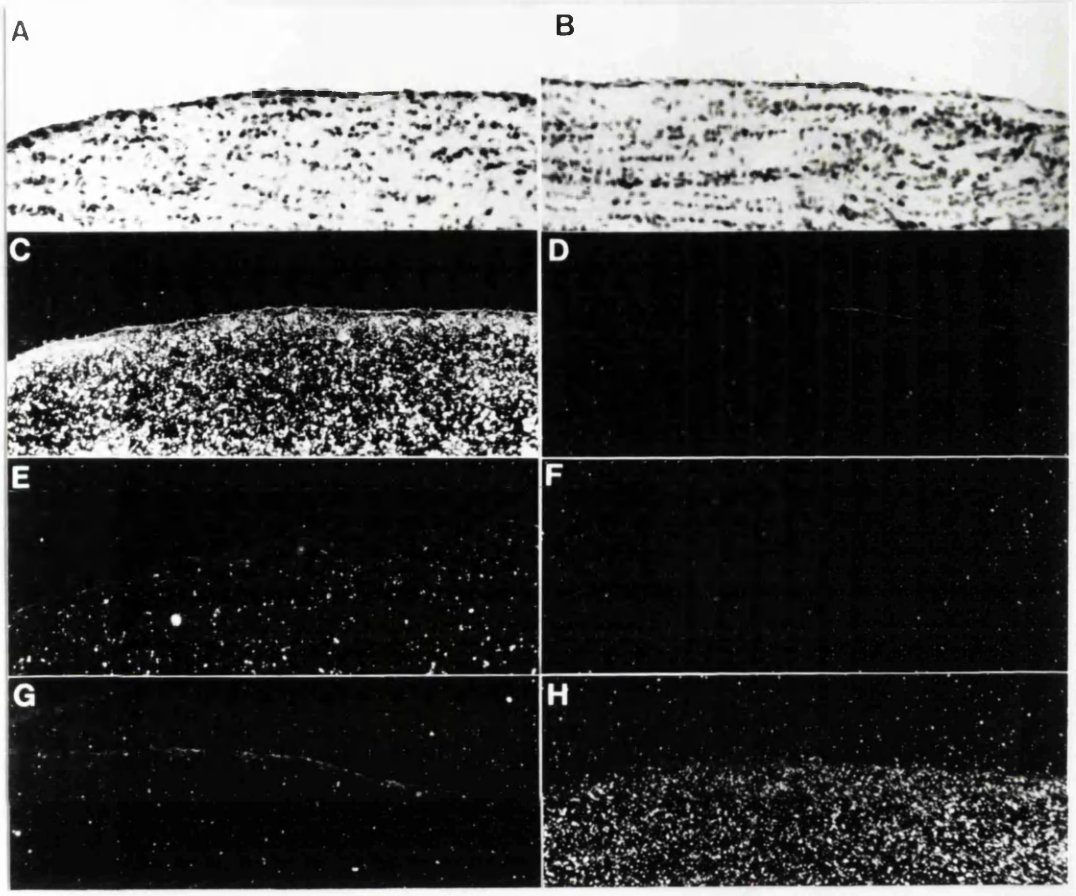

Cryosections (10μm thick) were subjected to *in situ* hybridization and autoradiography, using ^{35}S-labelled single stranded RNA probes, then counter stained with toluidine blue and viewed by bright-field (**A** and **B**) or dark field light microscopy. (**A**) Bright-field micrograph of a longitudinal section through the mid region of a P8 nerve, hybridized with the PDGF-A chain antisense probe. (**C**) Same section viewed in dark field-field to reveal autoradiographic signal. (**E**) Similar section, pretreated with RNAse A before hybridization with the PDGF-A chain antisense probe. (**G**) Section hybridization with the PDGF-A chain sense probe. (**B**) Section hybridization with the PDGF-B chain antisense probe, viewed in bright-field). (**D**) Same section viewed in dark-field. (**F**) Section hybridization with the PDGF-B chain sense probe. (**H**) Section hybridized with an antisense probe for GFAP mRNA. Positive signals are obtained only with the PDGF-A chain and GFAP antisense probes.

Discussion

The aim of these experiments was to identify the growth factor(s) secreted by type-1 astrocytes that induces O-2A progenitors cells from developing rat optic nerve to proliferate in culture. In the absence of any mitogen, the O-2A progenitors promptly stop dividing in culture and differentiate into oligodendrocytes or type 2 astrocytes, whereas proliferation and differentiation into oligodendrocytes continues *in vivo* for several weeks (Miller *et al.*, 1985). Hence the mitogen seems to be important not only for expanding the pool of progenitor cells but also for controlling the time and rate of production of differentiated progeny. The *in vitro* behaviour of O-2A progenitor cells isolated from the brain closely resembles that of their optic nerve counterparts (Behar *et al.*, 1988), so it is likely that my conclusions from studies on optic nerve also apply to other myelinated tracts in the CNS.

Cultured rat cortical astrocytes produce PDGF.

Several results from our laboratory support the idea that cultured rat cortical astrocytes produce PDGF. First the mitogenic activity secreted by cultured cortical type-1-like astrocytes co-migrates with PDGF on a size-exclusion column (Richardson *et al.*, 1988). Second, cortical astrocyte conditioned medium competes with PDGF for receptors on human foreskin fibroblasts (Richardson *et al.*, 1988). Third, astrocytes secrete PDGF that can be immunoprecipitated from the culture medium by anti-PDGF immunoglobulins (Richardson *et al.*, 1988). Fourth, the majority of mitogenic activity in astrocyte-conditioned medium is neutralized by anti-PDGF immunoglobulins (Richardson *et al.*, 1988). Taken together, these results suggest that PDGF may play an important role in the development of the O-2A lineage. I have

shown that PDGF-A chain mRNA is synthesized by cortical astrocytes and is present in developing rat brain.

What is the source of PDGF in the optic nerve *in vivo*? Apart from O-2A lineage cells, type 1 astrocytes form the majority of the cells in the optic nerve during the first two postnatal weeks, and would be expected to have a major influence on the extracellular environment throughout this period, when O-2A progenitor cells are dividing rapidly (Skoff *et al.*, 1976a, 1976b; Miller *et al,*. 1985). However, retinal ganglion cell axons that pass through the optic nerve may also influence the environment in some way (see next section). Although I cannot be certain that type 1 astrocytes secrete PDGF *in vivo*, secretion of PDGF does not appear to be a general consequence of placing cells in primary culture, since meningeal cells contain mRNA for PDGF (Figure 9 and Figure 13, panel C) yet secrete no detectable PDGF or mitogenic activity for O-2A progenitors (Richardson *et al.*, 1988).

The time course of appearance of PDGF mRNA in the brain (Figure 10) is consistent with the notion that cortical astrocytes are a source of PDGF-A chain mRNA in the CNS. The A chain mRNAs are barely detectable at E17, just after the time that small numbers of astrocytes first appear in the brain (Abney *et al.*, 1981) and optic nerve (Skoff *et al.*, 1976a, 1976b; Miller *et al,*. 1985) and increase several fold between E17 and E19 when GFAP mRNA first becomes obvious. Thereafter, the A chain mRNAs remain at relatively constant levels until adulthood.

PDGF-A chain, not B-chain is expressed in rat optic nerves.

Cultured cortical astrocytes closely resemble cultured type-1 astrocytes from the rat optic nerve; both are flat epitheliod cells and express some of the same antigenic markers *in vitro*. However, there may be differences between cortical astrocytes and type-1 astrocytes located in different regions of the CNS. The results

of my in situ hybridizations with PDGF-A and PDGF-B chain in the optic nerve suggests that type 1 astrocytes produce PDGF-A chain in the developing optic nerve. I have demonstrated the presence of PDGF-A chain mRNA in the optic nerves of P8 rats (Figure 13) and also in neonatal and adult nerves (not shown). The spatial distribution of PDGF-A chain mRNA is nearly uniform throughout the optic nerve except that a slightly higher grain density is observed just beneath the surface of the nerve (Figure 13). This may reflect the frequent siting of astrocyte cell bodies in this region (Miller *et al.*, 1985). This feature is barely discernible in figure 13, but in other sections was more obvious. I did not notice a similar dense layer with the GFAP probe, but since GFAP is an intracellular protein, whilst PDGF is secreted, we would not necessarily expect their mRNAs to reside in the same regions of the cell; PDGF may be translated preferentially in the cell body near the Golgi, whilst GFAP may be translated throughout the cell, including the cell processes. Sub-cellular localizations of specific mRNAs has been described in other cell types (Trapp *et al.*, 1987; Fontaine *et al.*, 1988).

Sources of PDGF: Neurons *versus* Astrocytes?

The recent observation that neurons, as well as some glia, express PDGF-A chain mRNA (Yeh *et al.*, 1991) suggests that a proportion of the PDGF-A chain mRNA seen in my northern blots of developing brain mRNA (Figure 10) might be attributable to neurons.

Is the rise in expression of PDGF-A mRNA detected in northern blots of developing rat brain due to neurons or astrocytes? Almost all neurons are in place by the day of birth (P0), most being postmitotic before E15 (Jackobson, 1978), when I first detect low levels of PDGF-A mRNA. In contrast glial cells increase in numbers during the early postnatal period (see Jacobson, 1978). The increase of

PDGF-A chain mRNA transcripts coincides reasonably well with the increase of expression of GFAP (an astrocyte specific marker). This suggests that astrocytes, not neurons, are probably responsible for the increased levels of PDGF-A chain mRNA occurring at this time.

However, cortical astrocytes express a predominant ~1.9 kb transcript for PDGF-A (Figure 9, lane 3), whereas in rat brain I can detect two major transcripts of ~2.3 and 1.9 kb (Figure 9, lane 1; Figure 10). This suggests that astrocytes and neurons may preferentially express different sized mRNA transcripts for PDGF-A chain. If this proves to be true, then the increase of the ~2.3 kb transcript may not be attributable to astrocytes, but may reflect up-regulation in neurons or glial cell type other than astrocytes.

PDGF-B chain mRNAs, in contrast to PDGF-A chain, decreases postnatally, a single transcript of ~2.1 kb being detected in the adult (Figure 11. panel B). Sasahara *et al,*. (1991) have shown that neurons in primates express PDGF B chain. I can detect little, if any, PDGF-B chain mRNA in cultures of cortical astrocytes (Figure 9, lane 9). Thus the expression of PDGF-B chain mRNA in the rat brain probably reflects expression in neurons rather than astrocytes, although endothelial cells also express PDGF-B chain (H.Mudhar, unpublished observations) and might contribute also.

Regardless of its, source PDGF-A mRNA is present in the brain during the time that O-2A progenitor cells are proliferating rapidly, suggesting that PDGF-A chain is important during gliogenesis.

Insulin-like growth factors are developmentally regulated in the CNS.

My results suggest that both IGF-I and IGF-II mRNA transcripts are developmentally regulated in rat brain and are in general agreement with those previously described by Lund *et al.* (1986). My observed IGF-I transcripts of ~1.9 and 7.1 kb (Figure 6) probably correspond to the 1.7 and 7.5 kb transcript described in rat brain by Lund *et al.* (1986). However, the ~3.4 and 3.8 kb transcripts (Figure 6) were not detected by Lund *et al.* (1986) and may have been seen due to my loading higher concentrations of poly(A)-containing RNA on my northern blot. The ~7.1 kb IGF-I transcript is only observed at E15, whereas the ~1.7, 3.4 and 3.8 kb transcripts were present until at least P12.

The detection of a single ~1.9 kb transcript in cultured cortical astrocytes (Figure 7) suggests that astrocytes may be one source of IGF-I in the rat brain. IGF-I mRNA is also strongly expressed in many cerebellar projection neurons during late neurogenesis, having a projected role in shaping specific synaptic connections or myelinization (Bondy, 1991).

I was unable to detect any IGF-II transcripts in the same northern used to detect both IGF-I (Figure 7) and PDGF-A chain (Figure 9). In contrast I found a major IGF-II transcript of ~4 kb and a minor one of ~2.7 kb in all fetal and postnatal ages of rat brain examined. My major transcript probably corresponds to the 3.9 kb transcript described by Lund *et al.* (1986). The minor species of IGF-II transcripts detected in brain of ~2 and 1.5 kb are only seen at E15. My results suggest that developmental regulation of both IGF-I and IGF-II transcripts occurs predominantly in the embryo, although mRNA is found until at least P12 for IGF-I and P3 for IGF-II.

Other workers have found that mRNA transcripts for IGF-I and IGF-II are expressed predominantly in the embryo, the levels of their mRNAs decrease postnatally, although transcripts are still found in the adult (Werner *et al.*, 1989; Rotwein *et al.*, 1988). These observations suggest that both IGF-I and IGF-II exert their effects on the developing nervous system during late embryonic development.

Barres *et al.* (1992), has suggested that both PDGF (at sub-mitogenic concentrations) and IGFs may act as survival factors for newly formed oligodendrocytes and their precursors *in vitro*. This suggests a potentially novel role for these factors in the development of the CNS.

Conclusions

In summary, my results have demonstrated that cortical astrocytes *in vitro* produce PDGF-A chain mRNA. The time course of appearance of PDGF-A mRNA in the rat brain coincides with the increases of GFAP mRNA, which is a specific astrocyte marker. This is consistent with the idea that astrocytes may be a source of PDGF in the brain. More recently PDGF-A chain mRNA has been shown to be expressed by neurons as well as by glial cells (Yeh *et al.*, 1991) and PDGF-B chain immunoreactivity has been demonstrated in neurons (Sasahara *et al.*, 1991). Thus astrocytes are not the only source of PDGF in the rat CNS. My *in situ* hybridization studies in the rat optic nerve *in vivo* have demonstrated that PDGF-A chain, not PDGF-B chain mRNA is expressed, and that the mRNA expression observed substantially overlaps with that for GFAP. Type 1 astrocytes may, therefore, be one source of PDGF in the rat optic nerve. Meningeal cells of the optic nerve and retinal

ganglion neurons which also express PDGF-A chain mRNA (H. Mudhar, unpublished observations) might also contribute.

My results suggest that both IGF-I and IGF-II mRNAs are present in the rat brain at a time that oligodendrocytes are being formed. Only IGF-I appears to be expressed by cortical astrocytes. Insulin-like growth factors are thought to influence oligodendrocyte formation (McMorris *et al.*, 1986) and have recently been shown to act not as mitogens for O-2A progenitor cells, but as survival factors (Barres *et al.*, 1992).

CHAPTER 4

PDGF RECEPTORS IN THE RAT CNS: DURING LATE NEUROGENESIS, PDGF ALPHA RECEPTOR EXPRESSION APPEARS TO BE RESTRICTED TO GLIAL CELLS OF THE OLIGODENDROCYTE LINEAGE.

INTRODUCTION

In my previous chapter of results I have demonstrated that PDGF-A chain mRNA is present in the rat CNS and cultured cortical astrocytes. Other workers have shown that PDGF homodimers are mitogenic on O-2A progenitor cells *in vitro* (Richardson *et al.*, 1988; Raff *et al.*, 1988; Noble *et al.*, 1988). In common with many other growth factors, PDGF elicits its biological effects by binding to transmembrane receptors with extracellular ligand-binding domains and intracellular tyrosine kinase domains. There are two PDGF receptors with different ligand specificities; PDGF alpha-receptors (PDGF-αR) can bind both A and B chains of PDGF (Hart *et al.*, 1988; Matsui *et al.*, 1989) whereas beta-receptors (PDGF-βR) bind only B chains (Gronwald *et al.*, 1988). The unoccupied receptors are monomeric and inactive, but PDGF binding induces receptor dimerization and activates their tyrosine kinase domains (Li and Schlessinger 1991; for review see Ullrich and Schlessinger 1990). Thus, the response of a given cell to PDGF depends on the PDGF receptor type(s) that it expresses as well as the PDGF isoform(s) that it encounters. In the CNS, PDGF-βR has been reported to be expressed by brain endothelial cells (Smits *et al.*, 1989; H. Mudhar, unpublished observations) and also by many CNS neurons (Smits *et al,*. 1991). O-2A progenitor cells express predominantly PDGF-αR (Hart *et al,*. 1989; McKinnon *et al,*. 1990), and are stimulated to divide *in vitro* by all three dimeric isoforms of PDGF, although PDGF-AA is more effective than PDGF-BB (Pringle *et al,*. 1989) because of the higher affinity of PDGF A chains for PDGF-αR (Heldin *et al,*. 1988). The aim of the experiments described in this chapter of results was to investigate the temporal and spatial distribution of PDGF-αR within the CNS, to determine which cell types are expressing PDGF-αR and to investigate whether PDGF-αR expression might be restricted to cells of the oligodendrocyte lineage. I performed *in situ* hybridization on rat CNS tissue from E16 to adult using a probe

which specifically recognises PDGF-αR. The results described in this chapter suggest that, during the ages studied, PDGF-αR expression within the CNS appears to be restricted to cells of the oligodendrocyte lineage, meningeal cells and choroid plexus.

Results.

To map the distribution of PDGF-αR mRNA in the developing rat CNS, I performed *in situ* hybridizations with a ^{35}S-RNA probe corresponding to part of the extracellular domain of the rat PDGF-αR. This probe recognized a single ~7 kb mRNA on northern blots of poly-A-containing RNA from perinatal rat brain (Figure 14). A PDGF-αR transcript of 6.8 kb was previously described (Lee *et al,*. 1990). Thus, my probe specifically recognizes PDGF-αR mRNA and does not cross-hybridize with PDGF-βR mRNA, a 5.3 kb species (Matsui *et al,*. 1989) that is also present in the rat CNS (Sasahara *et al,*. 1991). Cryostat sections (10 μm nominal thickness) of embryonic and postnatal rat brains (E16, E18, P0, P2, P6, P10, P20 and adult) were subjected to *in situ* hybridization with the PDGF-αR probe, as described in Methods. Subsequently, sections were subjected to autoradiography, lightly stained with hematoxylin and examined in the microscope under bright- and dark-field illumination.

Small numbers of PDGF-αR$^+$ cells are present in the rat forebrain by E16.

Figure 15 shows a coronal section through an E16 rat head, at the level of the anterior forebrain. PDGF-αR is expressed strongly in most craniofacial tissues, the anterior proliferating lens epithelium and in the meningeal cell layer that surrounds and bisects the forebrain; there is very little PDGF-αR signal in the forebrain itself at E16. The few isolated PDGF-αR$^+$ cells that are present in the E16 brain lie outside of the halo of densely packed cells that surrounds the ventricles (corresponding to the densely stained region delineated by dotted lines in the inset to Figure 15). This region comprises the ventricular and subventricular zones, which

are the major mitotically active areas and the primary source of new neurons and glia. It is noteworthy that at E16 most PDGF-αR$^+$ cells lie inferior (ventral) and lateral to the ventricles; few if any are present in the developing cerebral cortex at this age, even though E16-E17 is the peak time of production of postmitotic neurons in the rat cortex (see Jacobson, 1970 for review).

PDGF-αR$^+$ cells proliferate during late embryonic and early postnatal brain development.

Figure 16 shows a coronal section through the anterior forebrain at E18. PDGF-αR$^+$ cells are scattered throughout the thalamus and hypothalamus. Some PDGF-αR$^+$ cells are present at the lateral tips of the subcortical white matter at E18, but not in the more medial white or grey matter of the cortex. There are significantly more PDGF-αR$^+$ cells in the E18 forebrain than at E16 (compare figure 16 with 15), but most of these cells still lie outside of the subventricular zones.

Figure 17 shows a pair of consecutive sagittal sections through an P0 rat head, one hybridized with the PDGF-αR antisense probe (i.e. complementary to the mRNA) and the other with the sense probe. Only the antisense probe hybridizes, providing further verification of the specificity of the signal. The number of PDGF-αR$^+$ cells has increased further by the day of birth (Figure 17a and Table 2). Individual PDGF-αR$^+$ cells are apparent throughout the brain; their distribution is relatively uniform in many areas but, in general, they are less numerous in peripheral areas such as the inferior and superior colliculi, pons and the ventral-most hypothalamus. PDGF-αR$^+$ cells are abundant in the cerebral cortex at P0, especially in the subcortical white matter, including the cingulum (Figure 18). Relatively weakly

labelled PDGF-αR$^+$ cells are detected in the developing cerebellum at P0, mainly in the internal granule layer (Figure 19A,B).

PDGF-αR$^+$ cells multiply still further after birth (Table 2). By P3, there are large numbers of strongly labelled cells in the internal granule layer of the cerebellum, for example (Figure 19C,D). Figure 20 shows coronal and sagittal sections through a P10 rat brain. At this age PDGF-αR$^+$ cells are prominent in all regions of the brain including the outermost regions of the cerebral cortex. At P10 the density of PDGF-αR$^+$ cells is noticeably higher, however, in developing white matter tracts such as the subcortical white matter (Figure 20) and the foliar white matter of the cerebellum (Figure 19E,F). At P20, the distribution and density of PDGF-αR$^+$ cells in all regions of the brain (not shown) was very similar to the picture at P10.

The nuclear morphology of PDGF-αR$^+$ cells in the forebrain is indicative of glial cells, not neurons.

Figure 21 shows an enlarged view of part of the P10 cerebral cortex corresponding to the area within the frame in Figure 20A. Developed silver grains are associated with individual cells (or small groups of cells) possessing small, spherical nuclei that stain intensely with haematoxylin (black arrows). This nuclear morphology is usually regarded as a hallmark of glial cells, and oligodendroglia especially (Smart and Leblond, 1961; Bunge, 1968). Often, the labelled cells are in pairs, suggesting that they may have divided locally. Neurons with large, lightly-staining nuclei (white arrows) never labelled for PDGF-αR, either in the cerebral cortex (Figure 21) or in any other brain region that I examined.

PDGF-αR$^+$ cells accumulate in the developing optic nerve in a wave starting from the optic chiasm.

I find PDGF-αR$^+$ cells in the rat optic nerve, from around birth (Figure 22) through to adulthood (Figure 23). The optic nerve carries axons from ganglion neurons in the retina to the brain, but does not contain any neuronal cell bodies. Hence, the PDGF-αR$^+$ cells in the nerve correspond either to glial cells or, less likely, non-neural cells such as capillary endothelial cells or fibroblasts.

At P0, there are relatively few PDGF-αR$^+$ cells in the optic nerve; these are more numerous towards the optic chiasm, being almost absent from the retinal end of the nerve (Figure 22A,B). Two days later, at P2, PDGF-αR$^+$ cells occupy the optic nerve uniformly, except for a short region at the extreme retinal end (Figure 22C). The progressive appearance of PDGF-αR$^+$ cells from the chiasmal to the retinal end of the optic nerve is similar to the way that O-2A progenitor cells accumulate in the nerve. It has been suggested that this results from a wave of migration of O-2A progenitors from a germinal zone, presumably around the third ventricle, into the developing nerve *via* the optic chiasm (Small *et al,*. 1987)

There is a narrow band of PDGF-αR$^+$ cells at the inner face of the retina from P0 (Figure 22) through to adulthood (not shown). These cells lie in the inner limiting membrane, a basement membrane comprised of Muller glial cell endfeet and non-CNS cells (including blood vessels) that overlies the optic fibre layer.

PDGF-αR$^+$ cells persist in the adult CNS.

Figure 23 shows a coronal section through the forebrain of an adult (approximately six-months-old) rat. PDGF-αR$^+$ cells are visible in all regions of the section, including the optic nerves. Cell counts indicate that the number of cells expressing PDGF-αR in the thalamus declines from about 8% to about 4% of total cells between P10 and adulthood (Table 2). PDGF-αR$^+$ cells are also present in the molecular and internal granule layers of the adult cerebellum (Figure 19G,H); it is not possible to distinguish individual cells in the foliar white matter, because of the high scattering background from myelinated fibres.

O-2A lineage cells, but neither microglial cells nor cortical astrocytes, express PDGF-αR in vitro.

The *in situ* hybridization data presented above, together with previous ^{125}I-PDGF binding studies on optic nerve cells in culture (Hart *et al*., 1989), suggested to me that PDGF-αR might be expressed solely by O-2A lineage cells in the CNS. I investigated this possibility further by attempting to bind ^{125}I-PDGF-AA to various non-neuronal rat brain cells *in vitro*, since PDGF-AA should only bind to cells that possess PDGF-αR (Heldin *et al*,. 1988; Gronwald *et al*,. 1988). I established enriched cultures of microglial cells (the macrophages of the CNS) and cortical (type-1-like) astrocytes (see Methods for details). The enriched cultures of rat O-2A progenitor cells were prepared by Dr. E. Collarini. These different glial cell types were maintained for 24 hours in low-serum medium before incubating with ^{125}I-PDGF-AA in the presence or absence of a 100-fold excess of unlabelled PDGF-AA or PDGF-BB. NIH 3T3 cells, which are known to express PDGF-αR,

were included as a control. Bound ^{125}I-PDGF was estimated by gamma counting of solubilized cells. Table 3 shows the results of these competitive binding experiments. NIH 3T3 cells bound ^{125}I-PDGF-AA specifically, as expected. O-2A progenitor cells also bound ^{125}I-PDGF-AA specifically, confirming previous findings that O-2A lineage cells express PDGF-αR on their surface (Hart *et al,*. 1989). Neither cortical astrocytes nor microglia bound ^{125}I-PDGF-AA specifically, indicating that neither of these cell types express PDGF-αR. In other experiments (table 4), cortical astrocytes were found to bind ^{125}I-PDGF-BB, suggesting that these cells express PDGF-ßR *in vitro*.

Figure 14. Northern blot analysis of PDGF-αR mRNA in P13 rat brain.

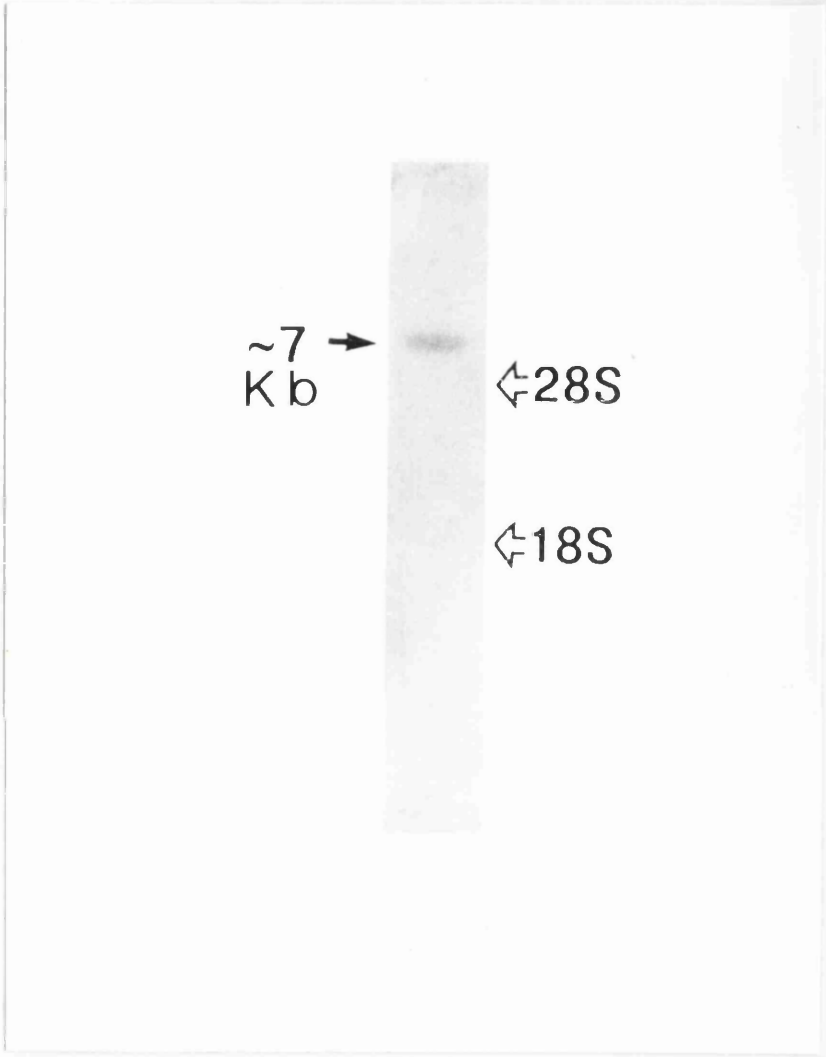

Poly(A)-containing mRNA (10 μg) was electrophoresed on a 1% agarose gel containing formaldehyde, transferred to nylon membrane and hybridized with a ^{32}P-labelled cDNA probe coding for the extracellular domain of PDGF-αR. My probe recognises a single mRNA species at ~7 kb. The positions of the ribosomal 18S and 28S subunits are shown for comparison.

Figure 15. Distribution of PDGF-αR mRNA in E16 rat head, visualized by *in situ* hybridization.

Illustrated is a coronal section at the level of the anterior forebrain. Cryosections (10 μm nominal thickness) were subjected to *in situ* hybridization and autoradiography, using ^{35}S-labelled single stranded RNA probes specific for PDGF-αR. The exposed silver grains were developed and the sections photographed in darkfield illumination. Many craniofacial structures are strongly labelled as are the anterior proliferating cells of the lens. A few PDGF-αR$^+$ cells are seen in the developing forebrain, away from the germinal zones surrounding the lateral ventricles. Scale bar, 100 μm. Inset: LV, lateral ventricle; SVZ, subventricular zone; Men, meningeal membrane; L, lens; Ret, retina.

Figure 15. Distribution of PDGF-αR mRNA in E16 rat head, visualized by *in situ* hybridization.

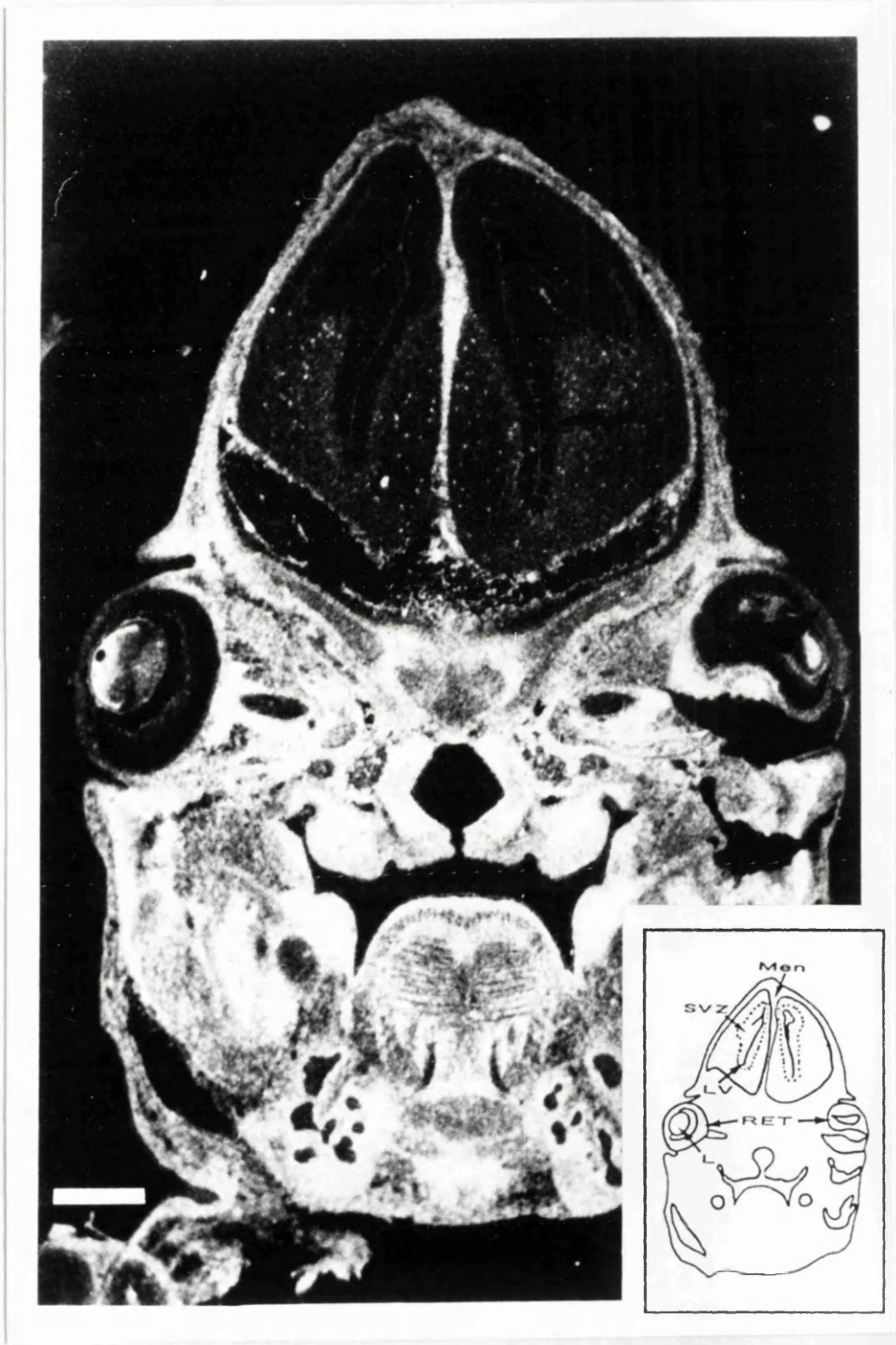

Figure 16. Distribution of PDGF-αR mRNA in the E18 forebrain (coronal section).

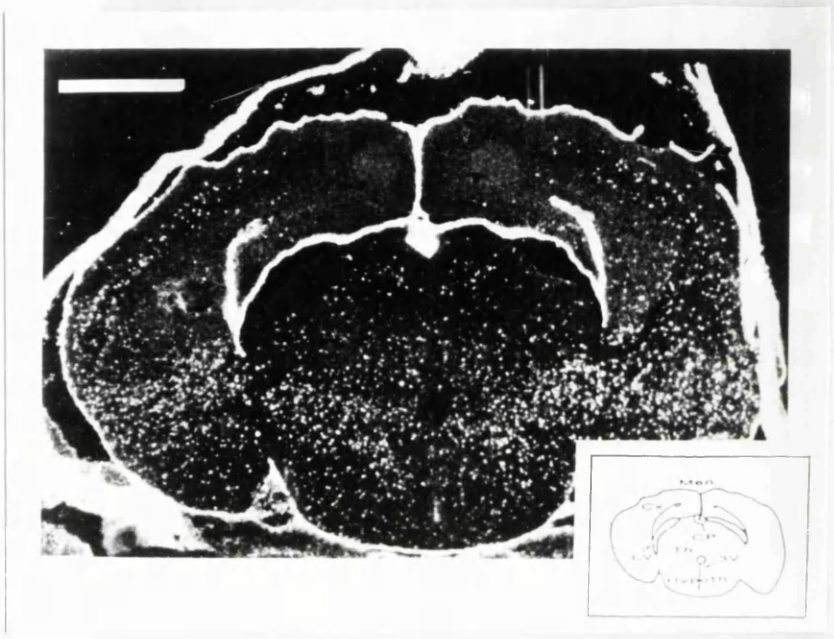

PDGF-αR^+ cells are more concentrated in the lower (ventral) half of the brain and at the lateral tips of the lateral ventricles. PDGF-αR^+ cells are also present in the more lateral regions of the cortical intermediate zone (developing subcortical white matter), but not in the more medial white or gray matter of the cortex. Scale bar, 100 μm. Inset: LV, lateral ventricle; 3V, third ventricle; Th, thalamus; Hypoth, hypothalamus; Cx, cerebral cortex; CP, choroid plexus; Men, meningeal membrane.

Figure 17. Distribution of PDGF-αR mRNA in the P0 rat head.

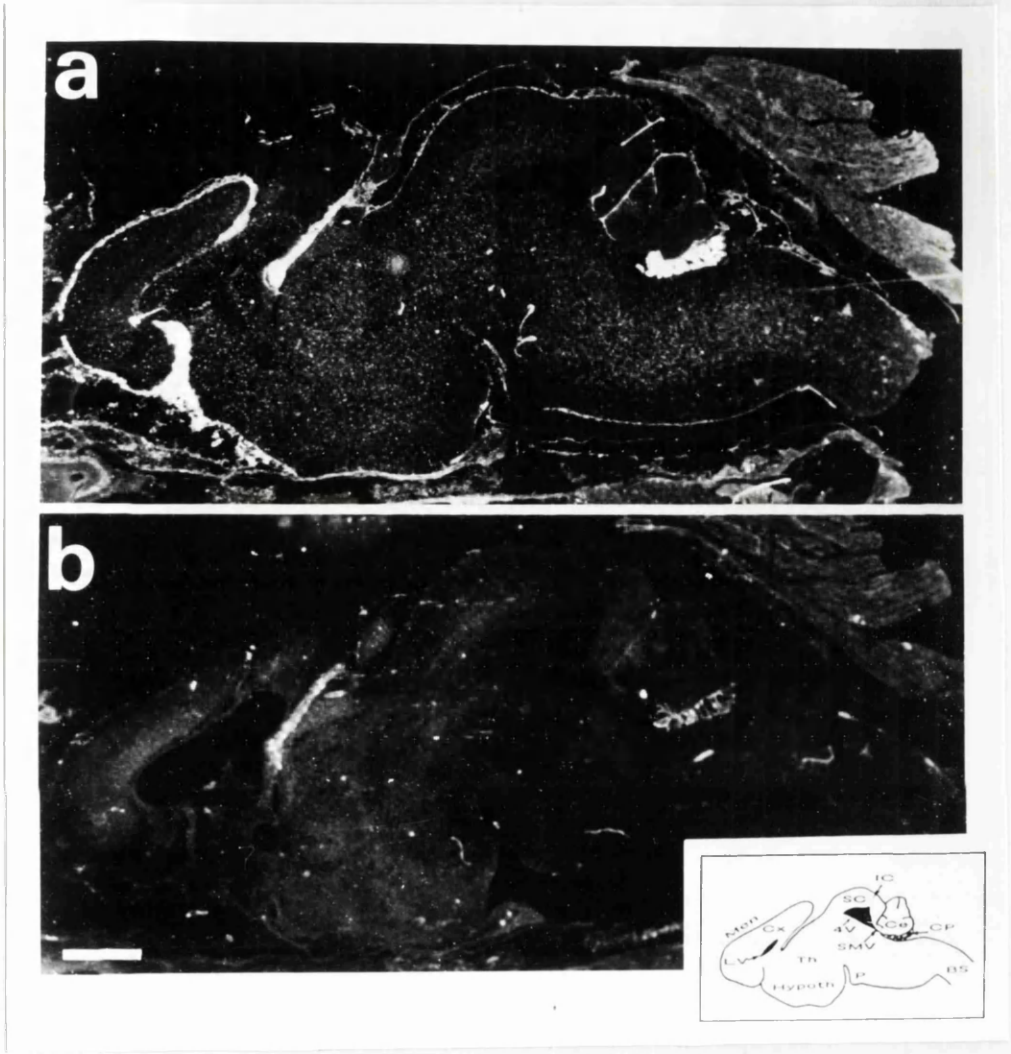

Panel *a*, sagittal section through a P0 rat head, hybridized with the ^{35}S-labelled PDGF-αR "antisense" probe, autoradiographed and photographed under dark-field illumination. Individual PDGF-αR$^+$ cells are apparent throughout the brain; their distribution is relatively uniform in many areas but, in general they are less numerous in peripheral areas such as the inferior and superior colliculi, pons and posterior hypothalamus. Panel *b*, adjacent section hybridized with the ^{35}S-labelled PDGF-αR "sense" probe shows no specific labelling. Scale bar, 100 μm. Inset: LV, lateral ventricle; 4V, fourth ventricle; Cx, cerebral cortex; CP, choroid plexus; Th, thalamus; Hypoth, Hypothalamus; P, pons; SC, superior colliculi; IC, inferior colliculi; SMV, superior medullary vellum; CE, cerebellum; BS, brain stem; Men, Meningeal membrane.

Figure 18. PDGF-αR$^+$ cells in the P0 cerebral cortex and developing hippocampus (coronal section).

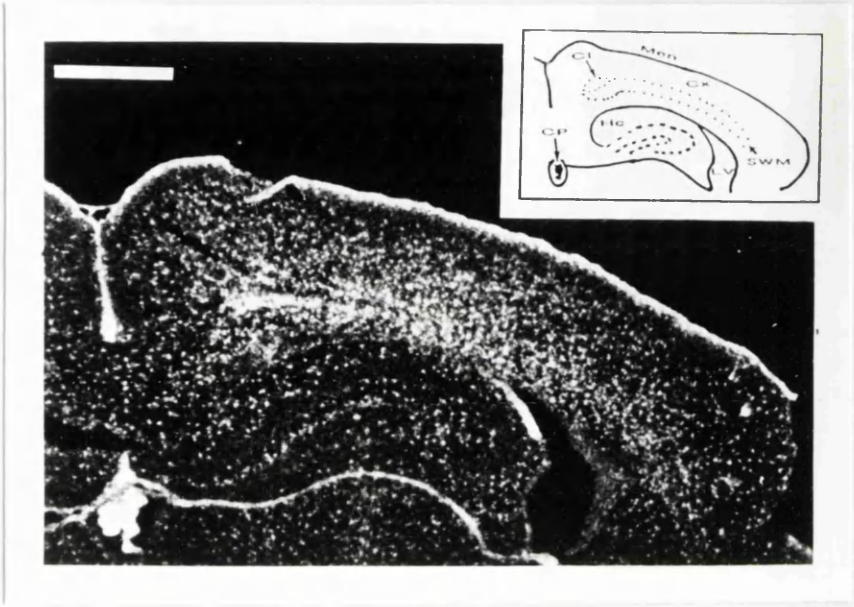

PDGF-αR$^+$ cells are present throughout the cortex up to the pial surface, but are more concentrated in the subcortical white matter, including the cingulum. Scale bar, 50 μm. Inset: Cx, cerebral cortex; SWM, subcortical white matter; Ci, cingulum; LV, lateral ventricle; Hc, hippocampus; CP, choroid plexus; Men, meningeal membrane.

Figure 19. Distribution of PDGF-αR$^+$ cells in the developing rat cerebellum.

Panels A and B, bright- and dark-field images of the P0 cerebellum and adjacent brain regions. A few weakly-positive cells are visible in the internal granule layer of the cerebellum (IGL), but almost none in the superior medullary vellum (SMV) or inferior colliculus (IC). Panels C and D, the P3 cerebellum. PDGF-αR$^+$ cells are more numerous and appear more intensely labelled than before; they are distributed throughout the IGL, but are absent from the molecular layer (ML) and external granule layer (EGL). Panels E and F, the P10 cerebellum. PDGF-αR$^+$ cells in the IGL are concentrated in the developing foliar white matter (WM). The ML and EGL are still negative for PDGF-αR. Panels g and h, the adult rat cerebellum. PDGF-αR$^+$ cells are now present in the (much expanded) ML and the IGL. The intense scattering from the foliar white matter tracts obscures the *in situ* hybridization signal there. At all ages examined, the choroid plexus (CP) and meningeal membranes (Men) are strongly positive for PDGF-αR. The Purkinje cells (which lie at the boundary between the ML and IGL) do not express detectable PDGF-αR. Scale bars, 100 μm.

Figure 19. Distribution of PDGF-αR$^+$ cells in the developing rat cerebellum.

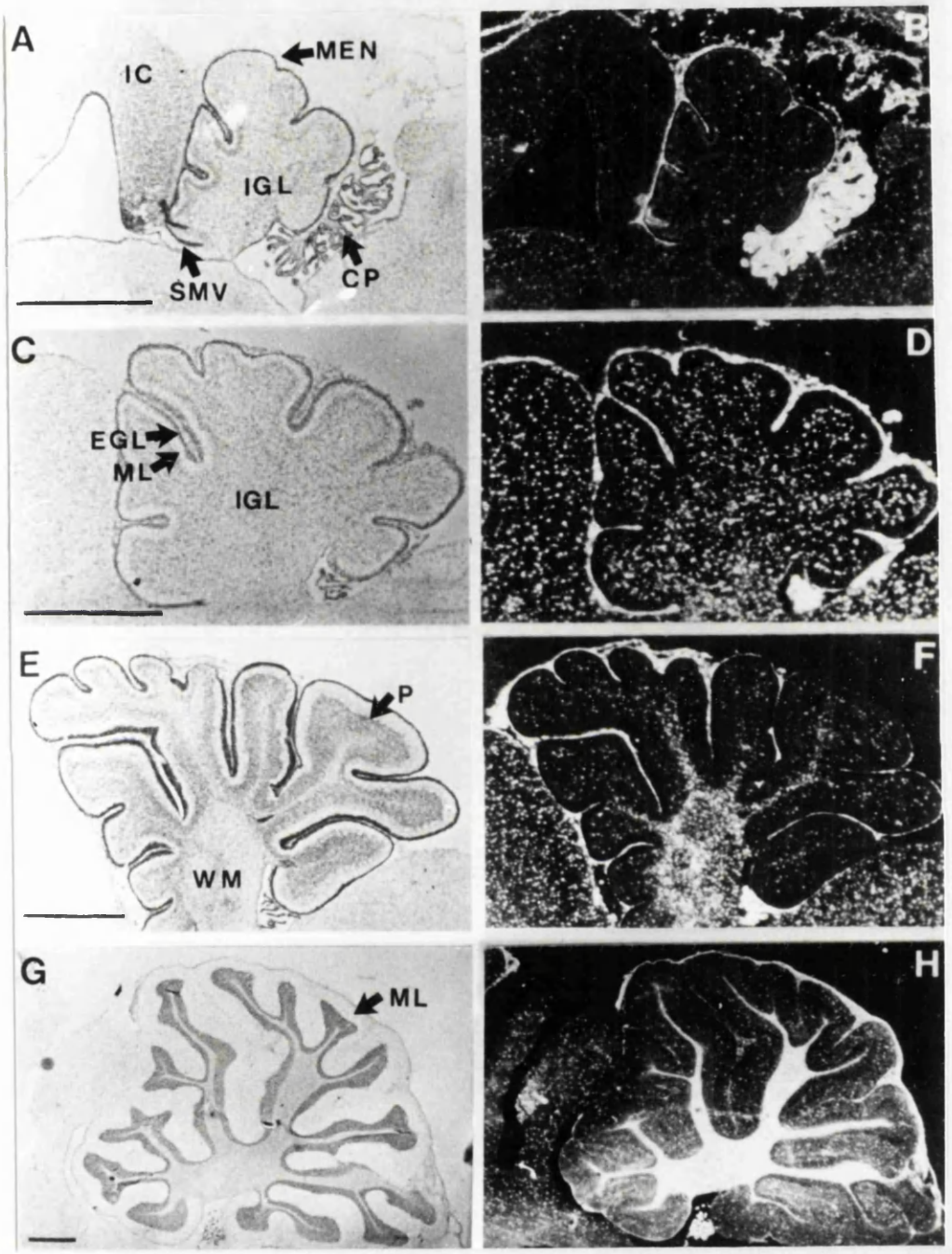

Figure 20. Expression of PDGF-αR mRNA in the P10 rat brain.

Panel A, sagittal section. Panel B, coronal section. PDGF-αR^+ cells are abundant and fairly evenly spaced throughout the brain, being somewhat more concentrated in the corpus callosum and the cerebellar white matter tracts. The choroid plexus within the lateral ventricles, and the meningeal membranes are strongly PDGF-αR^+ as before. Scale bar, 100 μm. Inset: Cx, cerebral cortex; CC, corpus callosum; Hc, hippocampus; Th, thalamus; Hypoth, hypothalamus; Ce, cerebellum; BS, brainstem; P, pons; SC and IC, superior and inferior colliculi; LV, lateral ventricles; OC, optic chiasm.

Figure 20. Expression of PDGF-αR mRNA in the P10 rat brain.

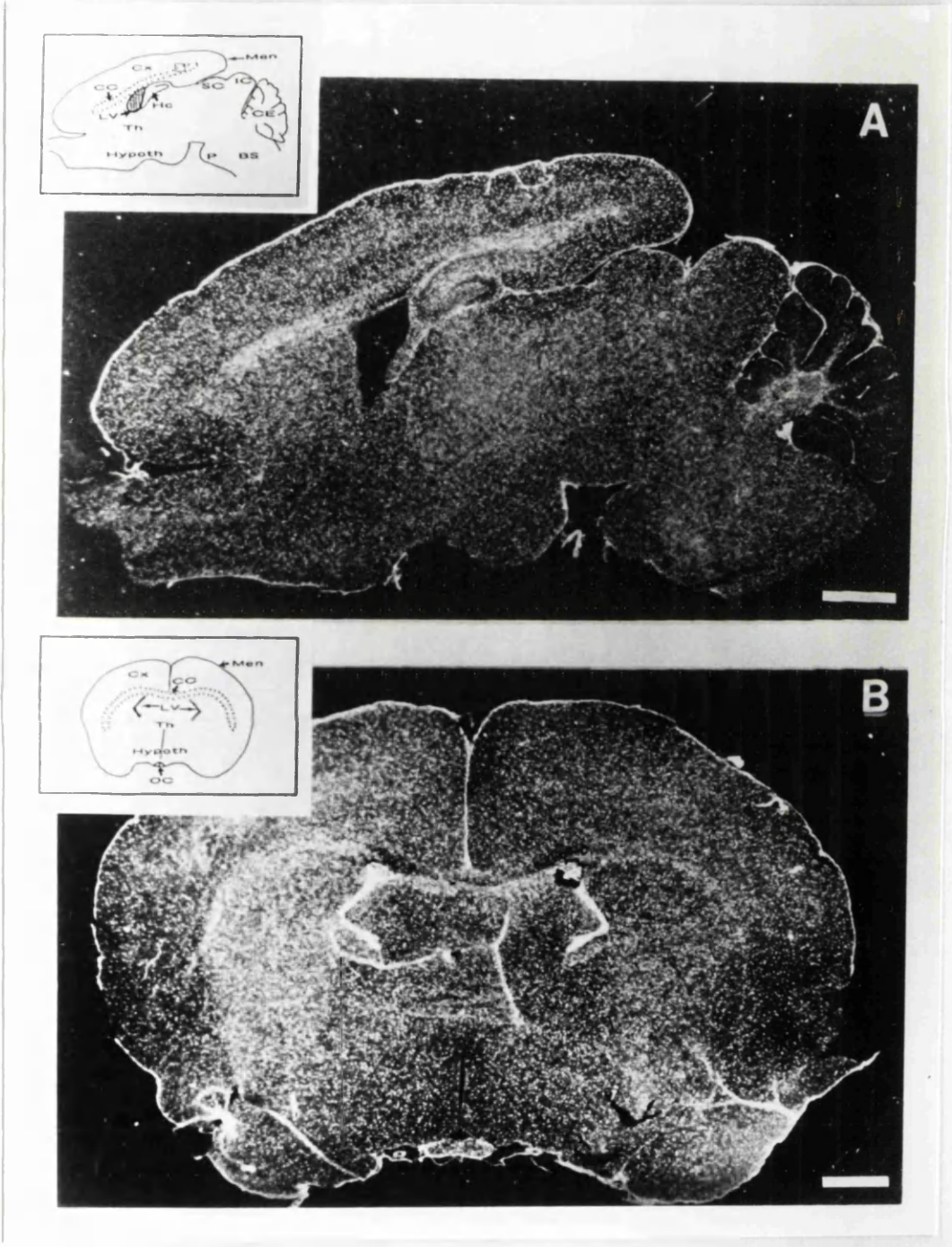

Figure 21. PDGF-αR$^+$ cells in the rat CNS are associated with cells having small densely stained nuclei.

Higher magnification bright field micrograph of the region within the frame of Figure 20A, comprising part of the corpus callosum (CC) and the polymorphous cell layer of the cerebral cortex (CX). Exposed silver grains are associated with cells with small, densely-stained nuclei (black arrows). Neurons with large nuclei (white arrows) are negative for PDGF-αR. Scale bar, 10 μm.

Figure 21. PDGF-αR$^+$ cells in the rat CNS are associated with cells having small densely stained nuclei.

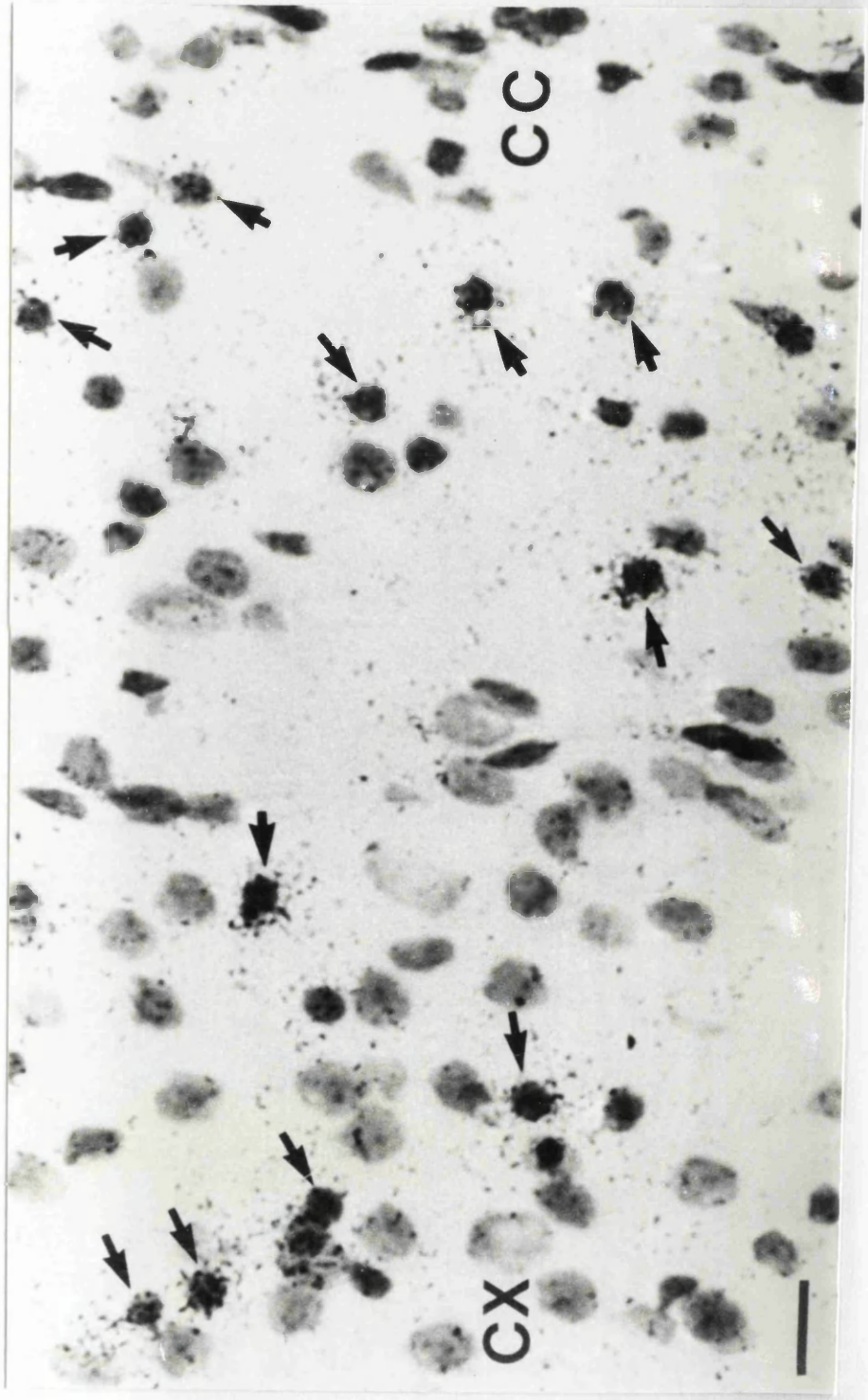

Figure 22. Distribution of PDGF-αR mRNA in the perinatal rat optic nerve (ON) and retina (RET).

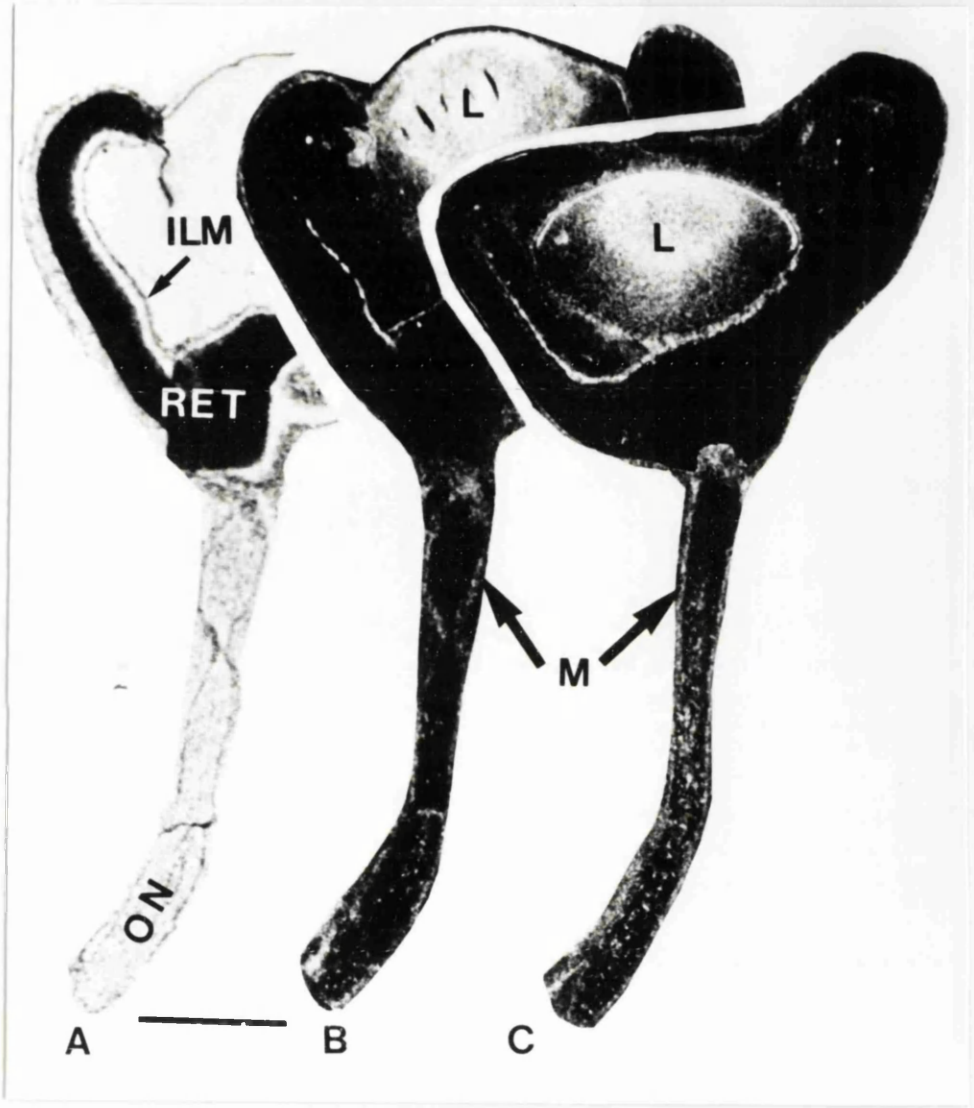

The Figure is a collage of three micrographs. Sections A and B, bright- and dark-field micrographs of a horizontal section through a P0 eye and optic nerve. A few PDGF-αR+ cells are visible in the optic nerve, mostly towards the chiasmal end of the nerve (i.e. away from the eye). Section C, equivalent dark-field image of a P2 eye and optic nerve. At this age, there are many more PDGF-αR^+ cells in the nerve, and these are fairly evenly distributed apart from an exclusion zone next to the eye. At both P0 and P2 there is also intense labelling of the inner limiting membrane (ILM) of the retina, the anterior epithelium of the lens (L) and the meninges (M) around the optic nerve. Scale bar, 100 μm.

Figure 23. Expression of PDGF-αR mRNA in the adult rat forebrain and optic nerves (coronal section).

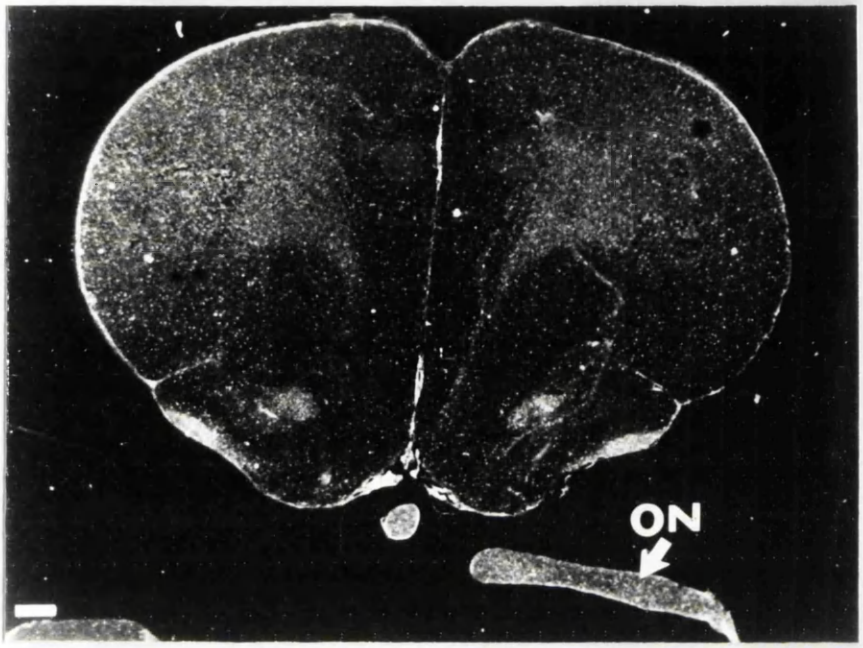

PDGF-αR^+ cells are found in all areas of the adult forebrain and also in the optic nerves (ON). Scale bar, 100 μm.

Figure 24. A speculative view of the spatio-temporal development of the O-2A lineage in terms of the expression of PDGF-αR and various antigenic markers of the O-2A lineage.

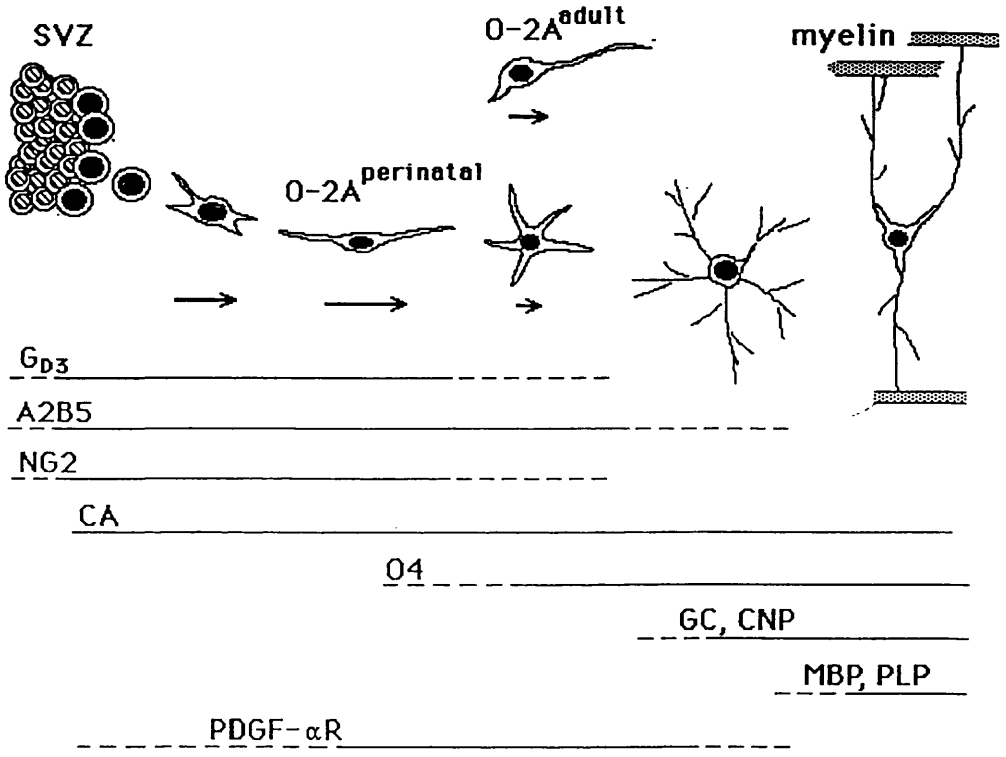

This diagram incorporates ideas and data from many studies, including my own. Antigenic markers not mentioned in the text are: O4, a monoclonal antibody raised against oligodendrocytes (Sommer and Schachner, 1980); PLP, proteolipid protein, a late structural protein of myelin. Dashed lines indicate uncertainty about the precise stage of gain or loss of the marker in question. Arrows indicate migratory cells; SVZ, subventricular zone.

Table 2. Numbers of PDGF-αR^+ cells in the rat CNS at various ages. PDGF-αR^+ cells were counted in dark-field micrographs of *in situ* autoradiographs of the hypothalamus and optic nerve. Total cells numbers were estimated from bright-field micrographs of the same sections, which had been lightly stained with hematoxylin. Between 1000-5000 total cells in at least three different fields of view were scored at each age, and the number of PDGF-αR^+ cells expressed as a percentage of the total. In the hypothalamus the proportion of PDGF-αR^+ cells increases from E16 to P10, when they account for ~8% of the total cells, and drops to ~4% of cells in the adult. In the optic nerve, the proportion of PDGF-αR^+ cells is ~11% at P7, and ~4% in the adult. Numbers of PDGF-αR^+ cells in whole optic nerves were calculated from these percentages and B. Barres' independent measurements (from DNA content) of the total number of cells in the nerve at each age (Barres *et al.* 1992). For comparison I have listed Vaughn's (1969) figures for the proportions of "small glioblasts", counted in electron micrographs of rat optic nerves. From their ultrastructure, these cells probably correspond to O-2A progenitors (Fulton *et al.* 1992). I have also listed numbers of presumptive O-2A progenitors visualized in wholemount preparations of rat optic nerves by quisqualate-stimulated cobalt uptake (Fulton *et al.* 1992). Numbers of O-2A progenitors *in vivo* have also been estimated by counting A2B5+GC$^-$ cells in suspensions of dissociated optic nerve cells (assuming complete recovery after the dissociation procedure). In this way, Miller *et al.* (1985) estimated 6×10^3 O-2A progenitors in the P7 nerve; Small *et al.* (1987) estimated 9×10^3 at P5 and 1.6×10^4 at P9.

Table 2. PDGF-αR$^+$ CELLS IN THE DEVELOPING CNS

HYPOTHALAMUS

Age	*% PDGFαR$^+$ cells*
E16	0.15 ±0.03
E18	3.2 ±0.5
P0	4.8 ±0.2
P10	7.8 ±0.1
P20	6.5 ±0.14
ADULT	4.3 ±0.35

OPTIC NERVES

Age	*% PDGFαR$^+$ cells*		*Total PDGFαR$^+$ cells per nerve*	
P7	11.1 ±0.1	*(~11.5%)**	1.6 x 10^4	*(~1.2 x 10^4)♯*
P15	9.3 ±0.7	*(~11.5%)**	2.4 x 10^4	*(~2.2 x 10^4)♯*
ADULT	3.6 ±0.7	*(~4%)**	1.9 x 10^4	*(~1.8 x 10^4)♯*

* Data taken from Vaughn (1969).
♯ Data taken from Fulton *et al.* (1992).

Table 3. ^{125}I-PDGF-AA binding to enriched cultures of glial cells from rat brain. Different populations of glial cells were isolated as described in Methods, and grown in 24-well plates until semi-confluent (approximately 10^4 cells/well). NIH 3T3 fibroblasts were included as a positive control. ^{125}I-PDGF-AA binding in the presence or absence of competing unlabelled PDGF-AA or PDGF-BB was assessed as described in Methods. Each experiment was performed in duplicate (both results shown) or triplicate (shown as mean ± standard error). Results tabulated are in counts per minute (CPM). NIH 3T3 cells and O-2A progenitors bound ^{125}I-PDGF-AA that could be competed with either PDGF-AA or PDGF-BB, as expected for cells that express PDGF-αR. Neither cultured cortical astrocytes nor microglial cells bound ^{125}I-PDGF-AA in a competable fashion, and therefore appear not to express PDGF-αR.

Table 3. ^{125}I-PDGF-AA BINDING TO ENRICHED CULTURES OF GLIAL CELLS

COMPETITOR:-	NONE	PDGF-AA	PDGF-BB	BACKGROUND (No cells)
O-2A PROGENITORS				
Expt 1	1,523±35	421±40	231±9	483±120
Expt 2	294±20	85±11	ND	ND
MICROGLIA				
Expt 3	473	984	1092	741
	598	1122	710	876
Expt 4	625	964	ND	717
	837	827	ND	776
CORTICAL ASTROCYTES				
Expt 5	139±15	199±31	167±26	ND
Expt 6	209	250	167	ND
	293	203	116	ND
NIH 3T3				
Expt 7	3,030±40	645±145	407±10	ND

Table 4. ^{125}I-PDGF-BB BINDING TO ENRICHED CULTURES OF CORTICAL ASTROCYTES

COMPETITOR:-	NONE	PDGF-AA	PDGF-BB
CORTICAL ASTROCYTES			
	1,899	1,572	558
	2,399	2,239	481

Table 4. ^{125}I-PDGF-BB binding to enriched cultures of cortical astrocytes. Rat cortical astrocytes were isolated as described in Methods, and grown in 24-well plates until semi-confluent (approximately 10^4 cells/well). ^{125}I-PDGF-BB binding in the presence or absence of competing unlabelled PDGF-AA or PDGF-BB was assessed as described in Methods. Each experiment was performed in duplicate and both results shown. Results tabulated are in counts per minute (CPM). Cortical astrocytes specifically bound ^{125}I-PDGF-BB, that could be competed with PDGF-BB, but not PDGF-AA. This results is consistent with cortical astrocytes expressing the PDGF-ß receptor.

Discussion.

I have used *in situ* hybridization to visualize cells that express PDGF-αR mRNA in the rat CNS. From the spatial distribution of PDGF-αR$^+$ cells in the mature CNS, and the way these cells accumulate during development, I conclude that PDGF-αR is expressed by a subset of glial cells, but not neurons. I further conclude that PDGF-αR may be restricted to a single glial cell lineage in the CNS, the oligodendrocyte-type-2 astrocyte (O-2A) lineage. This conclusion is based on correlations between the distribution of PDGF-αR mRNA and histochemical markers of the O-2A lineage *in situ* (Reynolds and Wilkin, 1988; Hardy and Reynolds, 1991; LeVine and Goldman, 1988a,b), and *in vitro* studies that demonstrate PDGF-αR on O-2A lineage cells (Hart *et al,*. 1989; McKinnon *et al,*. 1990) but not other types of glial cells in culture (Hart *et al,*. 1989 and table 3). PDGF-αR$^+$ cells were found in most regions of the CNS, but occurred relatively infrequently in the subventricular germinal layer, suggesting that O-2A lineage cells either originate before the times investigated in these experiments or that they may not start to express PDGF-αR until after (or just before) they migrate away from the subventricular zones towards their final destinations.

PDGF-αR is expressed by glial cells, not neurons.

The spatial distribution of PDGF-αR$^+$ cells in the postnatal rat CNS argues against these cells being neurons. Large numbers of PDGF-αR$^+$ cells are present in developing white matter tracts such as the corpus callosum (Figure 20), the foliar white matter of the cerebellum (Figure 19) and the optic nerve (Figure 22); these cells cannot all be neurons because there are few neuronal cell bodies in white matter generally, and none in the optic nerve. Even outside of white matter, the

pattern of PDGF-αR$^+$ cells is not what would be expected for neurons; PDGF-αR$^+$ cells are distributed rather uniformly throughout the CNS, and are quite widely spaced, whereas the cell bodies of neurons are often closely packed in groups or sheets. For example, neurons in the postnatal cerebral cortex are arranged in discrete lamellae, whereas PDGF-αR$^+$ cells show no sign of stratification, being distributed more-or-less evenly throughout the cortex (see Figure 20, for example). Moreover, cells that are easily recognizable as neurons because of their location and/or distinctive morphology, such as cerebellar Purkinje cells (Figure 19), retinal ganglion neurons (Figure 22) or hippocampal neurons (Figure 20), are invariably negative for PDGF-αR.

The time course on which PDGF-αR$^+$ cells populate the developing CNS also argues for these cells being of glial, not neuronal lineage. Most neurons in the rat CNS become postmitotic before birth, whereas PDGF-αR$^+$ cells continue to increase in number for some time after birth. In the cerebral cortex, for example, neurons are born in the subventricular zone between E11 and P0, with the peak time of production around E16/E17. As they are born, the neurons migrate away from the subventricular zone towards the pial surface, each wave of cells travelling further than the preceding one, so that those neurons that are born last end up closest to the pial surface (Jacobson, 1970). In contrast, PDGF-αR$^+$ cells do not appear in the cortex until about E18, at which time they are confined to the lateral extremities of the intermediate zone (developing subcortical white matter) (Figure 16). PDGF-αR$^+$ cells subsequently spread throughout the cortex and continue to increase in numbers until at least P10, before declining again in the adult (Figures 14 to 16; Table 2). Thus, the spatial distribution of PDGF-αR$^+$ cells in the developing and mature CNS, and the fact that they seem to proliferate postnatally, argue strongly that these cells correspond to glial cells, not neurons.

This conclusion is further supported by the appearance of the PDGF-αR$^+$ cell nuclei in haematoxylin-stained sections; invariably, the PDGF-αR hybridization signal is associated with small, round, densely-stained nuclei that are characteristic of glial cells (Figure 21). Blood vessels are readily apparent in these tissue sections, often being marked by rows of cells with elongated nuclei. These cells, which presumably represent endothelial cells and/or circulating blood cells, are always negative for PDGF-αR.

Is PDGF-αR restricted to the O-2A lineage?

O-2A lineage cells, but not other classes of glial cells, express PDGF-αR in vitro.

What is known about PDGF receptors on glial cells? Hart *et al,*. (1989) performed ^{125}I-PDGF binding experiments on cells freshly isolated from perinatal rat optic nerves, and the same cells grown for one day *in vitro*, and found that O-2A progenitor cells possess PDGF receptors with the binding characteristics of PDGF-αR, but no detectable PDGF-βR (Hart *et al,*. 1989). This finding has since been corroborated by northern and western blot analysis of O-2A progenitor-enriched cultures prepared from perinatal rat cerebral cortex (McKinnon *et al,*. 1990). Newly formed, postmitotic oligodendrocytes that develop in cultures of perinatal rat optic nerve cells initially retain PDGF-αR on their surface, but this is lost over the succeeding two or three days *in vitro* (Hart *et al,*. 1989). Type-1 astrocytes, the other major macroglial cell type in the optic nerve, do not appear to express either PDGF-αR or PDGF-βR. Of the remaining cells in these cultures, which can constitute up to 60% of the total and consist mainly of microglial cells, endothelial cells, fibroblasts and leptomeningeal cells, less than 5% possess detectable PDGF-αR or PDGF-βR (Hart *et al,*. 1989). I have performed ^{125}I-PDGF binding and northern blot analyses

on cultured astrocytes from rat cerebral cortex, and find that these cells possess PDGF-ßR, but not PDGF-αR (table 3 and table 4). Moreover, I can detect no specific binding of ^{125}I-PDGF-AA to microglial cells *in vitro*, indicating that microglia do not express PDGF-αR either (Table 3). Thus, apart from cells in the meningeal membranes and choroid plexus (Figs 14-16), the only cells in the CNS that are known to express PDGF-αR are O-2A progenitors and newly formed oligodendrocytes.

PDGF-αR$^+$ cells, like O-2A progenitors, appear to migrate into the postnatal optic nerve from the optic chiasm.

How does my data on the accumulation of PDGF-αR$^+$ cells in the developing CNS compare with what is known about the development of the O-2A lineage *in vivo*? There is persuasive circumstantial evidence that O-2A progenitors are migratory cells *in vivo*, moving into developing white matter tracts from nearby germinal zones. For example, Small *et al,*. (1987) found evidence consistent with the idea that O-2A progenitors migrate into the developing rat optic nerve from germinal zones in the brain *via* the optic chiasm. They cut optic nerves into thirds, dissociated the cells and counted O-2A progenitors in each third separately in suspension. On the day of birth, there were relatively few O-2A progenitors in the nerve, and these were distributed in a gradient increasing towards the chiasmal end of the nerve. By P5 this gradient of cell number had largely disappeared, and the total number of cells had increased appreciably. These results are comparable with my data on the accumulation of PDGF-αR$^+$ cells in the nerve. At birth, there are relatively few PDGF-αR$^+$ cells in the nerve and these are concentrated towards the chiasmal end of the nerve (Figure 22). By P2, the number of PDGF-αR$^+$ cells is several-fold higher (Table 2), and they are distributed fairly uniformly along the nerve except for a small exclusion zone next to the eye (Figure 22). This exclusion zone includes the

lamina cribrosa, a specialized structure that behaves as a physical barrier to prevent migration of O-2A progenitors into the retina (ffrench-Constant *et al,*. 1988), which in most mammals remains unmyelinated throughout life.

The total number of PDGF-αR^+ cells in the rat optic nerve, extrapolated from numbers counted in sections of isolated nerves (Table 2), is in good agreement with the total number of O-2A progenitor cells estimated by other workers (Table 2), providing further evidence that PDGF-αR^+ cells correspond to O-2A progenitors. Since the numbers of PDGF-αR^+ cells are much less than the number of mature oligodendrocytes in the P15 and adult nerves (Vaughn *et al,*. 1969), I conclude that oligodendrocytes stop expressing PDGF-αR soon after they differentiate *in vivo*, just as they do *in vitro* (Hart *et al,*. 1989).

PDGF-αR^+ cells in the cerebral cortex: comparison with previous studies of O-2A lineage development in situ.

At least two groups have studied the development of the O-2A lineage in the anterior forebrain by immunohistochemistry *in situ*. LeVine and Goldman (1988a,b) used a panel of antibodies including antibodies to ganglioside G_{D3}, which is expressed on the surface of immature neuroectodermal cells (Goldman *et al,*. 1984), antibodies to carbonic anhydrase (CA), which is expressed mainly in oligodendrocytes (Cammer, 1984) but also in some astrocytes (Cammer and Tansey, 1988), antibodies against galactocerebroside (GC), a specific marker for oligodendrocytes in the CNS (Raff *et al,*. 1978), and antibodies against myelin basic protein (MBP). From E16 into postnatal life, anti-G_{D3} labelled small, round cells in the subventricular zones of the lateral ventricles. Anti-CA labelled cells with a variety of shapes from large, round cells that also labelled with anti-G_{D3}, to cells with the antigenic phenotype

($G_{D3}^{-}GC^{+}MBP^{+}$) and morphology of mature oligodendrocytes. The large, round CA^{+} cells were first seen at E16 in the subventricular zones and in the intermediate zone (presumptive subcortical white matter); these were presumed to be the earliest cells committed to the oligodendrocyte lineage. At E18 the large, round cells were also found in the cingulum, and smaller $G_{D3}^{+}CA^{+}$ cells with a few thick processes appeared in the subventricular zones at the lateral tips of the lateral ventricles, and in the more lateral aspects of the subcortical white matter. Between E18 and E20 $G_{D3}^{+}CA^{+}$ cells spread throughout the formative cortical white matter and overlying gray matter.

Hardy and Reynolds (1991) also studied oligodendrocyte development in the cerebral cortex by immunohistochemistry with anti-G_{D3}, anti-vimentin, anti-GC and anti-MBP, as well as antibodies to the myelin-specific cyclic nucleotide phosphodiesterase (CNP). These authors did not look at stages earlier than E19 but, at this age and above, their results were generally concordant with those of LeVine and Goldman (1988a,b). At E19-E20 they observed G_{D3}^{+}vimentin^{-} cells that were either large and round, or smaller and bipolar, predominantly in the formative subcortical white matter, but also in the subventricular zones and the grey matter; some of these latter G_{D3}^{+} cells may have been immature neurons. Between P0 and P2, many G_{D3}^{+} cells were present in the subventricular zones and throughout the cortical grey and white matter; a few cells in the subventricular zone and inferior white matter co-expressed G_{D3} and GC at this time. By P3-P4, the number of G_{D3}^{+} cells had declined and these were found mainly in the cingulum and subcortical white matter adjacent to the subventricular zone. G_{D3}^{+} cells were seen in decreasing numbers up to P12, while the numbers of cells expressing GC, CNP and MBP increased.

Is it possible to integrate these results with my own data on PDGF-αR^+ cells in the forebrain? At E16, I see a few PDGF-αR^+ cells inferior to the lateral ventricles outside of the subventricular zones, but none in the cerebral cortex (Figure 15). I do not see PDGF-αR^+ cells in the cortex until E18, at which time they are confined to the lateral aspects of the presumptive subcortical white matter (Figure 16). I also see some PDGF-αR^+ cells at the periphery of the subventricular zones at the lateral extremities of the lateral ventricles at E18 (Figure 16), but none in the vicinity of the cingulum. At P0, PDGF-αR^+ cells are concentrated in the formative white matter, including the cingulum, and extend into the cortical grey matter up to the pial surface (Figs. 17 and 18). I believe that my data is compatible with those of LeVine and Goldman (1988a,b), if I assume that the G_{D3}^+ cells they observe in the subventricular zone are immature neurons, another explanation is that O-2A lineage cells may not start to express PDGF-αR until some time after they first become $G_{D3}^+CA^+$, i.e. after the "large, round" stage of their development. This might explain why I do not see any PDGF-αR^+ cells in the subventricular zone or intermediate zone at E16, or in the cingulum at E18. I presume that *in vivo*, as *in vitro*, the O-2A lineage cells retain PDGF-αR until shortly after they start to express early markers of oligodendrocyte differentiation such as GC (Hart *et al*,. 1989) (see Figure 24 for a schematic diagram).

It seems plausible, as suggested by LeVine and Goldman (1988a,b), that O-2A lineage cells migrate from subventricular germinal zones at or near the lateral tips of the lateral ventricles, first medially along the developing subcortical white matter tracts and then radially into the overlying cortex. This pattern of migration is also suggested by the way the distribution of PDGF-αR^+ cells evolves during cortical development (Figs 15 and 16). However, it is also possible that PDGF-αR^+ cells are

arise elsewhere in the CNS and I am observing the migration of these cells from the time they appear at the lateral tips of the lateral ventricles.

PDGF-αR$^+$ cells in the developing cerebellum.

LeVine and Goldman (1988a) observed $G_{D3}{}^+CA^+$ putative O-2A lineage cells with a gradation of morphologies in the P3 cerebellum, ranging from large, round cells without processes at the base of the cerebellum and in the presumptive germinal zones in the inferior colliculus (roof of the fourth ventricle), to more complex, process-bearing cells in the foliar white matter. Levine and co-workers studied a population of putative O-2A lineage cells in the developing rat cerebellum with antibodies to the NG2 chondroitin sulphate (Levine and Card, 1987; Levine and Stallcup, 1987). They found small numbers of NG2$^+$ cells in the cerebellar anlagen at E16; the number of these cells increased up to P5 and declined thereafter. In the adult, NG2$^+$ cells were especially prominent in the molecular layer. Reynolds and Wilkin (1988) found a few $G_{D3}{}^+$ cells in the developing inferior colliculus, the superior medullary vellum (the thin neck of tissue that connects the inferior colliculus to the base of the cerebellum) and the primitive folia of the P0 cerebellum. At P2, many $G_{D3}{}^+$ cells were present in the base of the cerebellum and throughout the folia, but not in the superior medullary vellum (SMV). From P2-P5, the $G_{D3}{}^+$ cells became progressively localized to the developing white matter tracts, and GC^+CNP^+ cells began to accumulate. After P7, the number of $G_{D3}{}^+$ cells dwindled, until at P12 they were no longer detected. Large numbers of cells expressing one or more oligodendrocyte markers developed after the first postnatal week, first in the foliar white matter tracts and later in the internal granule cell layer, Purkinje cell layer and, after P15, in the molecular layer.

These studies suggested that oligodendrocyte precursors migrate after birth from germinal zones around the roof of the fourth ventricle, through the SMV and peduncles into the developing cerebellum. My own data on the accumulation of PDGF-αR^+ cells in the cerebellum (Figure 19) is reasonably compatible with these previous investigations.

Thus my hypothesis, that PDGF-αR^+ cells in the CNS represent predominantly (or exclusively) O-2A lineage cells, seems both internally consistent and compatible with previously published data. I presume that O-2A progenitors continue to express PDGF-αR until shortly after they differentiate into oligodendrocytes, as they do *in vitro* (Hart *et al,*. 1989) (see Figure 24).

PDGF-αR^+ cells in the adult CNS: O-2A$^{\underline{adult}}$ progenitors?

I observe PDGF-αR^+ cells in most regions of the adult (approximately 6 months old) rat CNS including the optic nerve, cerebral cortex and the molecular layer of the cerebellum (Figures 23 and 19, panel H), although they are less abundant and appear less intensely labelled than in young animals. It is known that O-2A progenitor cells persist in the adult CNS (ffrench-Constant and Raff, 1986; Wolswijk and Noble, 1989), where they presumably are required to replace oligodendrocytes that die naturally or as a result of injury. Alternatively, they might perform some other function unrelated to myelination in the adult. These O-2A^{adult} progenitors have somewhat different properties *in vitro* than their perinatal counterparts; they divide more slowly and take longer to differentiate *in vitro*, for example (Wolswijk and Noble, 1989). It has been reported (Chan *et al,*. 1990) that O-2A^{adult} progenitors do not respond to PDGF *in vitro*, raising the possibility that they might no longer possess PDGF receptors. However, that study employed the PDGF-BB isoform, which has a significantly lower affinity than PDGF-AA for PDGF-αR (Heldin *et al,*.

1988). It may be that O-2A^{adult} progenitors express reduced levels of PDGF-αR and for this reason, together with the lower affinity of PDGF-αR for PDGF-BB, they do not readily respond to PDGF-BB. Other workers found that O-2A^{adult} progenitors do divide in response to PDGF-AA *in vitro* (Wolswijk *et al,*. 1991). Thus, it seems a reasonable supposition that PDGF-αR$^+$ cells in the adult CNS represent O-2A^{adult} progenitors and/or their newly differentiated progeny.

Conclusions.

In summary, I have provided circumstantial evidence that argues in favour of the idea that PDGF-αR is expressed by O-2A lineage cells in the CNS, but not by neurons or other types of glial cells. Definitive proof of this hypothesis would require double-labelling studies with antibodies directed against specific subtypes of CNS cells. Nevertheless, at the ages studied, the fact that PDGF-αR$^+$ cells occur mainly outside of the presumptive germinal zones in the subventricular layer suggests that these cells either originate before the times investigated in these experiments or that they may not start to express PDGF-αR until after (or just before) they have migrated away from the ventricular zones. The question of the origin of these cells is the subject of my next chapter of results.

CHAPTER 5

PLATELET DERIVED GROWTH FACTOR ALPHA RECEPTOR DEFINES A SINGULARITY IN THE DEVELOPING RAT SPINAL CORD: A POSSIBLE ORIGIN OF CELLS BELONGING TO THE OLIGODENDROCYTE LINEAGE

INTRODUCTION

In the previous chapter of results I have presented evidence suggesting that during late neurogenesis PDGF-αR expression might be restricted to cells of the oligodendrocyte lineage.

The ultimate origin of cells belonging to the oligodendrocyte lineage is presumably the ventricular zones, which are the major areas of mitosis within the CNS. At ages after E16 I observed few PDGF-αR^+ cells within the ventricular zones of the rat CNS. This led me to speculate that these PDGF-αR^+ cells did not begin to express PDGF-αR mRNA until after they had left the ventricular zone, or that these cells arose before E16. As O-2A progenitor cells are thought to be migratory *in vivo*, it is possible that these cells might arise elsewhere in the CNS and subsequently migrate to their final destinations. The distribution of PDGF-αR^+ cells within the developing cerebral cortex, particularly between E18 and P0, was suggestive of this. In the rat spinal cord Warf *et al.* (1991) observed that cells with the potential to become oligodendrocytes were present at E14. Thus, in the spinal cord, cells belonging to the oligodendrocyte lineage appear to be present at ages predating my previous study in the brain. To investigate the distribution of PDGF-αR^+ cells during early neurogenesis I performed *in situ* hybridization on rat spinal cord from E12 to E18, and also on rat brain from E12 to E15. The experiments described in this chapter, revealed a transient singularity of PDGF-αR expression in the ventricular zone of the embryonic spinal cord that I propose marks the emergence of the O-2A lineage in the cord. I also present evidence suggesting that oligodendrocyte precursors in the forebrain and midbrain originate in a restricted region of the ventricular zone of the third ventricle, in the ventral half of the developing diencephalon. My data also provides a striking illustration of the high

degree of spatial resolution with which gene expression and cell fate can be regulated along the dorsoventral axis of the neural tube.

RESULTS

To map the distribution of PDGF-αR mRNA in the developing rat CNS, I performed *in situ* hybridization experiments with a ^{35}S-RNA probe corresponding to part of the extracellular domain of the rat PDGF-αR. This probe specifically recognizes PDGF-αR mRNA (see figure 14) and does not cross-hybridize with PDGF-βR mRNA (see last chapter) which is also known to be present in the developing rat CNS (Sasahara *et al.*, 1991). Cryostat sections (15 μm nominal thickness) of embryonic rats (E12, E13, E14, E15, E16 and E18) were subjected to *in situ* hybridization with the PDGF-αR probe, as described in Methods. Subsequently, sections were subjected to autoradiography, lightly stained with hematoxylin and examined in the microscope under bright- and dark-field illumination. Control experiments with ^{35}S-RNA PDGF-αR probes homologous to PDGF-αR mRNA ("sense" probes) gave no autoradiographic signal above background at any of the ages studied.

Development of the spinal cord

Development of the spinal cord proceeds both in a rostral-caudal direction and also in a ventral-dorsal direction (Altman and Bayer, 1984; Nornes and Das, 1974). The spinal cord is divided at its midline into two halves delimitated by the sulcus limitans, the alar (dorsal) and basal (ventral) halves. By taking a series of sections from the sacral (caudal) level to the cervical (rostral) level approximately a day and half of development can be studied in one animal (Altman and Bayer, 1984). The ventral-dorsal development of the spinal cord follows a wave of mitotic divisions in the ventricular zone, which initiates ventrally and terminates dorsally. Initially motor

neurons originate from the ventral region of the basal ventricular zone, followed by the relay neurons which originate from the dorsal region of the basal ventricular zone. Finally the interneurons originate from the alar ventricular zone. Following their final cell division these neurons subsequently migrate to their final destinations within the spinal cord (Altman and Bayer, 1984; Nornes and Das, 1974).

PDGF-αR expression in the alar ventricular zone of the developing spinal cord

Figure 25 shows transverse sections from an E13 rat at the level of the brainstem (Figure 25, panels B and D) and lumbar region of the spinal cord (Figure 25, panels A and C), photographed in bright-field and dark-field illumination. PDGF-αR is strongly expressed in the meningeal membrane surrounding the spinal cord and brainstem, and also in surrounding non-CNS tissues. Within the dorsal half of the spinal cord, PDGF-αR expression is restricted to a narrow band of expression at the lumbar level (Figure 25, panel C, denoted by arrows) corresponding to a region within the alar (dorsal) ventricular zone. This PDGF-αR expression extends throughout the length of the cord and expands to fill the dorsal aspects of the brainstem ventricular zone (Figure 25, panel D). No PDGF-αR expression is seen in the spinal cord or brainstem at E12 (data not shown), suggesting that expression in this region of the CNS begins at around E13.

By E14 this dorsal PDGF-αR expression has extended to the fill the dorsal portion of the alar ventricular zone. This is illustrated in Figure 28 which shows transverse sections taken at the cervical, thoracic and sacral levels of an E14 spinal cord and photographed in dark-field and bright-field illumination. PDGF-αR expression, in the alar (dorsal) ventricular zone appears to diminish in a caudal-to-rostral direction (compare figure 28, panel D with panel F). PDGF-αR expression has disappeared from the dorsal ventricular zone at all levels of the spinal cord by

E16. This is illustrated in figure 29, which shows transverse sections taken at the cervical, thoracic and sacral levels of the spinal cord and photographed in dark-field and bright-field illumination. No PDGF-αR expression is observed in the dorsal half of the cord.

This transient PDGFαR expression in the alar plate presumably represents expression by developing sensory interneurons, which arise from this region of the alar ventricular zone (Altman and Bayer, 1984; Nornes and Das, 1974), This raises the question of whether these neurons can respond to PDGF (which is expressed at high levels in the cord, Yeh *et al.*, 1991) and if so how? However, whilst this restricted expression of PDGF-αR in the alar ventricular zone is intriguing, the most striking expression occurs in the basal half of the spinal cord.

PDGF-αR expression in the ventral (basal) region of the developing spinal cord at E14

Figure 26, panel A, shows a sagittal section of an E14 rat embryo and photographed in dark-field illumination. PDGF-αR is expressed strongly in many regions outside the CNS (described later). Within the spinal cord, a discrete column of PDGF-αR expression can be seen in the basal (ventral) half of the cord. This is captured in figure 26, panel A, at the sacral and lower lumbar levels of the cord (open white arrows) and can also be seen extending into the tegmentum of the hind brain and even someway into the medial tegmental neuroepithelium of the midbrain. This column of PDGF-αR expression extends throughout the spinal cord at this age, But lies just outside the plane of section at the thoracic and cervical levels in the section shown in Figure 26, panel A. This column of PDGF-αR expression is illustrated in more detail in figure 27 which shows a longitudinal section taken through an E14 spinal cord and photographed in dark-field illumination

Examination of transverse sections taken from different levels of an E14 embryo allowed me to follow the development of this ventral PDGF-αR expression over a time course of approximately one and half days. Figure 28 shows three sections taken from the sacral, thoracic and cervical levels of an E14 embryo and photographed in bright-field and dark-field illumination (the approximate levels of these sections is indicated in figure 26, panel A, by open black arrows). In the basal half of the spinal cord, at the sacral level, PDGF-αR expression (figure 28, panels A and D) is restricted to two tiny areas in the ventricular zone, on opposite sides of the central canal. At the thoracic level (developmentally more advanced than the sacral level by ~16 hours) this basal region of PDGF-αR expression appears larger and more intense, and an individual PDGF-αR^+ cell can be seen lying close to, but separate from this region (Figure 28, panel E). At the cervical level of the spinal cord this region of PDGFαR expression is further expanded, and individual PDGF-αR^+ cells appear to be dispersing from this central region into the grey matter (Figure 28, panel F).

The earliest time that I see PDGF-αR^+ cells in the basal half of the spinal cord is in the brainstem at E13 (Figure 25, panel D, white arrow). I can find no expression within the basal half of the spinal cord at any level at this age (eg. Figure 25, panel C). At E12 I can detect no PDGF-αR expression in any region of the spinal cord (data not shown).

PDGF-αR expression in the basal ventricular zone of the spinal cord at E14 is restricted to a column of cells, 2-3 cells wide

Figure 29 shows a high power bright-field photomicrograph of the E14 basal ventricular zone (illustrated in figure 28, panel A) at the lumbar level of the cord. The developed silver grains lie mainly outside of the depth of field of the photograph

and the restricted region of PDGF-αR expression is marked with arrows. PDGF-αR expression is restricted to the two adjacent cells within the ventricular zone, lying either side of the central canal. These PDGF-αR$^+$ cells within the ventricular zone do not appear to differ in any obvious way from their neighbouring cells. To my knowledge this extremely discrete localization of PDGF-αR expression within the basal ventricular zone appears to be unique and unlike the restricted expression patterns previously described for any other genes within the ventricular zone (see discussion).

In the E16 spinal cord, PDGF-αR$^+$ cells are distributed in rostral-caudal and ventral-dorsal gradients

Figure 26, panel B, shows a sagittal section taken through an E16 rat embryo and photographed in dark-field illumination. Unlike at E14 (Figure 26, panel A), many individual PDGF-αR$^+$ cells can be seen in the brain and the spinal cord. The restricted PDGF-αR expression pattern in the basal ventricular zone has largely disappeared by this age (see also Figure 30, panels D,E and F). Within the spinal cord, the distribution of PDGF-αR$^+$ cells show a distinct rostral-caudal and ventral-dorsal gradient of dispersion; there are many more PDGF-αR$^+$ cells at the cervical level of the cord that at the sacral level, and at any one level of the spinal cord the majority of these cells lie in the basal (ventral) half of the cord. This predominantly ventral distribution is illustrated clearly in Figure 30, which shows bright-field and dark-field photomicrographs of transverse sections through an E16 rat spinal cord taken at the lumbar level (panels A and D), the thoracic level (panels B and E) and the cervical level (panels C and F). The approximate levels of these sections are indicated in Figure 26, open black arrows. At the lumbar level (Figure 30, panels A and D) the majority of PDGF-αR$^+$ cells lie in the basal (ventral) half of the cord,

only a few PDGF-αR$^+$ cells being visible in the alar (dorsal) half. At the developmentally more advanced thoracic level (Figure 30, panels B and E) more PDGF-αR$^+$ cells are apparent and these are distributed more-or-less as in the lumbar region. At the even more developmentally advanced cervical level (Figure 30, panels C and F) there appear to be more PDGF-αR$^+$ cells than at any other level, the majority of which still lie in the basal (ventral) half of the cord.

These results suggest that PDGF-αR$^+$ cells are either migrating from the basal plate towards the alar plate, or that a wave of differentiation sweeps across the spinal cord from the basal to alar halves inducing isolated cells to express PDGF-αR.

PDGF-αR$^+$ cells are found throughout the spinal cord by E18.

Figure 31 shows transverse sections of an E18 spinal cord at the cervical (Figure 31, panel A) and lumbar level (Figure 31, panel B) photographed in dark-field illumination. The numbers of PDGF-αR$^+$ cells within the spinal cord has increased compared to E16 (compare figure 30 with figure 31), and PDGF-αR$^+$ cells are now found throughout the spinal cord, although the greatest density of cells is still found in the basal (ventral) half of the cord.

Figure 32 shows a bright-field photomicrograph of PDGF-αR$^+$ cells in the developing white matter of the spinal cord at E18. These cells have small densely stained nuclei, often regarded as a hallmark of glial cells. In some cases the nuclei of PDGF-αR$^+$ cells can be seen in various stages of cell division in both the white matter and grey matter of the cord (although this is not obvious in Figure 32). There are few, if any, neuronal cell bodies in the white matter of the spinal cord, suggesting that the PDGF-αR$^+$ cells are likely to be glial.

Figure 25. Distribution of PDGF-αR mRNA in the brainstem and spinal cord at E13.

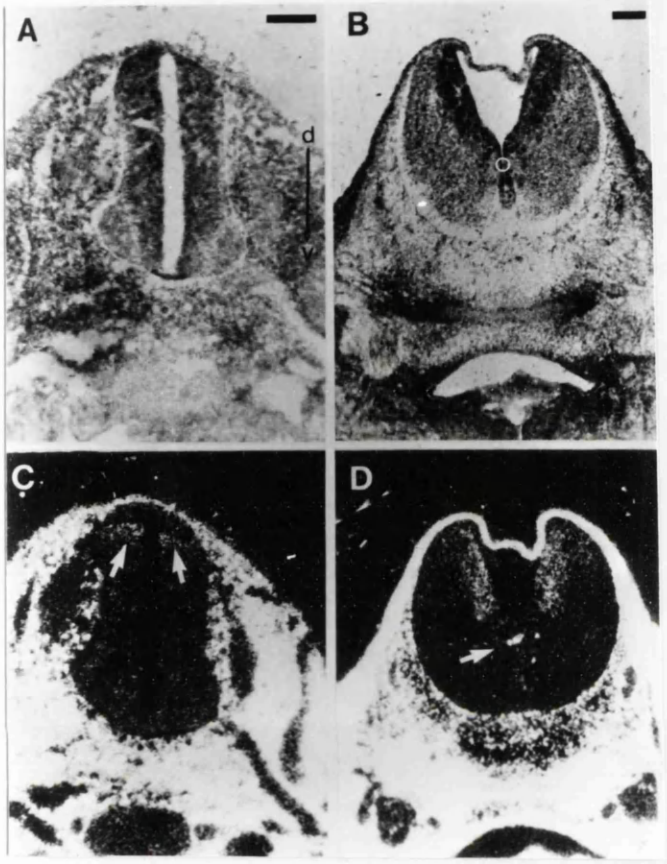

Illustrated are two transverse sections at the level of the brainstem and lumbar region of an E13 rat spinal cord. Cryosections (15 μm nominal thickness) were subjected to in situ hybridization and autoradiography, using ^{35}S-labelled single stranded RNA probes specific for PDGF-αR. The exposed silver grains were developed and the sections photographed in bright- and dark-field illumination. Panels A and C show the lumbar region of the spinal cord in bright- and dark field illumination. A discrete band of PDGF-αR expression can be seen in the alar plate (white arrows). Panels B and D show the brainstem, photographed in bright- and dark-field illumination. PDGF-αR expression is seen in the dorsal aspects of the brain stem. A discrete area of PDGF-αR expression is seen in the ventral half of the brain stem (white arrow). The staining is restricted to the ventricular zone and two individual PDGF-αR$^+$ cells, which can be seen lying to one side. The white ring in panel B illustrates the position of the discrete ventricular zone staining seen in panel D.

Scale bar, 100 μm.

Figure 26. Distribution of PDGF-αR mRNA in an E14 and E16 rat embryo.

Illustrated are two sagittal sections at the level of the midline and photographed in darkfield illumination. Many craniofacial structures are strongly labelled as is the cartilage surrounding the developing vertebrae, meninges, skin and intestines. The CNS has little PDGF-αR expression at E14 (panel A) but clearly visible is a discrete column of PDGF-αR expression in the ventral side of the basal ventricular zone. (lower white arrow). This column of cells can also be seen extending into the hind brain (upper white arrow). This column of expression extends the length of the spinal chord, as can be seen in a series of transverse sections cut at intervals along the cord (see figure 27), but is just out of the plane of section in panel A. Note the PDGF-αR expression in the brain at this age, which is restricted to two discrete regions within the diencephalon.

In the CNS, at E16 (panel B), many individual PDGF-αR^+ cells can be seen in the brain and the spinal cord. Within the spinal cord, the distribution of PDGF-αR^+ cells show a distinct rostral-caudal and ventral-dorsal gradient of dispersion. There are many more PDGF-αR^+ cells at the cervical level of the cord that at the sacral level, and at any one level of the spinal cord the majority of these cells lie in the basal (ventral) half of the cord. Individual PDGF-αR^+ cells can now be seen in the rat brain. The black arrows adjacent to the spinal cord in panels A and B, represent the approximate levels of the transverse sections shown in figures 28 and 29 respectively.

Scale bars, 100 μm.

Figure 26. Distribution of PDGF-αR mRNA in an E14 and E16 rat embryo.

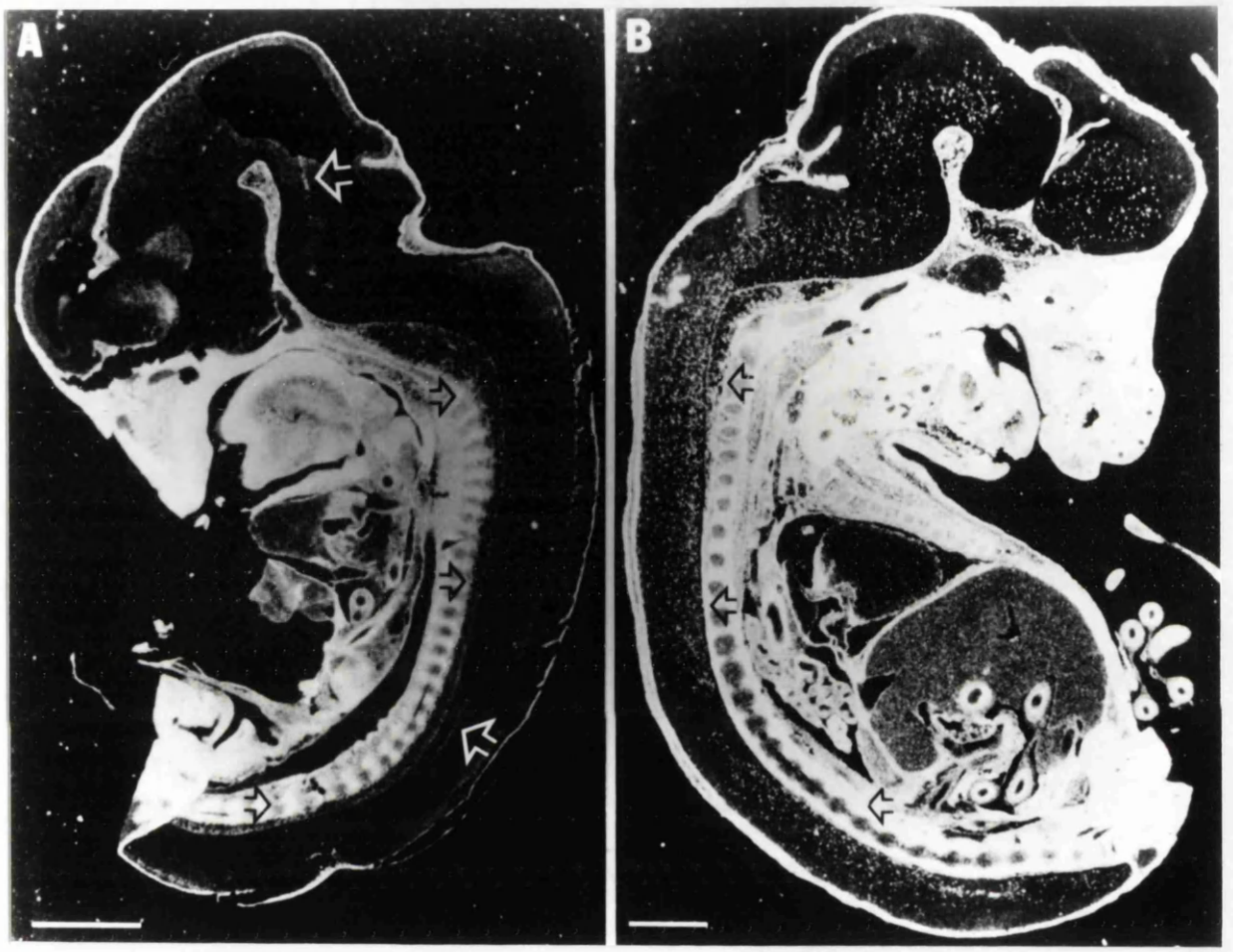

Figure 27. Distribution of PDGF-αR mRNA in the E14 spinal cord (longitudinal section).

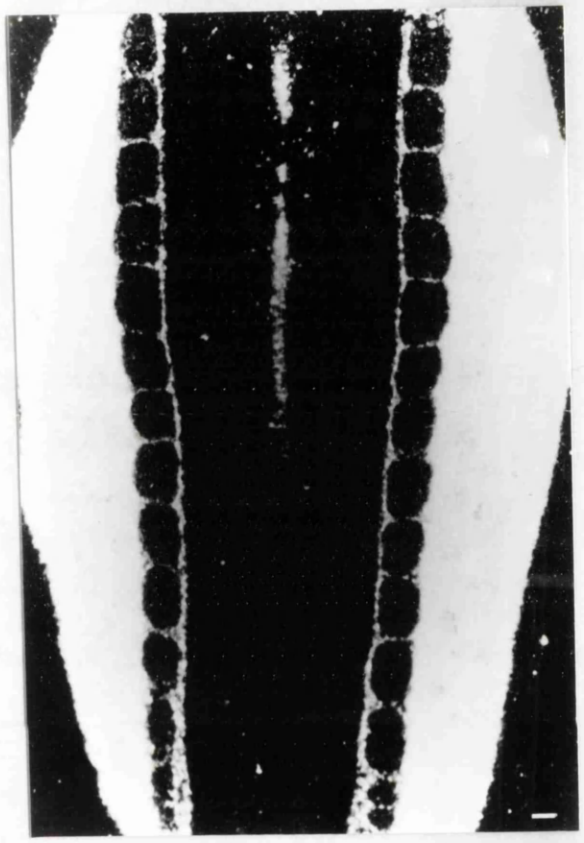

Illustrated is a dark-field photomicrograph of an E14 spinal cord longitudinal section. Within the spinal cord a distinct column of PDGF-αR expression can be seen. The section shows an area of spinal cord from mid thoracic to lumbar regions.
Scale bar, 100 μm.

Figure 28. Distribution of PDGF-αR mRNA in the E14 spinal cord

The figure shows bright- and dark-field images of an E14 rat spinal cord at the lumbar level (panels A and D), thoracic level (panels B and E) and cervical level (panels C and F). At the lumbar level PDGF-αR expression is restricted to the alar ventricular zone and two discrete regions lying either side of the central canal in the basal ventricular zone. At the thoracic level the PDGF-αR expression in the basal ventricular zone has expanded, an individual PDGF-αR$^+$ cells can be seen lying just outside of this region. At the cervical level, the basal ventricular zone PDGF-αR expression has increased further and several individual PDGF-αR$^+$ cells can be seen nearby. The alar ventricular zone staining decreases in intensity in a rostral-to-caudal direction. For comparison, the levels that these sections were cut is illustrated by black arrows in figure 26, panel A.

The black arrow (Panel A) indicates the dorsal (d) ventral (v) direction. The asterisk's denote the position of the ventral PDGF-αR expression on the bright field photographs.

Scale bar, 100 μm.

Figure 28. Distribution of PDGF-αR mRNA in the E14 spinal cord (transverse sections).

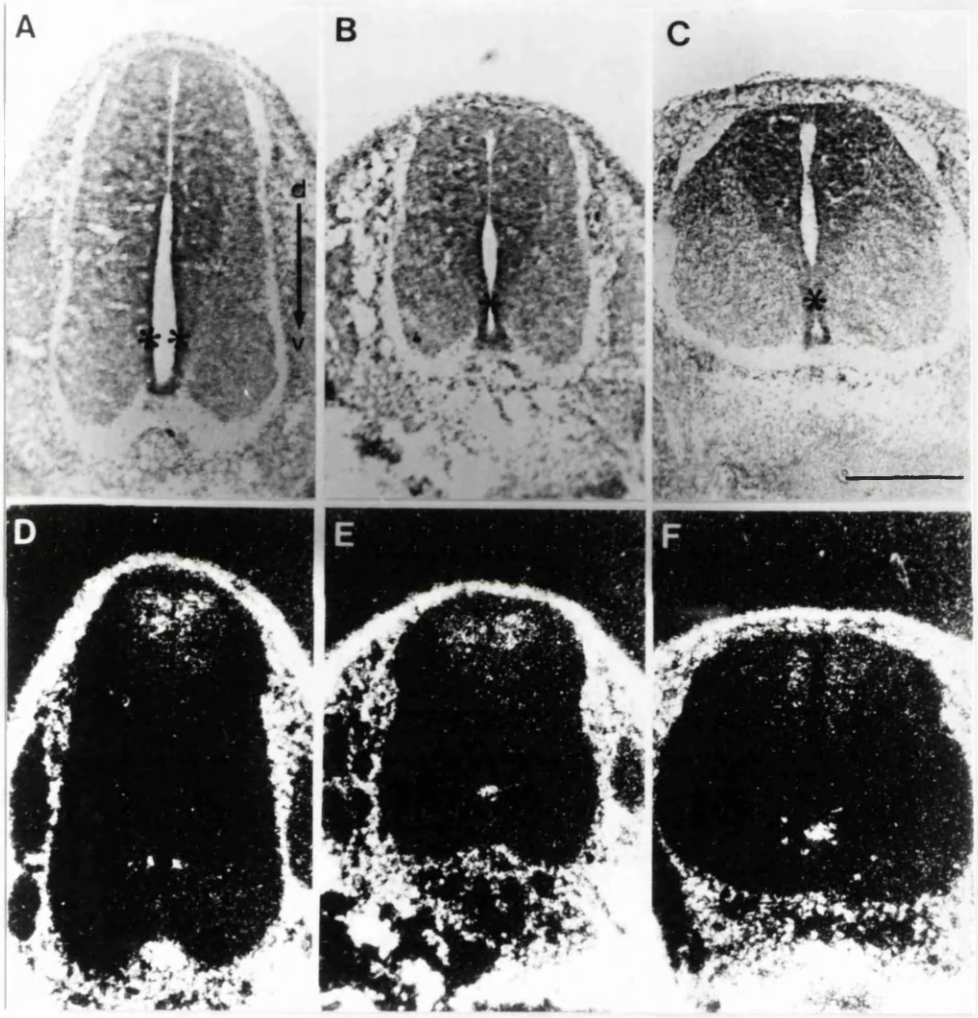

Figure 29. High power picture of the discrete PDGF-αR expression seen in the lumbar region of the spinal cord at E14.

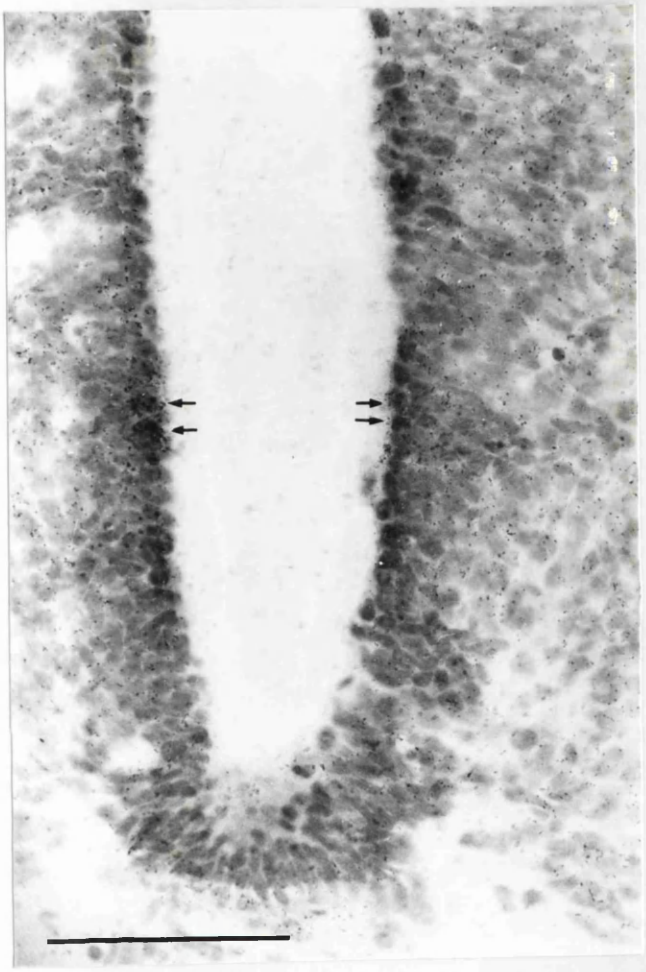

Illustrated is a high power bright-field photomicrograph of the E14 basal ventricular zone (illustrated in figure 28, panel A) at the lumbar level of the cord. The developed silver grains lie mainly outside of the depth of field of the photograph and the restricted region of PDGF-αR expression is marked with arrows. PDGF-αR expression is restricted to the two adjacent cells of the ventricular zone lying either side of the central canal. These PDGF-αR$^+$ cells within the ventricular zone do not appear to differ in any obvious way from their neighbouring cells.

Scale bar, 50 μm.

Figure 30. Distribution of PDGF-αR mRNA in the E16 spinal cord.

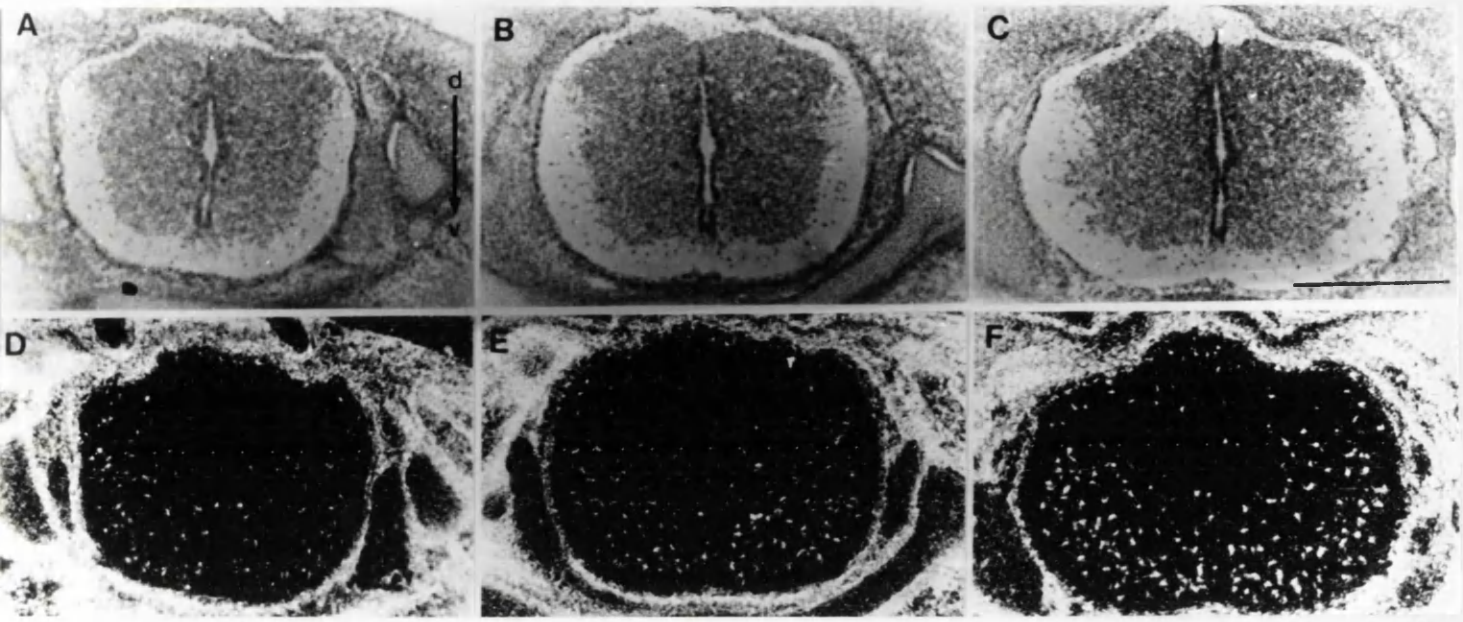

The figure shows bright- and dark-field images of an E16 rat spinal cord at the lumbar level (panels A and D), thoracic, (panels B and E) and cervical (panels C and F). There is no PDGF-αR expression in the ventricular zones at this age. Individual PDGF-αR$^+$ cells can be seen predominantly in the ventral half of the cord. The number of these cells increases as we move from lumbar to cervical levels. For comparison, the levels that these sections were cut is illustrated by black arrows in figure 26, panel B.

The black arrow (panel A) indicates the dorsal (d) ventral (v) direction.

Scale bar, 100 μm.

Figure 31. Distribution of PDGF-αR mRNA in the spinal cord at E18.

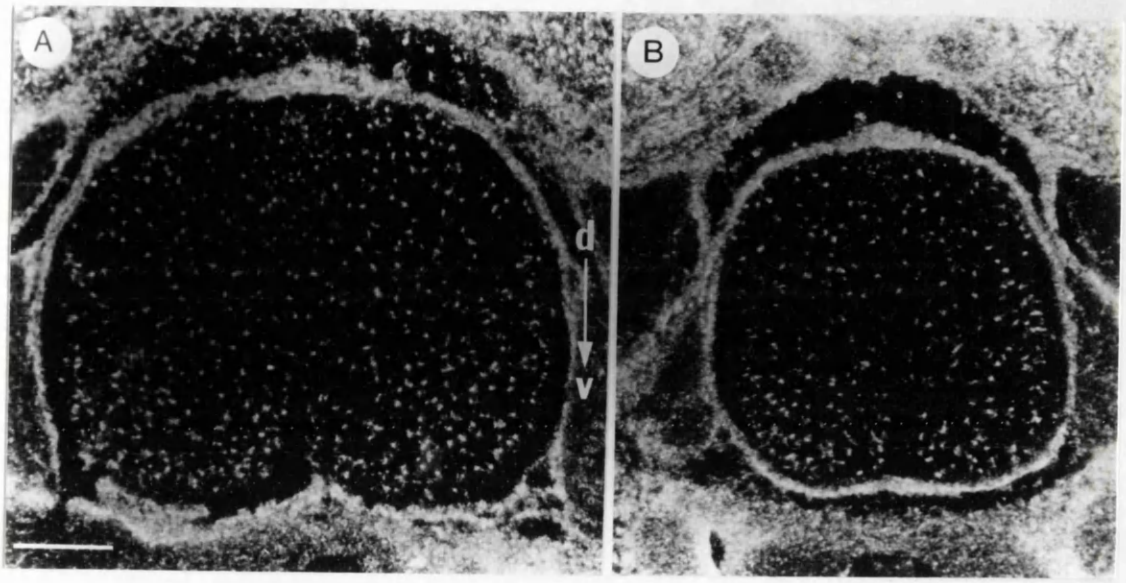

Illustrated are two dark-field photomicrographs of transverse sections of E18 spinal cord at the cervical level (Panel A) and lumbar level (Panel B). PDGF-αR$^+$ cells are now found throughout the spinal cord, with the greatest density of cells still lying in the basal (ventral) half of the cord.

The white arrow (Panel A) indicates the dorsal (d) ventral (v) direction.

Scale bar, 100 μm.

Figure 32. High power of PDGF-αR$^+$ cells in E18 spinal cord.

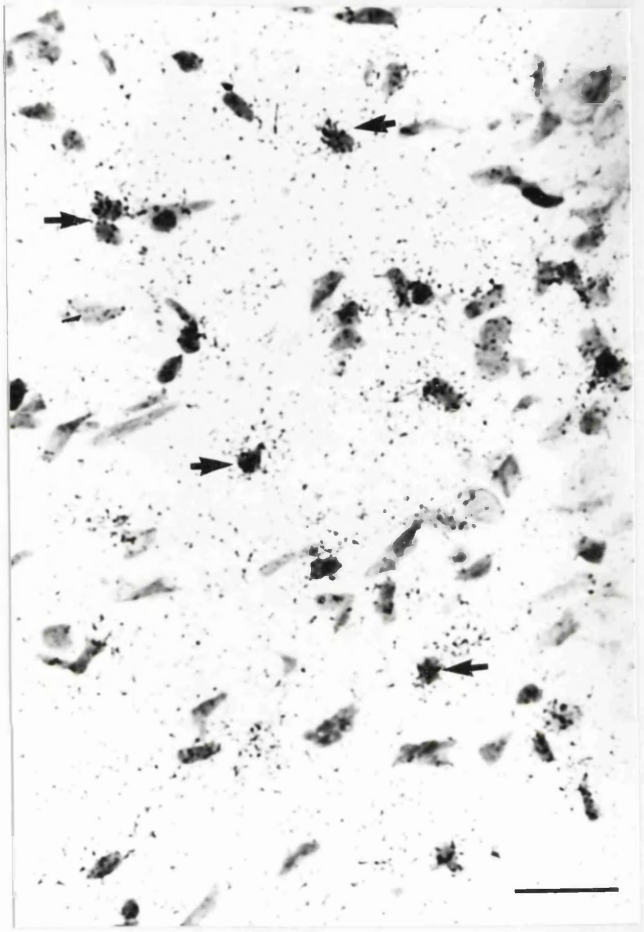

Illustrated is a high power bright-field photomicrograph of PDGF-αR$^+$ cells in the white matter of the spinal cord at E18. Exposed silver grains are associated with small densely stained nuclei (black arrows).

Scale bar, 10 μm.

PDGF-αR expression in the brain during early neurogenesis (E12-E15) is initially restricted to a dorsal and a ventral region of the diencephalic ventricular zone.

To map the distribution of PDGF-αR expression in the E12 and E13 brain I cut a series of coronal sections spaced approximately 300 μm apart throughout the brain for *in situ* hybridization. All the sections were processed at the same time under identical conditions. Control "sense" probes showed no hybridization above background (data not shown). The results illustrated in figure 33 are of representative sections taken from different regions of the forebrain.

Figure 33 (panels A, B and C) shows three E12 rat brain coronal sections taken at the forebrain level (The arrows on the inset to the figure legend of Figure 33 indicate the approximate positions and angles that the sections were cut). PDGF-αR is strongly expressed in many craniofacial regions and meninges. However, there is relatively little PDGF-αR expression within the CNS. No PDGF-αR expression can be detected in the anterior-most forebrain (panel A). More posteriorly, PDGF-αR expression appears to be restricted to two regions of the ventricular and subventricular zones adjacent to the third ventricle (panels B and C). This PDGF-αR expression lies in the dorsal half of the brain and defines an unclassified region of the ventricular zone of the diencephalon. Coronal sections taken posterior to those shown in figure 33 showed no PDGF-αR expression (data not shown), indicating that the dorsal expression in the diencephalon is restricted to the posterior forebrain.

Panels D, C and E of figure 33,show coronal sections taken from the forebrain of an E13 rat and have been taken at roughly equivalent levels to the E12 sections (panels A, B and C). There is still no PDGF-αR expression in the anterior forebrain (panel D). More posteriorly, PDGF-αR expression can still be seen in two regions on either side of the third ventricle in the dorsal half of the brain (panels E and F).

Note how this staining has intensified from E12 (Compare panels B and C with panels E and F) and the PDGF-αR expression does not extend to the meningeal surface as it did at E12. Another region of PDGF-αR expression can now be seen in the ventral half of the brain also in the ventricular zone of the third ventricle in the diencephalon (panel D). Similarly to E12, no PDGF-αR expression is found posterior to this level (data not shown). At this age nearly all the brain is comprised of ventricular and sub-ventricular zones, and PDGF-αR expression appears to be restricted to defined regions of this.

Individual PDGF-αR$^+$ cells are first seen in the brain at E14 and appear to arise from the ventral region of PDGF-αR expression seen in the diencephalon.

To map the distribution of PDGF-αR expression in E14 and E15 rat brains I cut a series of coronal sections spaced approximately 300 μm apart throughout the brain for *in situ* hybridization. The results illustrated in figures 34 and 35 are of representative sections taken from different regions of the brain. Figure 34, panel A, illustrates that there is still no PDGF-αR expression in the anterior-most forebrain at E14. The sections shown in panels B, C, D, E and F are spaced approximately 300 μm apart and came from a region corresponding to the posterior forebrain (the presence of the retina in these sections provides a useful landmark). Moving from anterior to posterior, panels B, C and D, illustrate that individual PDGF-αR$^+$ cells can now be seen in the ventral half of the brain and PDGF-αR expression can be seen in the ventral half of the ventricular zone of the third ventricle in an area corresponding to the diencephalon. It appears as if the individual PDGF-αR$^+$ cells are arising from this PDGF-αR expressing region of the ventricular zone. Note also that the choroid plexus expresses PDGF-αR. The section illustrated in panel E, is taken approximately 300 μm posterior to that of panel D illustrating that the

ventricular zone expression of PDGF-αR is fairly restricted in along the anterior-posterior axis. The ventral expression of PDGF-αR in the diencephalon has disappeared and PDGF-αR expression is now seen in a restricted region of the diencephalon, in the dorsal half of the brain (This PDGF-αR expression corresponds to the dorsal areas shown at E12 and E13, shown in figure 33, panels C, E and F). The restricted PDGF-αR expression within the diencephalon is also illustrated in figure 26, panel A, which shows a dark-field photomicrograph of an E14 embryo in sagittal section.

Figure 34, panel F, illustrates that no individual PDGF-αR$^+$ cells can be seen in this part of the brain, although the dorsal expression in the mesencephalon is still apparent (This section is approximately 300 μm posterior to that of Figure 34, panel E). Figure 34, panel G, shows a region of the midbrain and illustrates that no PDGF-αR expression is visible in the CNS in this area. Figure 34, panel H, shows a region of the hind brain at E14. A few individual PDGF-αR$^+$ cells can be seen in the ventral part of the brain and there is also a strong "V" of expression in the tegmentum, ventral to the aqueduct. I presume that this "V" of PDGF-αR expression corresponds to where the column of basal PDGF-αR expression from the spinal cord enters the tegmentum of the hind brain.

It appears from this survey of the E14 brain that PDGF-αR expression within the posterior forebrain is restricted to two regions, both in the diencephalon one dorsal and the other ventral. Both of these regions are also apparent in figure 26, panel A. Individual PDGF-αR$^+$ cells appear to arise from the ventral area of PDGF-αR expression in a region corresponding to the diencephalon. No individual PDGF-αR$^+$ cells were seen to arise from the dorsal region of PDGF-αR expression.

A similar survey at E15 (Figure 35, Panels A-F) again illustrates that the individual PDGF-αR$^+$ cells have a ventral origin. PDGF-αR$^+$ cells can now be

discerned in the anterior-most forebrain and are distributed ventrally (panels A and B). At the level of the posterior forebrain the individual PDGF-αR$^+$ cells are still predominantly ventral (panels C and D). There is strong PDGF-αR expression in the ventral half of the third ventricle (particularly around the Foramen of Monro, panel D) and much weaker expression in the dorsal part of the third ventricle (panels C and D). Individual PDGF-αR$^+$ cells are now seen in the midbrain (panel E) and again are distributed ventrally. In the hind brain PDGF-αR$^+$ cells still have a ventral distribution (panel F). The dorsal expression in the diencephalon is still apparent (panels C and D) and appears to extend throughout the dorsal aspects of the diencephalonic ventricular zone (eg. panel C).

By E16 all ventricular zone PDGF-αR expression has disappeared, (eg. figure 26, panel B and figure 15).

These results suggest that, between E12 and E13, PDGF-αR expression is restricted to two regions of the ventricular zone of the diencephalon. One located dorsally and the other ventrally around the third ventricle. Individual PDGF-αR$^+$ cells apparently arise from the ventral region of PDGF-αR expression in the diencephalon. These individual PDGF-αR$^+$ cells appear to disseminate from this region to fill the brain both anteriorly and posteriorly. Although their initial distribution is predominantly ventral the PDGF-αR$^+$ cells eventually populate all regions of the brain, ventrally and dorsally, including the cerebral cortex (see previous chapter). I presume that the dorsal region of PDGF-αR expression seen in the diencephalon represents expression by neuronal precursors.

PDGF-αR expression is widespread outside the CNS.

Figure 26 shows two sagittal sections taken through E14 (panel A) and E16 (panel B) embryos hybridized with the PDGF-αR anti-sense probe and photographed under dark-field illumination. PDGF-αR expression is not restricted to the CNS; both at E14 and E16 (Figure 2, panels A and B) strong hybridization can be seen in much of the developing embryo, notably the craniofacial regions, the cartilage surrounding the developing vertebrae, meningeal membranes, skin and intestines; in fact most mesodermal and neural crest-derived tissues. The CNS, in comparison to the rest of the embryo, has rather little PDGF-αR expression.

Figure 33. PDGF-αR mRNA expression in the rat forebrain at E12 and E13.

Panels A, B and C show three coronal sections taken from an E12 rat head at the level of the developing forebrain, photographed in dark-field illumination. There is strong PDGF-αR expression outside of the CNS, in the meninges and craniofacial structures. The only PDGF-αR expression in the CNS (Panels B and C) occurs in the dorsal half of the brain, in a region corresponding to part of the diencephalon. Panels D, E and F show three coronal sections taken from an E13 rat head forebrain. PDGF-αR expression is apparent in the dorsal part of the brain (panels E and F), also in a region corresponding to part of the diencephalon. PDGF-αR expression is now seen in the ventral half of the diencephalon (Panel F).

Panels A and D, B and E, C and F are taken from approximately equivalent regions of the developing rat brain. This is illustrated in the inset, where the arrows point to the approximate angle and position the sections were cut.

Inset: D, Diencephalon; T, Telencephalon; M, Mesencephalon; My, Myencephalon.

Scale bar, 100μm.

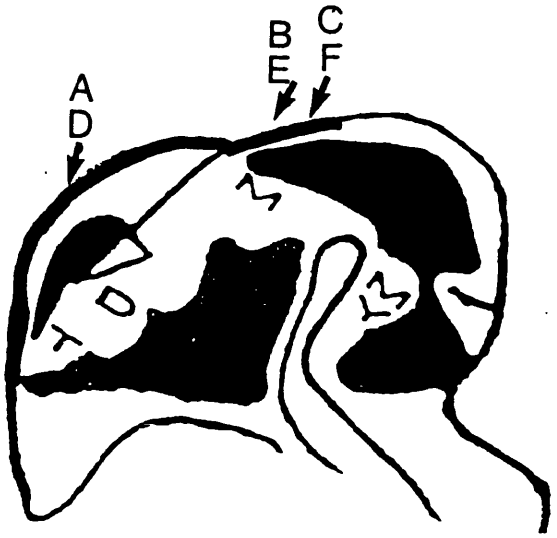

Figure 33. PDGF-αR mRNA expression in the rat forebrain at E12 and E13.

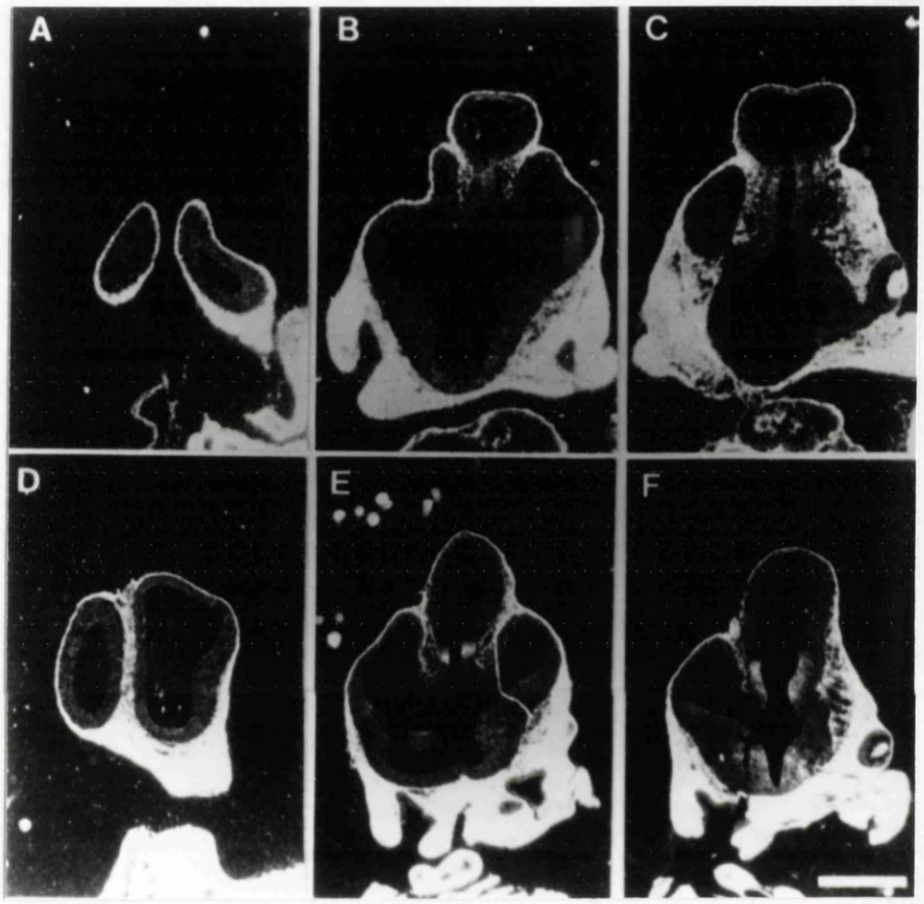

Panels A-H show eight coronal sections taken from an E14 rat head and photographed under dark-field illumination. The approximate positions the sections were taken from is illustrated in the inset. Panels B-F give more detailed picture of the posterior forebrain and lie approximately 300 μm apart. Individual PDGF-αR$^+$ cells can be distinguished in the ventral half of the brain and are predominantly located around the posterior forebrain (Panels B-E). PDGF-αR expression is still apparent in the ventral region of the developing diencephalon (Panels B-D) and also in the dorsal half of the diencephalon (panels E and F). There is no PDGF-αR expression in the midbrain (Panel G). The "V" of PDGF-αR expression seen in the hindbrain (Panel H) is probably a continuation of the ventral column of PDGF-αR expression seen in the spinal cord. The choroid plexus also stains strongly for PDGF-αR mRNA (Panels B-F)

Inset: FBr, Forebrain; Mbr, Midbrain; HBr; Hindbrain.

Scale bar, 100 μm.

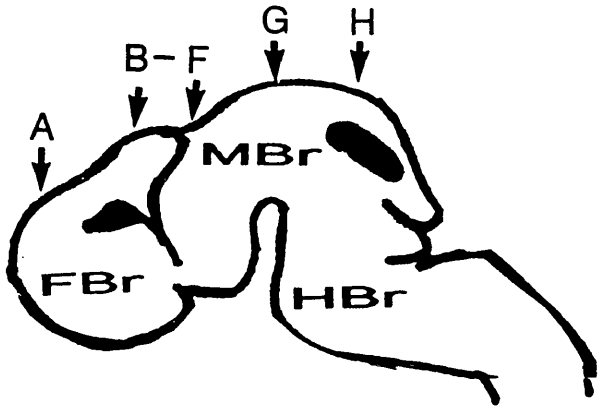

Figure 34. PDGF-αR mRNA expression in the rat brain at E14.

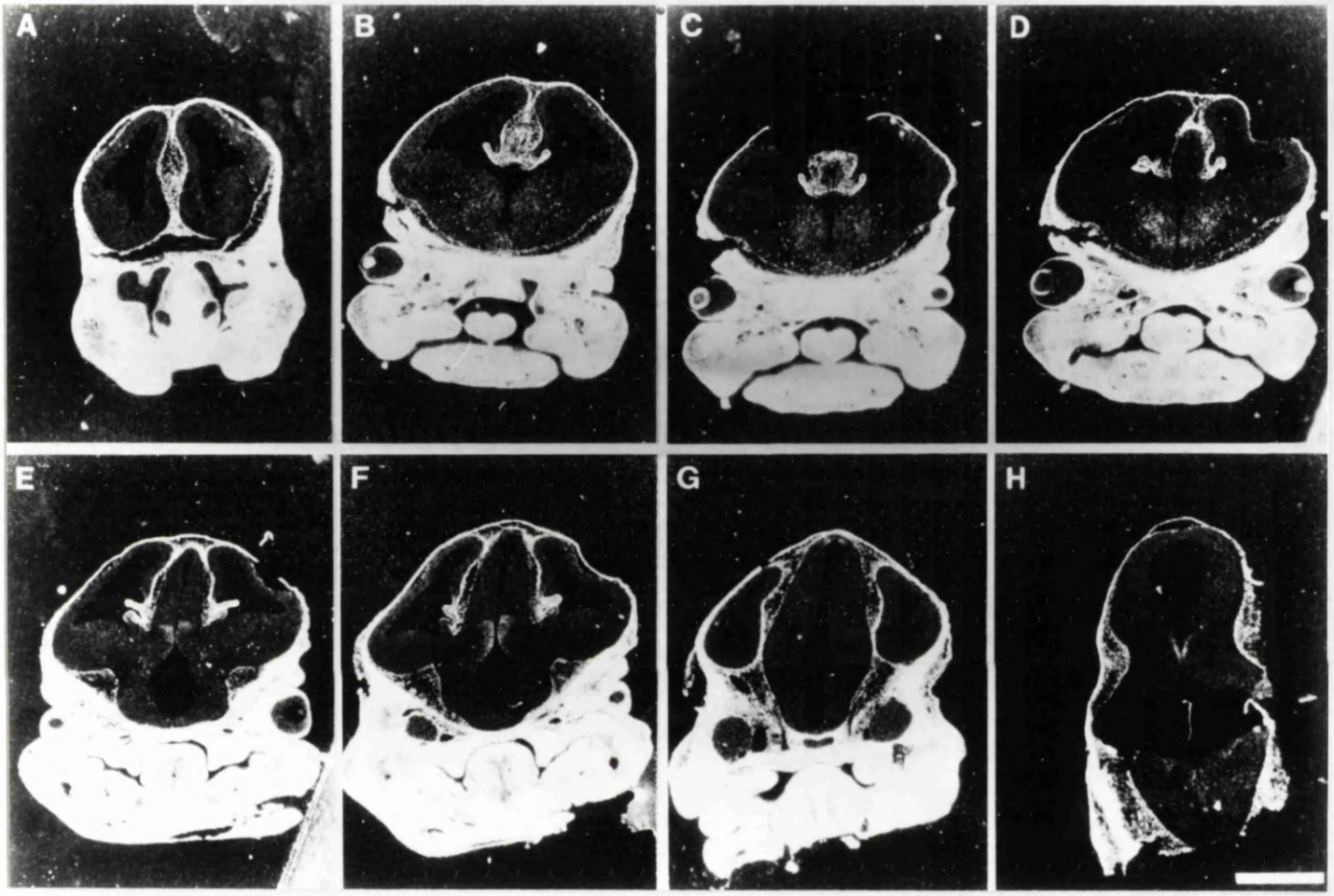

Figure 35. PDGF-αR expression in the rat brain at E15.

Panels A-F show six coronal sections taken from an E15 rat head and photographed under dark-field illumination. The approximate positions the sections were taken from is illustrated in the inset. There are many more individual PDGF-αR$^+$ cells visible at this age, with a predominantly ventral distribution. There is strong PDGF-αR expression in the ventral half of the third ventricle (Panels C and D). PDGF-αR expression can also be seen in the dorsal half of the brain, lying either side of the diencephalonic ventricular zone (Panels C and D). PDGF-αR$^+$ cells are now seen in the midbrain (Panel E) and hindbrain (Panel F).

Inset: FBr, Forebrain; Mbr, Midbrain; HBr; Hindbrain.

Scale bar, 100 μm.

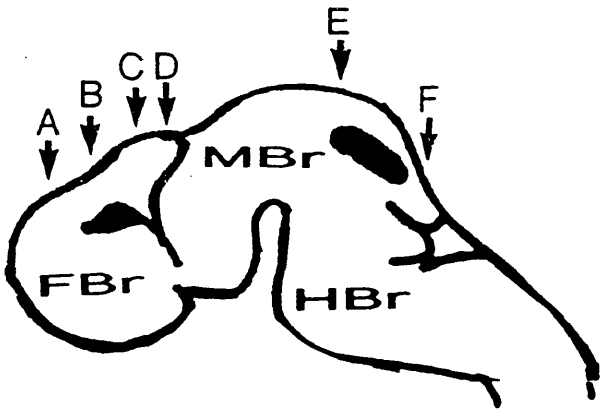

Figure 35. PDGF-αR expression in the rat brain at E15.

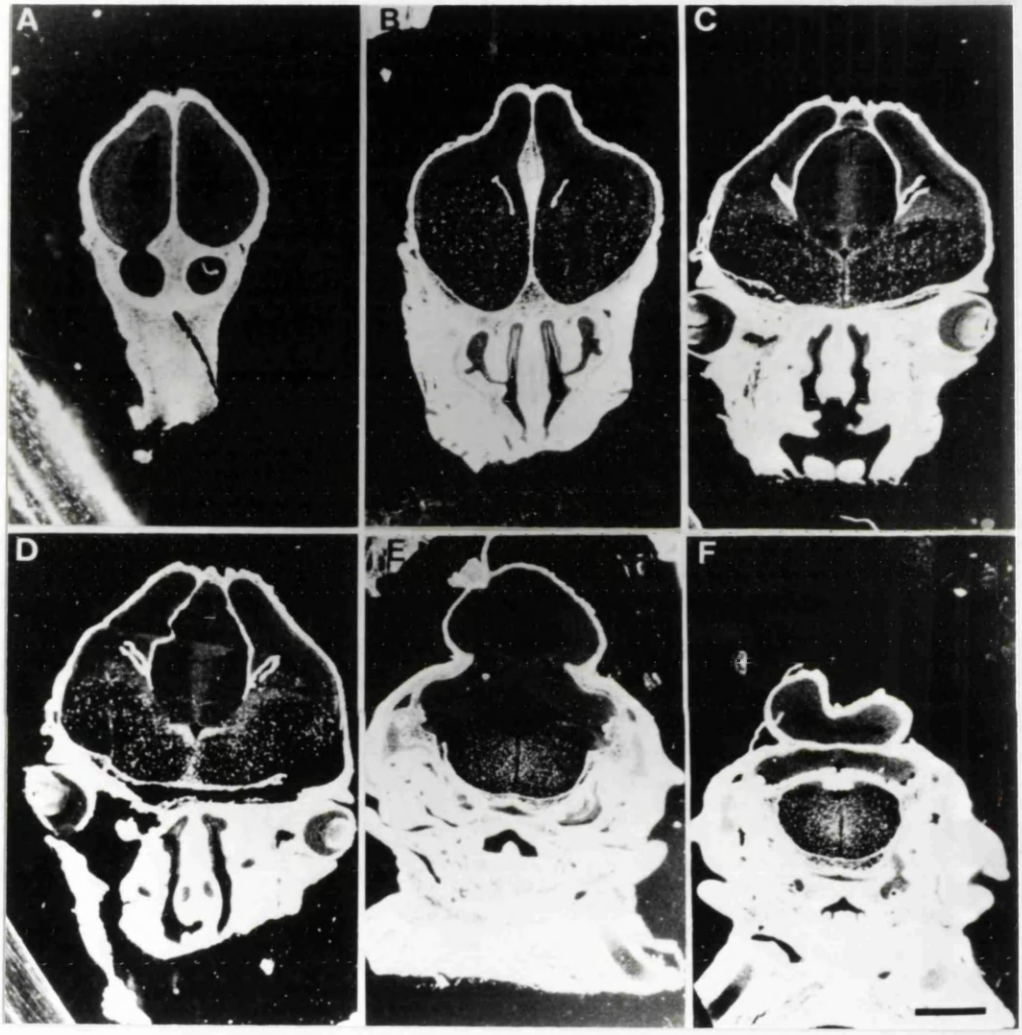

DISCUSSION

PDGF-αR is expressed transiently by interneuron precursors in the alar plate of the spinal cord

At the cervical level of the spinal cord, PDGF-αR is expressed transiently between E12 and E14 near the dorsal tip of the central canal (dorsal aspect of the alar ventricular zone). This region of the ventricular zone gives rise to interneurons, the last major population of neurons to form in the spinal cord (Nornes and Das, 1974; Altman and Bayer, 1984). The first interneurons become post-mitotic at the cervical level of the spinal cord around E14 (Nornes and Das, 1974; Altman and Bayer, 1984), and the peak of interneuron production occurs around E15. Therefore, PDGF-αR expression in the alar ventricular zone appears to precede interneuron differentiation. It is possible, therefore, that PDGF might act as a mitogen for developing interneurons in the later stages of their development. It will be interesting to discover if other populations of spinal cord neurons that are born earlier than interneurons (e.g. motor neurons) also express PDGF-αR before they become post-mitotic.

PDGF-αR$^+$ cells in the basal ventricular zone probably represent glial cells, not neuronal precursors

The most salient aspect of the present work is the discovery of a transient column of PDGF-αR expression in the ventricular zone in the basal region of the embryonic spinal cord. This column is first discernible in the brainstem at E13 and in the lumbar region of the spinal cord at E14. The spatial and temporal distribution

of these PDGF-αR$^+$ cells in the rat spinal cord argues against their being neurons. Large numbers of PDGF-αR$^+$ cells can be seen in the developing white matter of the spinal cord; these cells cannot all be neurons because there are few, if any, neuronal cell bodies in white matter. Even outside of the developing white matter, the pattern of PDGF-αR$^+$ cells is not what would be expected for neurons; by E18 PDGF-αR$^+$ cells are distributed throughout the spinal cord, and are quite widely spaced (Figure 31), whereas neurons, in the spinal cord are often closely packed in groups. For example motor neurons are located in the lateral aspects of the dorsal horn (see figure 25, panel A for example). Many of the PDGF-αR$^+$ cells outside of the ventricular zone can be seen to be dividing, a property of glial cells, not neurons. Moreover, cells that are easily recognizable as neurons because of their location, such as motor neurons, are invariably negative for PDGF-αR.

The time course that PDGF-αR$^+$ cells arise in the basal ventricular zone occurs after neuronal differentiation in this area has ceased. The basal ventricular zone initially gives rise to motor neurons; the first motor neurons arise at E11 and all production of motor neurons has ceased, in the basal ventricular zone by E13 (Nornes and Das, 1974; Altman and Bayer, 1984). As they are born these neurons migrate away from the ventricular zone before coming to rest forming columns of motor neurons in the ventral horns of the spinal cord (Nornes and Das, 1974; Altman and Bayer, 1984). PDGF-αR$^+$ cells subsequently spread throughout the spinal cord, and increase in numbers. Thus the spatial distribution of PDGF-αR$^+$ cells in the developing spinal cord, and the fact that they seem to proliferate, argues strongly that these cells correspond to glial cells, not neurons.

This conclusion is further supported by the appearance of the PDGF-αR$^+$ cell nuclei in haematoxylin-stained sections (Figure 32); the PDGF-αR hybridisation

signal is usually associated with small, densely stained nuclei, that are characteristic of glial cells (Smart and Leblond 1961). Blood vessels are readily apparent in these spinal cord sections, often being marked by rows of cells with elongated nuclei. These cells, which presumably represent endothelial cells and/or circulating blood cells, are always negative for PDGF-αR.

The temporal and spatial distribution of PDGF-αR$^+$ cells arising from the basal ventricular zone: comparison with previous studies of oligodendrocyte development in the spinal cord.

I have previously demonstrated (see last chapter) that during late neurogenesis in the brain, PDGF-αR expression appears to be restricted to cells of the oligodendrocyte lineage. How do my present findings (regarding these ventrally arising PDGF-αR$^+$ cells) compare with previous studies on oligodendrocyte formation in the spinal cord? Few studies exist on gliogenesis in the spinal cord, but recently a paper by Warf *et al.*, (1991) has shed some light on the process of oligodendrocyte formation. Warf *et al.* (1991) dissected the spinal cord of embryonic rats at different levels. They further dissected these segments into ventral and dorsal halves, dissociated the cells and cultured them *in vitro*. Using antibodies against galactocerebroside (GC), an oligodendrocyte specific marker, they were able to follow the development of oligodendrocytes. They showed that, at E14, all segmental levels of the spinal cord have the capacity to give rise to oligodendrocytes, although no GC$^+$ cells were found in the initial cultures. This suggests, that in the E14 spinal cord, there exists a population of cells with the capacity to give rise to oligodendrocytes (oligodendrocyte precursors). GC$^+$ oligodendrocytes arose in these cultures on the same time schedule as they would have done *in vivo*. Furthermore, at E14, only the ventral regions of the spinal cord had the capacity to give rise to oligodendrocytes.

During subsequent development, dorsal regions of the spinal cord gradually acquired the capacity to form oligodendrocytes. The numbers of oligodendrocytes forming in the dorsal spinal cord cultures was notably less than the numbers seen in the ventral spinal cord cultures for the ages studied implying a ventral-dorsal gradient of oligodendrocyte differentiation. Oligodendrocyte differentiation also occurred in a rostral-caudal direction, the first oligodendrocytes being observed at the cervical level of the spinal cord at E16 and at the sacral level at E17.

How does my present study of the distribution of PDGF-αR^+ cells arising from the basal ventricular zone of the spinal cord compare with the study of Warf *et al.* (1991)?

PDGF-αR^+ cells are first seen in the basal ventricular zone at E14, at a time when only this region of the spinal cord has the capacity to generate oligodendrocytes. Between E14 and E16 PDGF-αR^+ cells are predominantly found in the ventral half of the spinal cord. Cultures made from the dorsal or ventral halves of spinal cord from these ages show that the ventral half of the spinal cord has the greatest capacity to give rise to oligodendrocytes (Warf *et al.*, 1991); E14 cultures of dorsal cells contained only 86 ± 110 (sic) oligodendrocytes while ventral cultures contained 17,100 ± 2800. Presumably the oligodendrocytes in the dorsal spinal cord cultures arose from contamination with ventral spinal cord tissue during the micro-dissection. The numbers of oligodendrocytes increased till at E16 they found 1570 ± 30 oligodendrocytes in the dorsal cultures and 24,850 ± 1871 in the ventral cultures. Thus the spatial and temporal distribution of PDGF-αR^+ cells *in vivo* correlates well with the capacity of the spinal cord to generate oligodendrocytes *in vitro*. By E18 PDGF-αR^+ cells are distributed throughout the spinal cord, with perhaps the greatest density of cells lying in the ventral half. A not dissimilar picture to that of oligodendrocytes formation dorsal half seen by Warf *et al.*, (1991), who observed approximately twice as many oligodendrocytes arising from the ventral half of the

cord, compared to the dorsal half at this age (21,500 ± 2989 and 12,400 ± 1650 respectively). Therefore there are striking parallels between my PDGF-αR data and those of Warf *et al.* (1991).

PDGF-αR expression in the brain from E12 to E15.

I investigated the distribution of PDGF-αR expression in the developing brain from E12 to E15. The dynamic changes in morphology of the brain occurring during this period make interpretation of events more difficult than in the spinal cord, where much more is known about the developmental time course of neuronal maturation. Studies detailing neuronal development in the diencephalon have suggested that from E12 to E20, the diencephalic ventricular zone gives rise to most of the neurons of the hypothalamus (Altman and Bayer 1978a,b,c). Their tritiated thymidine studies showed that neurons were born in the ventricular and subventricular zones. They subsequently migrated away from these ventricular zones and came to rest forming defined neuronal regions of the hypothalamus. The neuronal development of the hypothalamus is complex and as described by Altman and Bayer (1978b), "indicates that the hypothalamus is composed of several zones of sequentially acquired neuronal systems. Two major chronological gradients were discerned: in the anterior hypothalamus a topologically distorted lateral-to-medial gradient, and in the posterior hypothalamus, specifically in its caudal portion, a horizontally orientated gradient was partially combined with a lateral-to-medial gradient." Little, however, is known about glial cell development at these ages. To my knowledge, no studies exist detailing the formation of oligodendrocytes at these early ages, so I cannot compare my results with previous studies. However, the distribution of PDGF-αR$^+$ cells in this region has no obvious correlation with any of the neuronal migration patterns described by Altman and Bayer (1978a,b,c), suggesting that PDGF-αR$^+$ cells are not neuronal.

There are, however, certain parallels between the PDGF-αR expression in the spinal cord and the brain. There are two regions of PDGF-αR expression, one lying dorsally and the other ventrally in the diencephalon. Individual cells, which strongly express PDGF-αR, can be seen apparently arising from the ventral region of the ventricular zone of the diencephalon, in particular at the Foramen of Monro. As in the spinal cord these PDGF-αR$^+$ cells initially have a ventral distribution, before disseminating throughout the brain. However, unlike the spinal cord, PDGF-αR expression seems to be restricted in the anterior-posterior axis, to a region of the diencephalon and does not extend along the length of the brain. The individual PDGF-αR$^+$ cells appear to arise from the ventral region of PDGF-αR expression in the diencephalon and to disseminate throughout the brain from this region.

Highly restricted PDGF-αR expression in the basal ventricular zone of the spinal cord

One of the most striking aspects of PDGF-αR expression in the basal (ventral) half of the spinal cord is its initial restriction in the transverse plane to two cells lying either side of the central canal (Figure 29). This provides a striking illustration of the high degree of spatial resolution with which gene expression and cell fate can be regulated along the dorsoventral axis of the neural tube. During early neurogenesis the expression of other growth factor receptors has also been shown to be restricted to the ventricular zone. In the chicken spinal cord at E5, fibroblast growth factor receptor (FGF-R) expression is restricted to the ventricular zone cells, and is expressed in both alar and basal halves of the spinal cord (Heuer *et al.*, 1990). In the rat, between E12 and E17, FGF-R expression is restricted to the ventricular zones of the spinal cord and brain (Wanaka *et al.*, 1991). Nerve growth factor receptor in E5 chicken embryos has a reciprocal pattern of expression to that of FGF-R, being

found in the postmitotic neurons, outside of the ventricular zone (Heuer *et al.*, 1990).

Similarly the expression of PDGF-ß receptor in the early embryonic rat brain is localized throughout the ventricular zones of the brain at E12 (Mudhar *et al.*, in preparation).

Two members of the *Wnt* gene family, a group of cysteine-rich proteins implicated in intercellular signalling during several stages of vertebrate development, show restricted patterns of expression in the developing mouse spinal cord and brain (Roelink and Nusse, 1991). One member of this family, *Wnt*-3 is expressed at low levels in the alar laminae and ventral horns, whereas *Wnt*-3A expression is confined to the roof plate (Roelink and Nusse, 1991).

Although expression of these growth factor receptors is localized to the ventricular zones during early neurogenesis, they are expressed throughout the ventricular zones, and do not exhibit the highly restricted expression seen with PDGF-αR. At present this highly restricted expression within the ventricular zone appears to be unique for PDGF-αR.

Control of PDGF-αR expression in dorso-ventral axis of the neural tube

The restricted expression of PDGF-αR in both the alar and basal ventricular zones is presumably controlled by other genes, which direct these particular cells to express PDGF-αR. One group of genes which display a dorsal or ventral restricted expression in the spinal cord are some of the homeotic genes. The expression of the H*ox*-2 cluster of homeobox genes in the developing mouse spinal cord shows such a pattern of expression. At E11.5 the H*ox*-2 cluster of homeotic genes are expressed throughout the murine spinal cord. As development proceeds the pattern of

expression of the *Hox*-2 genes changes and by E14.5 their expression is restricted to the alar (dorsal) half of the spinal cord (Graham *et al.*, 1991).

Similarly many genes containing the "paired box" motif (*Pax* genes) show restricted expression patterns within the spinal cord. *Pax*-3 and *Pax*-7 are expressed in the ventricular zone of the alar plate (Goulding *et al.*, 1991; Jostes *et al.*, 1991), *Pax*-3 expression is also found in the roof plate (Goulding *et al.*, 1991). *Pax*-6 is expressed in the entire basal plate, excluding the floor plate (reviewed in Gruss and Walther 1992). *Pax*-2, *Pax*-5 and *Pax*-8 are restricted to a subset of cells in the ventricular zone of the alar and basal plates, however, their expression does not extend to the central canal (Plachov *et al.*, 1990; Nornes *et al.*, 1990; reviewed in Gruss and Walther, 1992).

Presumably these genes regulate the expression of other subordinate genes that collectively define cell phenotype. The basic dorso-ventral axis of cells within the spinal cord appears to be controlled by the notochord and floor plate. Grafting additional notochord or floor plate to ectopic positions in developing chicken embryos results in changes in cell fate (Yamada *et al.*, 1991). For example, if an additional notochord or floor plate is placed dorsally to the spinal cord a second population of motor neurons arises in the alar plate. The notochord and floor plate appear to determine the polarity of the spinal cord, and presumably will affect the expression of other genes, such as homeotic genes, which are thought to control the overall process of differentiation in some way. Which ultimately is likely to control PDGF-αR expression in the ventricular zones in an, as of yet, undefined manner.

Conclusions

During early neurogenesis PDGF-αR expression is restricted to dorsal and ventral regions of the ventricular zone in both the brain and spinal cord. In the

spinal cord and brain the dorsal expression of PDGF-αR appears to be restricted to neuronal precursor cells. Thus PDGF-αR expression in the CNS is not totally restricted to cells of the oligodendrocyte lineage at this time. The highly restricted PDGF-αR column of expression in the basal (ventral) ventricular zone of the spinal cord appears to be unique, and unlike any previously described restricted expression within a ventricular zone. The spatial and temporal distribution of these ventrally derived PDGF-αR$^+$ cells argues, but does not prove, that the individual PDGF-αR$^+$ cells may include cells of the oligodendrocyte lineage. If PDGF-αR cells do belong to this lineage, then oligodendrocyte precursor cells, in both the brain and spinal cord, arise from discrete areas of the ventricular zone in the ventral half of the CNS. These cells are born over a short window of time, around E14, and subsequently appear to disseminate throughout the CNS, whilst continuing to proliferate. Thus my data suggests that oligodendrocyte in the brain may be derived from two highly localized germinal zones; oligodendrocytes in the hindbrain (and possibly part of the mid brain) may arise from the columns of PDGF-αR cells that extend from the hindbrain along the length of the spinal cord, while oligodendrocytes in the forebrain and anterior midbrain may arise at the Foramen of Monro.

CHAPTER 6

GENERAL DISCUSSION

One of the aims of this work was to elucidate the nature of the mitogen produced by cortical astrocytes that influences O-2A progenitor cell differentiation. This has turned out to be a form of PDGF. I have demonstrated that PDGF-A chain mRNA is produced by cortical astrocytes *in vitro*, and that the time course of appearance of PDGF-A chain mRNA transcripts in the rat brain is consistent with astrocytes being a source of PDGF-A chain *in vivo*. The distribution of PDGF-A chain mRNA in the rat optic nerve suggests that astrocytes may be a source of PDGF-A chain in the optic nerve.

O-2A progenitor cells express PDGF-αR on their surface (Hart *et al.*, 1989; McKinnon *et al.*, 1990; also see table 3 of this thesis). To investigate the possibility that PDGF-αR might be a useful marker to trace O-2A progenitor cell development in the rat CNS I performed *in situ* hybridization using a probe specific for the PDGF-αR. The spatial and temporal distribution of PDGF-αR$^+$ cells in the rat CNS (presented in this thesis) has led me to speculate that the expression of PDGF-αR may be restricted to cells of this lineage during late neurogenesis (after E16). During earlier stages of neurogenesis (E12-E14) PDGF-αR expression is also found in dorsal regions of the ventricular zone, which presumably give rise to neurons. The experiments described in chapter 5, revealed a transient singularity of PDGF-αR expression in the basal ventricular zone of the embryonic spinal cord that I propose marks the emergence of the O-2A lineage in the cord. My data provides a striking illustration of the high degree of spatial resolution with which gene expression and cell fate can be regulated along the dorsoventral axis of the neural tube. I also presented evidence suggesting that oligodendrocyte precursors in the forebrain and midbrain originate in a restricted region of the ventricular zone of the third ventricle, in the ventral half of the developing diencephalon (Foramen of Monro). Needless to say, much more work will be required to substantiate these hypotheses, and some future approaches are discussed later in this chapter.

Sources of PDGF in the CNS: neurons *versus* glia

Where does the PDGF in the optic nerve originate? The two most obvious potential sources are glial cells in the nerve, and the axons of retinal ganglion neurons which traverse the nerve. The idea that axons might be a source of mitogens for the glial cells in the optic nerve is an attractive one as it would be logical to assume that they somehow influence the glial cells that physically interact with them, and also because it has long been known that peripheral nervous system (PNS) axons carry surface-bound mitogens for Schwan cells, the PNS equivalent of oligodendrocytes (reviewed by Lemke 1990; Collarini and Richardson, 1992). However, the results of optic nerve transection experiments seemed to refute the notion that retinal ganglion axons are important for O-2A progenitor cell proliferation *in vivo* (David *et al.*, 1984; Privat *et al.*, 1981). The optic nerves of newborn rats were unilaterally transected just behind the eye; this results in the degeneration of the axons in the distal nerve within a day or so. When the surviving nerve stump was examined one week later, there was a large reduction of O-2A lineage cells (about 9-fold) relative to the contralateral, untransected nerve, whereas there was a less than two-fold reduction in the number of type-1 astrocytes (David *et al.*, 1984). However, the mitotic index of the remaining O-2A progenitors did not differ between transected and untransected nerves, suggesting that axons are important, not for proliferation, but rather for survival of O-2A lineage cells (David *et al.*, 1984). An alternative interpretation might be that axons are required for migration of O-2A progenitors into the optic nerve from the optic chiasm. Regardless of the reason for the reduction in total O-2A lineage cells, it appeared that the axons of retinal ganglion neurons were not critical for O-2A progenitor proliferation. A likely alternative source of mitogens for O-2A progenitors in the

optic nerve was type-1 astrocytes, because these cells constitute more than half of the total glial cells in the newborn nerve. This possibility was supported by the demonstration that cultured astrocytes from rat cerebral cortex, which resemble type-1 astrocytes in optic nerve cell cultures, produced a mitogen for O-2A progenitor cells in *vitro* (Noble *et al.*, 1984). Moreover, astrocyte-conditioned medium could reconstitute the correct timing of oligodendrocyte development *in vitro* (Raff *et al.*, 1985). I have subsequently showed that cultured rat cortical astrocytes make PDGF-A chain mRNA and that the distribution of PDGF-A chain mRNA in the rat optic nerve has a similar distribution to that of GFAP mRNA (an astrocyte specific marker). Rat cortical astrocytes have also been shown to secrete PDGF, probably PDGF-AA, and antibodies against human PDGF can neutralize up to 90% of the mitogenic activity for O-2A progenitors in astrocyte-conditioned medium (Richardson *et al.*, 1988). Thus, the available evidence supports the view that O-2A progenitors in the optic nerve are stimulated to divide by PDGF-AA produced by type-1 astrocytes.

Recently it has been shown that many neurons in the CNS, as well as some white matter glia (type-1 astrocytes?), contain mRNA encoding the PDGF A chain (Yeh *et al.*, 1991). Many CNS neurons, but not glia, also contain the PDGF B chain (Sasahara *et al.*, 1991). These observations, together with experiments showing that cultured cerebellar interneurons produce PDGF-like mitogenic activity for O-2A progenitors from cerebellum or optic nerve (Levine, 1989), suggest that neurons might be a major source of PDGF in the CNS. Whether neurons secrete PDGF where it would be available to stimulate O-2A progenitor proliferation remains to be seen. Most likely, this would require that PDGF be released from axons, for which there is no mechanism known at present. The function(s) of neuron-derived PDGF is intriguing and is likely to be a focus of future research.

Is PDGF-αR a marker for Oligodendrocyte lineage cells *in vivo*?

^{125}I-PDGF binding studies on O-2A progenitor cells from brain and optic nerve have shown that these cells express PDGF-αR on their surface, both when grown *in vitro* (Hart *et al.*, 1989a; table 3, this thesis) and when directly isolated from optic nerves (Hart *et al.*, 1989a). When grown *in vitro*, O-2A progenitor cells also respond mitogenically to all three forms of PDGF homodimers, (Pringle *et al.*, 1989; Richardson *et al.*, 1988; Raff *et al.*, 1988; Noble *et al.*, 1988), an attribute of cells expressing PDGF-αR (Hart *et al.*, 1988; Matsui *et al.*, 1989). Furthermore, northern and western blotting has shown that both PDGF-αR mRNA and immunoreactivity can be found in O-2A progenitor-enriched cultures prepared from rat cerebral cortex (McKinnon *et al.*, 1990). These results strongly suggest that O-2A progenitor cells express PDGF-αR.

The results presented in chapter 4 of this thesis have provided circumstantial evidence that during late neurogenesis (after E16) PDGF-αR might be restricted to cells of the oligodendrocyte lineage (with the exception of choroid plexus and the meningeal membranes). My conclusions were based on the following points. Firstly I showed that PDGF-αR$^+$ cells did not appear in the forebrain in significant numbers until around E16, by which time a large proportion of neurons have already formed (Jacobson, 1970), and PDGF-αR$^+$ cells continued to increase in number up to and after birth, coinciding with the period of maximum gliogenesis (eg. Jacobson, 1970). Secondly the distribution of PDGF-αR$^+$ cells in the postnatal brain did not correlate in any obvious way with the spatial organization of neurons; on the contrary they were most numerous in developing white matter tracts, which are generally devoid of neuronal cell bodies. Thirdly, the PDGF-αR hybridization signal was associated only with cells possessing small, densely-staining nuclei that are typical of glial cells (Smart and Leblond, 1961; Bunge, 1968). Fourth, there were many PDGF-αR$^+$ cells

in the postnatal optic nerve, which contains glial cells and axons but no neuronal cell bodies. These PDGF-αR$^+$ cells were initially more numerous near the optic chiasm but later become evenly distributed throughout the optic nerve, mirroring in time and space the manner in which O-2A progenitor cells accumulate in the nerve during development (Small *et al.* 1987). Furthermore, the number of PDGF-αR$^+$ cells (table 2) in the optic nerve is very similar to the number of O-2A progenitors estimated by other means (Miller *et al.*, 1985; Small *et al.,* 1987; Fulton *et al.* 1992; Barres *et al.*, 1992).

PDGF-αR, however, is not expressed exclusively by cells of the oligodendrocyte lineage during early neurogenesis. Prior to E16, transient PDGF-αR expression is seen in the dorsal ventricular zone of the spinal cord, a region that gives rise to sensory interneurons. A second dorsal region of PDGF-αR expression is seen in the brain which appears to define a region of the diencephalon. This PDGF-αR expression is also transient, lasting for approximately 4 days. PDGF-αR expression in these dorsal ventricular zones has disappeared by E16. Unlike the ventral ventricular zone PDGF-αR expression (see below) no individual PDGF-αR$^+$ cells can be seen disseminating from these zones, suggesting that any neurons (or glial cells) arising from these regions lose PDGF-αR expression as a consequence of their differentiation. The interesting aspects of these observations are that PDGF-αR expression defines discrete areas of the dorsal neural ventricular zone in both the brain and spinal cord, and begs the question of how PDGF might affect the development of the precursor cells in these areas?

The column of PDGF-αR expression in the basal (ventral) ventricular zone of the spinal cord and the ventral region of PDGF-αR expression in the ventricular zone of the diencephalon both appear to give rise to individual PDGF-αR$^+$ cells that disseminate from these zones and subsequently populate the rest of the CNS, beginning around E14. It is therefore the PDGF-αR$^+$ cells arising from these

ventrally located ventricular zones which I propose correspond to cells belonging to the oligodendrocyte lineage. Presumably these ventricular zone cells begin to express PDGF-αR as they commit to the oligodendrocyte lineage and that they continue to express PDGF-αR until they differentiate into oligodendrocytes as they do *in vitro* (Hart *et al.*, 1989a). These individual PDGF-αR$^+$ cells are spatially separated from the dorsal PDGF-αR expression and this latter expression has disappeared prior to the individual PDGF-αR$^+$ cells reaching these regions.

In order to determine the true identity of cells that express PDGF-αR, more antigenic or molecular markers need to be developed which unambiguously recognise these cells. Many of the markers used to recognise cells of the oligodendrocyte lineage *in vivo*, also recognise other cell types *in vivo*, making it difficult to interpret the observed staining. Transgenic animals may help to elucidate this problem. The promoter region of the PDGF-αR could be cloned and a construct made with the *E.Coli* ß-galactosidase (*Lac-Z*) gene under its control. Transgenic mice generated with this construct might express ß-galactosidase in every cell expressing PDGF-αR. The expression of the *E.coli* ß-galactosidase (*Lac-Z*) gene is readily detected histochemically or immunohistochemically. Cells within the CNS expressing PDGF-αR could then be readily detected both in sections and in dissociated cell cultures. In combination with present antigenic markers (such as A2B5, GC, and GFAP for example) the phenotype of cells expressing PDGF-αR could be determined *in vitro*.

It might be possible to use antibodies directed against the extracellular domain of the PDGF-αR to facilitate "panning" of cells expressing PDGF-αR from dissociated brains, thus enabling purification of PDGF-αR expressing cells. By culturing "panned" PDGF-αR cells, isolated from dorsal and ventral halves of rat brains at E14 or E15, it should be possible to determine whether the ventrally derived PDGF-αR$^+$ cells differentiate into oligodendrocyte. If antibodies directed against the PDGF-αR do not facilitate direct "panning" of PDGF-αR$^+$ cells, it might

be possible to use the PDGF-αR promoter to drive expression of a novel surface antigen in PDGF-αR^+ cells (in transgenic mice) which might facilitate "panning" of these cells.

As the CNS develops the ventrally derived PDGF-αR^+ cells appear to disseminate from these regions and eventually populate the entire CNS. While it is not possible to conclude from my data that these cells are migratory there is, however, a certain amount of evidence that O-2A progenitor cells are migratory (Small *et al.*, 1987; Noble *et al.*, 1989; LeVine and Goldman, 1988a.b). Small *et al.* (1987) found that by cutting P0 optic nerves into thirds and counting the dissociated O-2A progenitor cells present in each portion, that the cells were present in a gradient increasing towards the chiasmal end. By P5 this gradient of O-2A progenitor cells had largely disappeared, and the total number of cells had increased. These results have been taken to imply that O-2A progenitor cells migrate into the optic nerve via the optic chiasm, from germinal zones in the brain. Noble *et al.* (1989) has demonstrated, using time-lapse photography, that O-2A progenitor cells are highly motile *in vitro*. LeVine and Goldman (1988a,b) using antibodies which recognise different stages of the oligodendrocyte lineage, have suggested that O-2A progenitor cells, appearing in both the rat cerebrum and cerebellum are migrating into these regions. Thus the available evidence, albeit circumstantial, suggests that O-2A progenitor cells are migratory. My data is compatible with these cells being migratory, however, I cannot eliminate the possibility that a wave of morphogenic differentiation is moving across the CNS in a ventral to dorsal direction causing isolated cells to express PDGF-αR. Thus, definitive evidence of the migratory nature of O-2A progenitor cells *in vivo* has still to be demonstrated.

How does my hypothesis about the origin of cells belonging to the oligodendrocyte lineage agree with previously described hypotheses on the origin of oligodendrocytes and glial cells? Morphological and immunocytochemical analyses

of the developing CNS have resulted in two distinct hypotheses to explain the origin of astrocytes and oligodendrocytes. It has been proposed that immature glial cells develop in the ventricular zones of the developing CNS and subsequently migrate to their final positions within the CNS (Smart, 1961; Privat and Leblond, 1972; LeVine and Goldman 1988a,b). Morphological studies have suggested that immature glial cells leave the ventricular zones and enter both white and grey matter of the CNS before differentiation (Smart, 1961; Privat and Leblond, 1972). Antigenic studies, using antibodies which recognise different stages of the oligodendrocyte lineage, have suggested that oligodendrocytes populating the cerebrum arise from the lateral aspects of the ventricular zone of the lateral ventricle (LeVine and Goldman, 1988a,b). Alternatively, it has been proposed that both astrocytes and oligodendrocytes differentiate from the embryonic radial glial cells of the developing CNS (Choi *et al.*, 1983; Choi and Kim, 1985; Hirano and Goldman, 1988). Radially orientated glial cells in the presumptive white matter of the postnatal rat spinal chords have been demonstrated to express antigens characteristic of oligodendrocytes as well as radial glial cells. Radial glial cells begin to dissipate from the CNS at roughly the same time as glial cells appear, providing some support for a radial glial origin of oligodendrocytes (Choi *et al.*, 1983; Choi and Kim, 1985; Hirano and Goldman, 1988). While my findings do not support this latter theory of oligodendrocyte formation, they do provide support for the first. The major difference is that I propose that oligodendrocyte precursors arise from highly defined regions of the ventricular zone over a relatively short time period around E14. O-2A progenitor cells are capable of dividing within the CNS (Hardy and Reynolds, 1991; Reynolds and Wilkins, 1991). Therefore, it is not inconceivable that a short period of oligodendrocyte precursor cell production might enable sufficient oligodendrocytes to be generated to myelinate the entire CNS. If my theory eventually proves to be correct, then it suggests a modification of current ideas in this field.

Cell fate selection in the ventricular zone

There are at least two views of how the immature neuroepithelial cells in the ventricular zones might give rise to the diversity of differentiated cell types in the mature CNS. The extreme genetic viewpoint holds that each proliferating ventricular zone cell is dedicated to the production of a single cell type, or a predetermined sequence of cell types, regardless of environmental influences. The extreme epigenetic view holds that the ventricular cells and their progeny remain uncommitted until after their final division, their final cell phenotype being determined by environmental factors in the environment in which they find themselves. There is evidence for both genetic and epigenetic influences on the final differentiated phenotype of progenitor cells. Cell lineage analysis in the chick spinal cord has provided evidence that the progenitors of motor neurons are pluripotent, capable of giving rise to motor neurons, interneurons and glial cells (Leber *et al.*, 1990). Similarly progenitor cells in both the mouse and rat retina are capable of differentiating into any of several different types of neurons and Müller glial cells (Turner *et al.*, 1990; Turner and Sepko, 1987). In the rat cerebral cortex, however, the evidence suggests that from E14 there are separate progenitors at the ventricular surface that are dedicated to producing only neurons or glial cells (Luskin *et al.*, 1988; Price and Thurlow, 1988). However, due to the difficulty of distinguishing different neuronal types by morphology at the light microscope level, it is still unclear as to whether the neuronal precursors are pluripotent or only give rise to one type of neuron. Electron microscopic studies suggest that separate progenitor cells give rise to pyramidal and nonpyramidal neurons in the rat telencephalon (Parnavelas *et al.*, (1991).

Experiments where parts of the spinal cord are removed and the subsequent development of the remaining cord followed, have shown that the spinal cord

develops normally, except that the cell types which would have developed in the dissected part are missing (Wenger, 1950). This suggest that cells at any dorsoventral level of the cord are generated from progenitor cells in the ventricular zone at the same level. This led Wenger (1950) to propose that the ventricular zone of the spinal cord is a mosaic of specialized units each comprised of progenitor cells dedicated to the production of specific types of neurons or glial cells. The data presented in this thesis (chapter 5) indicates that a subset of progenitor cells in the ventricular zone of the rat spinal cord is already committed to the expression of PDGF-αR, and presumably to their choice of cell lineage before they start their migration away from the ventricular surface. However, I cannot make inferences about the mechanism (genetic or epigenetic) by which the decision to express PDGF-αR is made. My data does, however, provide a clear and striking example of regional specialization of the ventricular zone in the dorsoventral axis; whether this represents an exception or the rule remains to be determined.

What defines the singularity of PDGF-αR expression in the basal ventricular zone of the spinal cord?

My results have shown that a discrete region of PDGF-αR expression occurs in the dorsal ventral axis of the rat spinal cord. Whilst many homeotic genes have been shown to have restricted dorsal/ventral expression in the spinal cord ventricular zones, none have been shown to have the exquisite expression displayed by PDGF-αR. It is possible that the definition of this region may arise from cells reading information from a variety of overlapping regions of homeotic gene expression, resulting in PDGF-αR expression as a consequence.

The dorsoventral polarity of the spinal cord has been shown to be influenced by the floor plate and notochord. Grafting additional notochord or floor plate to

ectopic positions in developing chicken embryos results in changes in cell fate (Yamada *et al.*, 1991). For example, if an additional notochord or floor plate is placed dorsally to the spinal cord a second population of motor neurons arises in the alar plate. The notochord and floor plate appear to determine the polarity of the spinal cord, and presumably will affect the expression of other genes, such as homeotic genes, which are thought to control the differentiation of cells by regulating many downstream genes that collectively define cell phenotype. It will be of great interest to see if PDGF-αR expression in the chicken CNS exhibits a similar distribution to that observed in rat. If so, then it will be possible to determine what effect ectopic grafting of the notochord has on PDGF-αR expression in the chicken spinal cord and could yield important information regarding cell fate selection in the dorsoventral axis of the neural tube.

It will also be of interest to see if PDGF-αR expression should prove to have a similar pattern of expression within the CNS of zebrafish. This would allow us to study the effects of genetic mutants in zebrafish which may effect this patterning of PDGF-αR expression in the CNS dorsoventral axis. One such mutant, cyclops, blocks specification of the floor plate and appears to affect ventrally derived CNS structures (Hatta *et al.*, 1991). I am currently focusing my research on cloning both the chicken and zebrafish PDGF-αR genes, with these aims in mind.

CHAPTER 7

REFERENCES

Alosia, F., Giampaola, A., Giovanni, R., Peschle, C., Levi, G., 1992.
Developmental appearance, antigenic profile, and proliferation of glial cells of the human embryonic spinal cord: An immunocytochemical study using dissociated cultured cells.
Glia. **5**: 171-181.

Altman, J., Bayer, S.A., 1978a.
Development of the diencephalon in the rat. I. Autotradiographic study of the time of origin and settling patterns of neurons of the hypothalamus.
J. Comp. Neur. **182**: 945-972.

Altman, J., Bayer, S.A., 1978b.
Development of the diencephalon in the rat. II. Correlation of the embryonic development of the hypothalamus with the time of origin of its neurons.
J. Comp. Neur. **182**: 973-993.

Altman, J., Bayer, S.A., 1978c.
Development of the diencephalon in the rat. III. Ontogeny of the specialized ventricular linings of the hypothalmic third ventricle.
J. Comp. Neur. **182**: 995-1015.

Altman, J., Bayer, S.A. (1984).
The development of the rat spinal cord.
Adv. in Anat. Embry. and Cell Biol. **85**: 1-166.

Anderson, D.M., Lyman, S.D., Baird, A., Wignall, J.M., Eisenman, J., Rauch, C.,March, C.J., Boswell, S.H., Gimpel, S.D., Cosman, D., Williams, D.E., 1990.
Molecular cloning of mast cell growth factor, a haematopoietin that is activate in both membrane bound and soluble forms.
Cell. **63**: 235-243

Auffray, C., Rougeon, F., 1980.
Purification of mouse immunoglobulin heavy-chain messenger RNAs from total myeloma tumor.
Eur. J. Biochem. **107**: 303-314.

Bandtlow, C.E., Heumann, R., Schwab, M.E., Thoenen, H., 1987.
Cellular location of nerve growth factor by *in situ* hybridization,
EMBO J. **6**: 891-899.

Banerjee, U., Renfranz, P.J., Pollock, J.A., Benzer, S., 1987a.
Molecular characterization and expression of *sevenless*, a gene involved in neuronal pattern formation in the *Drosophila* eye.
Cell. **49**: 281-289.

Banerjee, U., Renfranz, P.J., Hinton, D.R., Rabin, B.A., Benzer, S., 1987b.
The *sevenless*$^+$ protein is expressed apically in cell membranes of the developing *Drosophila* retina; It is not restricted to cell R7.
Cell. **51**: 151-158.

Barres, B.A., Hart, I.K., Coles, H.C., Burne, J.F., Voyvodic, J.T., Richardson, W.D., Raff, M.C., 1992.
Cell death and control of cell survival in the oligodendrocyte lineage.
Cell. in press.

Bartlett, P.F., Noble, M.D., Pruss, R.M., Raff, M.C., Rattray, S., Williams, C.A., 1981.
Rat neural antigen (RAN-2): A cell surface antigen on astrocytes, ependymal cells, Muller cells and lepto-meninges defined by a monoclonal antibody.
Brain Res. **204**: 339-351.

Basler, K., Hafen, E., 1989.
Ubiquitous expression of *sevenless*: Position-dependend specification of cell fate.
Science. **243**: 931-934.

Bayer, S., Altman, J., 1987.
Development of the preoptic area: time and site of origin, migratory routes, and settling pattern of its neurons.
J. Comp. Neurol. **265**: 65-95.

Behar, T., McMorris, F.A., Novotný, E.A., Barker, J.L., Dubois-Dalcq, M., 1988.
Growth and differentiation properties of O-2A progenitors purified from rat cerebral hemispheres.
J. Neuroscience Res. **21**: 168-180.

Benda, P., Lightbody, J., Sato, G., Levine, L., Sweet, W., 1968.
Differentiated rat glial cell strain in tissue culture.
Science. **161**: 370-371.

Betsholtz, C., Johnsson, A., Heldin, C,H., Westermark, B., Lind, P.,Urdea, M,S., Eddy, R., Shows, T.B., Philpot, K., Mellor, A.L., Knott, T.J., Scott, J., 1986.
cDNA sequence and chromosomal localization of platelet-derived growth factor A-chain and its expression in tumour cell lines.
Nature. **320**: 695-699.

Bodner, M., Castrillo, J., Theill, L.E., Deerinck, T., Ellisman, M., Karin, M., 1988.
The pituitary-specific transcription favtor GHF-1 is a homeobox-containing protein.
Cell. **55**: 505-518.

Bögler, O., Wren, D., Barnett, S.C., Land, H., Noble, M., 1990.
Cooperation between two growth factors promotes extended self-renewal and inhibits differentiation of O-2A progenitor cells.
Proc. Natl. Acad. Sci. USA. **87**: 6368-6372.

Bondy, 1991. see page 209.

Boulder Committee, 1970.
Embryonic vertebrate central nervous system: revised terminology.
Anat. Rec. **166**: 257-262.

Bunge, R.P., 1968.
Glial cells and the central myelin sheath.
Physiol. Rev. **48**: 197-251.

Burgess, W.H., Maciag, T., 1989.
The heparin-binding (fibroblast) growth factor family of proteins.
Annu. Rev. Biochem. **58**: 575-606.

Cammer, W., 1984.
Carbonic anhydrase in oligodendrocytes and myelin in the central nervous system.
Annals N. Y. Acad. Sci. **429**: 494-497.

Cammer, W., Tansey, F.A., 1988.
Carbonic anhydrase immunostaining in astrocytes in the rat cerebral cortex.
J. Neurochem. **50**: 319-322.

Carpenter, M.B., 1976.
Human Neuroanatomy, 7th Ed.
Baltimore: Williams and Wilkin Company.

Chabot, B., Stephenson, D.A., Chapman, V.M., Besmer, P., Bernstein, A., 1988.
The proto-oncogene *c-kit* encoding a transmembrane tyrosine kinase receptor maps to the mouse *W* locus.
Nature. **335**: 88-89.

Chan, C.L., Wigley, C.B., Berry, M., 1990.
Oligodendrocyte-type 2 astrocyte (O-2A) progenitor cells from neonatal and adult rat optic nerve differ in their responsiveness to platelet-derived growth factor.
Dev. Brain Res. **55**: 275-282.

Choi and Kim, 1985. see page 209. | Choi *et al.*, 1983. see page 209.

Chugani, D.C., Kedersha, N.L., Rome, L.H., 1991.
Vault immunofluorescence in the brain: new insights regarding the origin of microglia.
J. Neurosci. **11**: 256-268.

Clegg *et al.*, 1987. see page 209.

Collarini, E.J., Richardson, W.D., 1992.
Neurotophic Factors; Academic Press Inc. pp-489-507.

Collarini, E.J., Kuhn, R., Marshall, C.J., Monuki, E.S., Lemke, G., Richardson, W.D., 1992.
Down-regulation of the POU transcription factor SCIP is an early event in oligodendrocyte differentiation *in vitro*.
Development. In press.

Copeland, N.G., Gilbert, D.J., Cho, B.C., Donovan, P.J., Jenkins, N.A., Cosman, D., Anderson, D., Lyman,S.D., Williams., 1990
Mast cell growth factor maps near the steel locus on mouse chromosone 10 and is deleted in a number of steel alleles.
Cell. **63**: 175-183

Cox, K.H., Deleon, D.V., Angerer, L.M., Angerer, L.M., 1986.
Detection of mRNAs in sea urchin embryos by *in situ* hybridization using asymmetric RNA probes.
Dev. Biol. **101**: 485-502.

Dale, L., Mathews, G., Tabe, L., Colman, A., 1989.
Developmental expression of the protein product *Vg*1, a localized maternal mRNA in the frog *Xenopus laevis*.
EMBO J. **8**: 1057-1065

Dalia Favera, R., Gallo, R.C., Gialionga, A., Croce, C., 1982.
Chromosonal localization of the human homologue (c-*sis*) of the simiam sarcoma virus *onc* gene.
Science. **218**: 686-688.

David, S., Miller, R.H., Patel, R., Raff, M. 1984.
Effects of neonatal transection on glial cell development in the rat optic nerve: evidence that the oligodendrocyte-type 2 astrocyte cell lineage depends on axons for its survival.
J. Neurocytol. **13**: 961-974.

Doolittle, R.F., Hunkappiller, M.W., Hood, L.E., Devare, S.G., Robbins, K.C., Aaronson, S.A., Antoniades, H.N., 1983.
Simian sarcoma virus onc gene, v-*sis*, is derived from the gene (or genes) encoding a platelet-derived growth factor.
Science. **221**: 275-277.

Dubois-Dalcq, M., 1987.
Characterization of a slowly proliferative cell along the oligodendrocyte pathway.
EMBO **6**: 2587-2595.

Dutly, F., Schwab, M.E., 1991.

Neurons and astrocytes influence the development of purified O-2A progenitor cells.

Glia. **4**: 559-571.

Eccleston, P.A., Silberberg, D.H., 1985.

Fibroblast growth factor is a mitogen for oligodendrocytes in vitro.

Dev. Brain Res. **21**: 315-318.

Eisenbarth, G.S., Walsh, F.S., Nirenburg, M., 1979.

Monoclonal antibody to a plasma membrane antigen of neurons.

Proc. Natl. Acad. Sci. USA. **76**: 4913-4917.

Eng, L.F., Vanderhaeghen, J.T., Bignami, A., Gerstl, B., 1971.

An acidic protein isolated from fibrous astrocytes.

Brain Res. **28**: 351-357

Eva, A., Robbins, K.C., Andersen, P.R., Srinivasan, A., Tronick, S.R., Reddy, E.P., Ellmore, N.W., Galen, A.T., Lautenberger, J.A., Papas, T.S., Westin, E.H., Wong-Staal, F., Gallo, R.C., Aaronson, S.A., 1982.

Cellular genes analogous to retroviral onc genes are transcribed in human tumour cells.

Nature. **295**: 116-119.

Feinberg, A.P., Vogelstein, B., 1984.

A technique for radiolabelling DNA restriction endonuclease fragments to high specific actvity.

Addendum. Anal. Biochem. **173**: 266-267.

Ferguson, I.A., Schweitzer, J.B., Johnson, E.M., 1990.

Basic fibroblast growth factor: Receptor-mediated internalization, metabolism, and anterograde axonal transport in retinal ganglion cells.

J. Neuroscience. **10**: 2176-2189.

ffrench-Constant, C., Miller, R.H., Burne, J.F., Raff, M.C., 1988.

Evidence that migratory oligodendrocyte-type-2 astrocyte (O-2A) progenitor cells are kept out of the rat retina by a barrier at the eye end of the optic nerve.

J. Neurocytol. **17**: 13-25.

ffrench-Constant, C., Raff, M.C., 1986.

Proliferating bipotential glial progenitor cells in the adult rat optic nerve.

Nature. **319**: 499-502.

Fontaine, B., Sassoon, D., Buckingham, M., Changeux, J.-P., 1988.

Detection of the nicotinic acetylcholine receptor α-subunit mRNA by *in situ* hybridization at the neuromuscular junctions of 15-day-old chick striated muscles.

EMBO J. **7**: 603-609.

Fulton, B.P., Burne, J.F., Raff, M.C., 1992.

Visualization of O-2A progenitor cells in developing and adult rat optic nerve by quisqualate-stimulated cobalt uptake.

J. Neurosci. in press.

Gehring, W.J., 1987.

Homeo boxes in the study of development.

Science. **236**: 1245-1252.

Geisser, E.N., Ryan, M.A., Housman, D.E., 1988.

The dominant-white spotting (*W*) locus of the mouse encodes the c-*kit* proto-oncogene.

Cell. **55**: 185-192

Gilmore, S.A., 1971.

Neuroglial population in the spinal white matter of neonatal and early postnatal rats: An autoradiographic study of numbers of neuroglia and changes in their proliferative activity.

Anat. Rec. **171**: 283-292.

Giulian, D., Baker, T.J., 1986.

Characterization of ameboid microglia isolated from developing mammalian brain.

J. Neurosci. **6**: 2163-2178.

Goldman, J.E., Hirano, M., Yu, R.K., Seyfried, T.N., 1984.

G_{D3} ganglioside is a glycolipid characteristic of immature neuroectodermal cells.

J. Neuroimmunol. **7**: 179-192.

Gospodarowicz, D., Ferrera, N., Schweigerer, L., Neufeld, G., 1987.

Structural characterization and biological functions of fibroblast growth factor.

Endocr. Rev. **8**: 95-113.

Gospodarowicz, D., Lepine, J., Massoglia, S., Wood, I., 1984.

Comparison of the ability of basement membranes produced by corneal endothelial and mouse-derived endodermal PF-HR-9 cells to support the proliferation and differentiation of bovine kidney tubule epithelial cells *in vitro*.

J. Cell Biol. **99**: 947-961.

Gospodarowicz, D., Vlodavsky, I., Savion, N., 1981.

The role of fibroblast growth factor and the extracellular matrix in the control of proliferation and differentiation of corneal endothelial cells.

Vision Res. **21**: 87-103.

Gospodarowicz, D., Weseman, J., Moran, J., Linstrom, J., 1976.

Effect of fibroblast growth factor on the division and fusion of myoblasts.

J. Cell. Biol. **70**: 395-399.

Goulding, M.D., Chalepakis, G., Deutsch, U., Erselius, J.R, Gruss,

P., 1991.

Pax-3, a novel murine DNA binding protein expressed during early neurogenesis.

EMBO J. **10**: 1135-1147.

Graham, A., Papalopulu, N., Krumlauf, R., 1989.

The murine and drosophila homeobox gene complexes have common features of organization and expression.

Cell. **57**: 367-378.

Graham, A., Maden, M., and Krumlauf, R., 1991.

The murine Hox-2 genes display dynamic dorsventral patterns of expression during central nervous system development.

Development. **112**: 255-264.

Greenwald, I., Seydoux, G., 1990.

Analysis of gain-of-function mutations of the *lin-12* gene of *Caenorhabditis elegans*.

Nature. **346**: 197-199.

Greenwald, I., 1985.

lin-12, A nematode homeotic gene, is homologous to a set of mammalian proteins that includes epidermal growth factor.

Cell. **43**: 583-590

Gronwald, R.G.K., Grant, F.J., Haldeman, B.A., Hart, C.E., OHara, P.J., Hagen, F.S., Ross, R., Bowen-Pope, D.F., Murray, M.J., 1988.

Cloning and expression of a cDNA coding for the human platelet-derived growth factor receptor: Evidence for more than one receptor class.

Proc. Natl. Acad. Sci. USA. **85**: 3435-3439.

Gruss, P., Walther, C., 1992.

Pax in development.

Cell. **69**: 719-722.

Guilian, D., Baker, T.J., 1986.

Characterization of amoeboid microglia isolated from developing mammalian brain.

J. Neurosci. **6**: 2163-2178.

Hafen, E., Basler, K., Edstroem, J., Rubin, G.M., 1987.

Sevenless, a cell-specific homeotic gene of *drosophila*, encodes a putative transmembrane receptor with a tyrosine kinase domain.

Science. **236**: 55-63.

Hammacher, A., Hellman, U., Johnsson, A., Ostman, A., Gunnarsson, K., Westermark, B., Wasteson, A., Heldin, C.-H., 1988.

A major part of platelet-derived growth factor purified from human platelets is a heterodimer of one A and one B chain.

J. Biol. Chem. **263**: 16493-16498.

Hanahan, D., 1983.

Studies on transformation of *Escherichia coli* with plasmids.

J. Mol. Biol. **166**: 557-580.

Hanahan, D., 1985.

DNA cloning: A practical approach.

IRL Press. Oxford and Washington. Vol 1: 109-136.

Hardie, R.C., 1984.

Progress in sensory physiology.

Springer-Verlag. Vol 5: 1-79.

Hardy, R., Reynolds, R., 1991.

Proliferation and differentiation potential of rat forebrain oligdendroglial progenitors both *in vitro* and *in vivo*

Development. **111**: 1061-1080.

Harris, W.A., Stark, W.S., Walker, J.A.,1976.

Genetic dissection of the photoreceptor system in the compound eye of *Drosophila melanogaster*.

J. Physiol. **256**: 415-439.

Hart, C.E., Forstrom, J.W., Kelly, J.D., Seifert, R.A., Smith, R.A., Ross, R., Murray, M.J., Bowen-Pope, D.F., 1988.

Two classes of PDGF receptor recognise different isoforms of PDGF.

Science. **240**: 1529-1531.

Hart, I.K., Richardson, W.D., Heldin, C-H., Westermark, B., Raff, M.C., 1989a.

PDGF receptors on the cells of the oligodendrocyte -type-2 astrocyte (O-2A) cell lineage.

Development. **105**: 595-603.

Hart, I.K., Richardson, W.D., Bolsover, R.S., Raff, M.C. 1989b.
PDGF and intracellular signaling in the timing of oligodendrocyte differentiation.
J. Cell Biol. **109**: 3411-3417.

Hatta, K., Kimmel, C.B., Ho, R.K., Walker, C., 1991.
The cylops mutation blocks specification of the floor plate of the zebrafish central nervous system.
Nature. **350**: 339-341.

Heath, J.K., Shi, W.K., 1986.
Developmentally regulated expression of insulin-like growth factors by differentiated murine teratocarcinomas and extra-embryonic mesoderm.
J. Embryol. Exp. Morphol. **95**: 193-212.

Heath, J.K., Isacke, C.M., 1984.
PC13 embryonal carcinoma-derived growth factor.
EMBO J. **3**: 1957-1962.

Heldin, C.-H., Bäckström, G., Östman, A., Hammacher, A., Rönnstrand, L., Rubin, K., Nistér, M., Westermark, B., 1988.
Binding of different dimeric forms of PDGF to human fibroblasts: evidence for two separate receptor types.
EMBO J. **7**: 1387-1393

Heldin, C.-H., Johnsson, A., Wennergren, S., Wernstedt, C., Betsholtz, C., Westermark, B., 1986.
A human osteosarcoma cell line secretes a growth factor structurally related to a homodimer of PDGF A-chains.
Nature. **319**: 511-514.

Heuer, J.G., von Bartheld, C.S., Kinoshita, Y., Evers, P.C., Bothwell, M., 1990.
Alternating phases of FGF receptor and NGF receptor expression in the developing chicken nervous system.
Neuron. **5**: 283-296.

Hirano, M., Goldman, J.E., 1988.
Gliogenesis in the rat spinal cord: Evidence for origin of astrocytes and oligodendrocytes from radial precursors.
J. Neursci. Res. **21**: 155-167.

Holt, C.E., Bertsch, T.H., Ellis, H.M., Harris, W.A., 1988.
Cellular determination in the **Xenopus** retina is independent of lineage and birth date.
Neuron. **1**: 15-26.

Heuer, F.G., Von Bartheld, C.S., Kinoshita, Y., Evers, P.C., Bothwell, M., 1990.
Alternating phases of FGF receptor and NGF receptor expression in the developing chicken nervous system.
Neuron. **5**: 283-296.

Huang, E., Nocka, K., Beier, D.R., Chu, T.Y., Buck, J., Lahm, H.W., Wellner, D., Leder, P., Besmer, P., 1990
The hematopoietic growth factor KL is encoded by the *Sl* locus and is the ligand of the c-*kit* receptor, the gene product of the *W* locus.
Cell. **63**: 225-233

Ignotz, R.A., Massagué, J., 1986.
Transforming growth factor-ß stimulates the expression of fibronectin and collagen and their incorporation into the extracellular matrix.
J. Biol. Chem. **261**: 4337-4345.

Ingraham, H.A., Chen, R., Mangalam, H.J., Elsholtz, H.P., Flynn, S.E., Lin, C.R., Simmonns, D.M., Swanson, L., Rosenfeld, M.G., 1988.
A tissue specific transcription factor containing a homeodomain specifies a pituitary phenotype.
Cell. **55**: 519-529.

Jacobson, M., 1978
Developmental Neurobiology (2nd edition).
Plenum press, New York and London.

Josephs, S.F., Ratner, L., Clarke, M.F., Westin, E.H., Reitz, M.S., Wong-Staal, F., 1984.
Transforming potential of human c-sis nucleotide sequences encoding platelet-derived growth factor.
Science. **225**: 636-639.

Jostes, B., Walther, C., Gruss, P., 1991.
The murine paired box gene, Pax7, is expressed specifically during the development of the nervous and muscular system.
Mech. Dev. **33**: 27-38.

Kimble, J., 1981
Alteration in cell lineage following laser ablation of cells in the somatic gonad of *Caenorhabditis elegans*
Dev. Biol. **87**: 286-300.

Kimble, J., Hirsh, D., 1979.
Postembryonic cell lineages of the hermaphrodite and male gonads in *Caenorhabditis elegans*
Dev. Biol. **70**: 396-417.

Kimelman, D., Kirschner, M., 1987.
Synergistic induction of mesoderm by FGF and TGF-ß and the identification of a mRNA coding for FGF in the early *Xenopus* embryo.
Cell. **51**: 869-877.

Kimelman, D., Abraham, J.A., Haaparanta, T., Palisi, T.M., Kirschner, M.W., 1988.
The presence of fibroblast growth factor in the frog egg: its role as a natural mesoderm inducer.
Science. **242**: 1053-1056.

Kingsbury, B.F., 1932.
The developmental significance of the floor-plate of the brain and spinal cord.
J. Comp. Neur. **50**: 177-201.

Klar, A., Baldassare, M., Jessel, T.M. (1992).
F-Spondin: A gene expressed at high levels in the floor plate encodes a secreted protein that promotes neural cell adhesion and neurite extension.
Cell. **69**: 95-110.

Kondaiah, P., Sands, M.J., Smith, J.M., Fields, A., Roberts, A.B., Sporn, M.B., Melton, D.A., 1990.
Identification of a novel transforming growth factor-beta (TGF-beta 5) mRNA in *Xenopus laevis*.
J. Biol. Chem. **265**: 1089-1093.

Laiho, M., Saksela, O., Andreasen, P.A., Keski-Oja, J., 1986.
Enhanced production and extracellular deposition of the endothelial-type plasminogen activator inhibitor in cultured lung fibroblasts by transforming growth factor beta.
J. Cell. Biol. **103**: 2403-2410.

Lawrence, J.B., Singer, R.H., 1985.

Quantitative analysis of *in situ* hybridization methods for the detection of actin gene expression.

Nucleic Acids Res. **13**: 1777-1799.

Lawrence, P.A., Green, S.M.,1979.

Cell lineage in the developing retina of *Drosophila.*

Dev. Biol. **71**: 142-152.

Leber, S.M., Breedlove, S.M., Sanes, J.R., 1990.

Lineage, arrangement, and death of clonally related motoneurons in chick spinal cord.

J. Neurosci. **10**: 2451-2462.

Lee, H.L., Bowen-Pope, D.F., Reed, R.R., 1990.

Isolation and characterization of the α platelet derived growth factor receptor from rat olfactory epithelium.

Mol. Cell Biol. **10**: 2237-2246.

Lemke, G. 1990.

Glial growth factors.

Semin. in Neurosci. **2**:437-443.

Levine, J.M., Card, J.P., 1987.

Light and electron microscopic localization of a cell surface antigen (NG2) in the rat cerebellum: association with smooth protoplasmic astrocytes.

J. Neurosci. **7**: 2711-2720.

Levine, J.M., Stallcup, W.B., 1987.

Plasticity of developing cerebellar cells *in vitro* studied with antibodies against the NG2 antigen.

J. Neurosci. **7**: 2721-2731.

Levine, J.M., 1989.

Neuronal influences on glial progenitor cell development.

Neuron. **3**: 103-113.

LeVine, S.M., Goldman, J.E., 1988a.

Spatial and temporal patterns of Oligodendrocyte differentiation in rat cerebrum and cerebellum.

J. Comp. Neurol. **277**: 441-455.

LeVine, S.M., Goldman, J.E., 1988b.

Embryonic divergence of oligodendrocyte and astrocyte lineages in developing rat cerebrum.

J. Neurosci. **8**: 3992-4006.

Lewis, S.A., Balcarek, J.M., Krek, V., Shelanski, M., Cowan, N.J., 1984.

Sequence of a cDNA clone encoding mouse glial fibrillary acidic protein: Structural conservation of intermediate filaments.

Proc. Natl. Acad. Sci. USA. **81**: 2743-2746.

Li, W., Schlessinger, J., 1991.

Platelet derived growth factor (PDGF)-induced disulphide-linked dimerization of PDGF receptor in living cells.

Mol. Cell Biol. **11**: 3756-3761.

Lonberg, N., Gilbert, W., 1983.

Primary structure of chicken muscle pyruvate kinase mRNA.

Proc. Natl. Acad. Sci. USA. **80**: 3661-3665.

Long, J.A., Burlingame, P.L., 1938.

The development of the external form of the rat with observations on the origin of the extraembryonic coelom and foetal membranes.

University of California Publications in Zoology. **43**: 143-184.

Lund, P.K., Moats-Staats, B.M., Hynes, M.A., Simmons, J.G., Jansen, M. D'Ercoles, J.D., Van Wyk, J.J., 1986.
Somatomedin-C/Insulin-like growth factor-I and insulin-like growth factor-II mRNAs in rat fetal and adult tissues.
J. Biol. Chem. **261**: 14539-14544.

Luskin, M.B., Pearlman, A.L., Sanes, J.R., 1988.
Cell lineage in the cerebral cortex of the mouse studied *in vivo* and *in vitro* with a recombinant retrovirus.
Neuron. **1**: 635-647.

Mandel, M., Higa, A., 1970.
Calcium dependant bacteriophage DNA infection.
J. Mol. Biol. **53**: 154-162

Matsui, T., Heidaran, M., Miki, T., Popescu, N., La Rochelle, W., Kraus, M., Pierce, J., Aaronson, S., 1989.
Isolation of a novel receptor cDNA establishes the existence of two PDGF receptor genes.
Science. **243**: 800-804.

McCulloch, E.A., Siminovitch, L., Till, J.E., 1964.
Spleen-colony formation in anemic mice of genotype W/W^{v}.
Science. **144**: 844-846.

McCarthy, K.D., De Vellis, J., 1980.
Preparation of separate astroglial and oligodendroglial cultures from rat cerebral tissue.
J. Cell Biol. **85**: 890-902.

McKinnon, R.D., Matsui, T., Dubois-Dalcq, M., Aaronson, S.A., 1990.
FGF modulates the PDGF-driven pathway of oligodendrocyte development.
Neuron. **5**: 603-614.

Mercola, M., Melton, D.A., Stiles, C.D., 1988.
Platelet-derived growth factor A-chain is maternally encoded in *Xenopus* embryos.
Science. **241**: 1223-1225.

Melamed, J., Trujillo-Cenoz, O., 1975.
The fine structure of the eye imaginal disks in muscoid flies.
J. Ultrastr. Res. **51**: 79-93.

Miller, R.H., David, S., Patel, R., Abney, E.R., Raff, M.C., 1985.
A quantitative immunohistochemical study of macroglial cell development in the rat optic nerve: *in vivo* evidence for two distinct astrocyte lineages.
Dev. Biol. **111**: 35-41.

Miller, R.H., Fulton, B.P., Raff, M.C., 1989a.
A novel type of glial cell associated with nodes of Ranvier in the rat optic nerve.
Eur. J. Neurosci. **1**: 172-180.

Miller, R.H., ffrench-Constant, C., Raff, M.C., 1989b.
The macroglial cells of the rat optic nerve.
Ann. Rev. Neurosci. **12**: 517-534.

Miller, R.H., Szigeti, V., 1991.
Clonal analysis of astrocyte diversity in neonatal rat spinal cord cultures.
Development. **113**: 353-362.

Miodzik, M., Hiromi, Y., Weber, U., Goodman, C.S., Rubin, G.M., 1990.
The *Drosophila seven-up* gene, a member of the steroid receptor gene superfamily controls photoreceptor cell fates.
Cell. **60**:211-224.

Morris, R.J, Beech, J.N., Heizmann, C.W. 1988.
Two distinc phases and mechanisms of axonal growth shown by primary vestibular fibres in the brain, demonstrated by parvalbumin immunocytochemistry.
Neurosci. **27**: 571-596.

Morrison-Graham, K., Schatteman, G.C., Bork, T., Bowen-Pope, D.F., Weston, J.A., 1992.
A PDGF receptor mutation in the mouse (*Patch*) perturbs the development of a non-neuronal subset of neural crest-derived cells.
Development. **115**: 133-142.

Murray, N.E., Brammer, W.J., Murray, K., 1977.
Lamboid phages that simplify the recovery of *in vitro* recombinants.
Molec. Genes and Genet. **150**: 53-59

Nister, M., Hammacher, A., Mellstrom, K., Siegbahn, A., Ronnstrand, L., Westermark, B., Heldin, C.H., 1988.
A glioma-derived PDGF A chain homodimer has different functional activities from a PDGF AB heterodimer purified from human platelets.
Cell. **52**: 791-799.

Noble, M., Murray, K., 1984.
Purified astrocytes promote the *in vitro* division of a bipotential cell.
EMBO **3**: 2243-2247.

Noble, M., Murray, K., Stroobant, P., Waterfield, M.D., Riddle, P., 1989.
Platelet-derived growth factor promotes division and motility and inhibits premature differentiation of the oligodendrocyte/type-2 astrocyte progenitor cell.
Nature. **333**: 560-562.

Nordlund, M., Hong, D., Fei, X., Ratner, N., 1992.
Schwann cells and cells in the oligodendrocyte lineage proliferate in response to a 50,000 dalton membrane-associated mitogen present in developing brain.
Glia. **5**: 182-192.

Nornes, H.O., Das, G.D., 1974.
Temporal pattern of neurogenesis in spinal cord of rat. I. An autoradiographic study:- Time and sites of origin and migration and settling patterns of neuroblasts.
Br. Res. **73**: 121-138.

Nornes, H.O., Hart, H., Carry, M., 1980.
Pattern of ascending and descending fibres in embryonic spinal cord of chick:I. Role of positional information.
J. Comp Neur. **192**: 119-132.

Nornes, H.O., Dressler, G.R., Knapik, E.W., Deutsch, U., Gruss, P., 1990.
Spatially and temporally restricted expression of Pax2 during murine neurogenesis.
Development. **109**: 797-809.

Orr-Urtreger, A., Bedford, M.T., Myoung-Sool, D., Eisenbach, L., Lonai, P., 1992.
Developmental expression of the α receptor for platelet-derived growth factor, which is deleted in the embryonic lethal *Patch* mutation.
Development. **115**: 289-303

Parnavelas, J.G., Barfield, J.A., Franke, E., Luskin, M.B., 1991.
Separate progenitor cells give rise to pyramidal and nonpyramidal neurons in the rat telencephalon.
Cerebral Cortex. **1**: 463-468.

Plachov, D., Chowdhury, K., Walther, C., Simon, D., Guenet, J.L, Gruss, P. 1990.
Pax8, a murine paired box gene expressed in the developing excretory system and thyroid gland.
Development. **110**: 643-651.

Price, J., Thurlow, L., 1988.
Cell lineage in the rat cerebral cortex: a study using retroviral-mediated gene transfer.
Development. **104**: 473-482.

Pringle, N., Collarini , E.J., Mosley, M.J., Heldin, C.-H., Westermark, B., Richardson, W.D., 1989.
PDGF A chain homodimers drive proliferation of bipotential (O-2A) glial progenitor cells in the developing rat optic nerve.
EMBO. **8**: 1049-1056.

Privat, A., Valat, J., Fulcrand, J. 1981.
Proliferation of neuroglial cell lines in the degenerating optic nerve of young rats.
J. Neuropathol. Exp. Neurol. **40**: 46-60.

Privat, A., Leblond, C.P., 1972
The subependymal layer and neighbouring region in the brain of the young rat.
J. Comp. Neurol. **146**: 277-302.

Qui, F., Ray, P., Brown, K., Barker, P.E., Jhanwar, S., Ruddle, F.H., Besner, P., 1988.
Primary structure of *c-kit*, relationship with the CSF-1/PDGF receptor kinase family-extracellular domain and c-terminus.
EMBO J. **7**:1003-1011.

Raff, M.C., 1989.
Glial cell diversification in the rat optic nerve.
Science. **243**: 1450-1455.

Raff, M.C., Lillien, L.E., Richardson, W.D., Burne, J.F., Noble, M.D., 1988.
Platelet-derived growth factor from astrocytes drives the clock that times the oligodendrocyte development in culture.
Nature. **333**: 562-565.

Raff, M.C., Abney, E.R., Fok-Seang, J., 1985.
Reconstitution of a developmental clock *in vitro*: a critical role for astrocytes in the timing of oligodendrocyte differentiation.
Cell. **42**: 61-69.

Raff, M.C., Abney, E.r., Miller, R.H., 1984.
Two glial cell lineages diverge prenatally in rat optic nerve.
Dev. Biol. **106**: 53-60.

Raff, M.C., Miller, R.H., Noble, M., 1983.
A glial progenitor cell that develops *in vitro* into an astrocyte or an oligodendrocyte depending on the culture medium.
Nature. **303**: 390-396.

Raff, M.C., Mirsky, R., Fields, K.L., Lisak, R.P., Dorfman, S.H., Silberberg, D.H., Gregson, N.A., Liebowitz, S., Kennedy, M., 1978.
Galactocerebroside: a specific cell surface antigenic marker for oligodendrocytes in culture.
Nature. **274**: 813-816.

Rakic, P., 1972.
Mode of cell migration to the superficial layers of fetal monkey neocortex.
J. Comp. Neurol. **145** : 61-84.

Rangini, Z., Ben-Yehuda, A., Shapira, E., Gruenbaum, Y., Fainsod, A., 1991.
CHox E, a chicken homeogene of the H2.0 type exhibits dorso-ventral restriction in the proliferating region of the spinal cord.
Mech. Dev. **35**: 13-24.

Ranscht, B., Clapshaw, P.A., Price, J., Noble, M., Seifert, W., 1982.
Development of oligodendrocytes and Schwann cells studied with a monoclonal antibody against galactocerebroside.
Proc. Natl. Acad. Sci. USA. **79**: 2709-2713.

Rappolee, D.A., Brenner, C.A., Schultz, R., Mark, D., Werb, Z., 1988.
Developmental expression of PDGF, TGF-α, and TGF-ß genes in preimplantation mouse embryos.
Science. **241**: 1823-1825.

Reinke, R., Zipursky, S.L., 1988.
Cell-cell interaction in the *drosophila* retina: *The bride of sevenless* is required in photoreceptor cell R8 for R7 development.
Cell. **55**: 321-330

Rexed, B., 1952.

The cytoarchitectonic organization of the spinalcord in the cat.

J. Comp. Neur. **96**: 415-495.

Reverberi , G., Minganti, A., 1946

Fenomeni di evocazione nello sviluppo dell'uovo di Ascidie.

Publ. Staz. Zool. Napoli. **20**: 199-252.

Reynolds, R., Wilkin, G.P., 1988.

Development of macroglial cells in rat cerebellum. II. An *in situ* immunohistochemical study of oligodendroglial lineage from precursor to mature myelinating cell.

Development **102**: 1-16.

Reynolds, R., Wilkins, G.P., 1991.

Oligodendroglial progenitor cells but not oligodendroglia divide during normal development of the rat cerebellum.

J. Neurocytol. **20**: 216-224.

Richardson, W.D., Pringle, N., Mosley, M.J., Westermark, B., Dubois-Dalcq, M., 1988.

A role for platelet-derived growth factor in normal gliogenesis in the central nervous system.

Cell. **53**: 309-319.

Richardson, W.D., Raff, M., Noble, M., 1990.
The oligodendrocyte-type-2 astrocyte lineage.
Semin. Neurosci. **2**: 445-454.

Rifkin, D.B., Moscatelli, D., 1989.
Recent developments in the cell biology of basic fibroblast growth factor.
J. Cell Biol. **109**: 1-6.

Rizzino, A., Bowen-Pope, D.F., 1985.
Production of PDGF like factors by embryonal carcinoma cells and response to PDGF by endoderm-like cells.
Dev. Biol. **110**: 15-22.

Roberts, A.B., Anzano, M.A., Lamb, L.C., Smith, J.M., Sporn, M.B., 1981.
New class of transforming growth factors potentiated by epidermal growth factor: isolation from non-neoplastic tissues.
Proc. Natl. Acad. Sci. USA. **78**: 5339-5340.

Roelink, H., Nusse, R., 1991.
Expression of two members of the Wnt family during mouse development-restricted temporal and spatial patterns in the developing neural tube.
Genes and Dev. **5**: 381-388.

Rosa, F., Roberts, A.B., Danielpour, D., Dart, L.L., Sporn, M.B., Dawid, I.B., 1988.
Mesoderm induction in amphibians: The role of TGF-ß2-like factors.
Science. **239**: 783-785.

Ross, R., Raines, E.W., Bowen-Pope, D.F., 1986.
The biology of platelet-derived growth factor.
Cell. **46**: 155-169.

Rotwein, P., Burgess, S.K., Milbrandt, J.T., Krause, J.E., 1988.

Differential expression of insulin-like growth factor genes in rat central nervous system development.

Proc. Natl. Acad. Sci. USA. **85**: 265-269.

Russell, E.S., 1949.

Analysis of pleiotropism at the *W*-locus in the mouse: Relationship between the effects of *W* and W^{v} substitution on hair pigmentation and on erythrocytes.

Genetics. **34**: 708-728.

Saint, R., Kalionis, B., Lockett, T.J., Elizur, A., 1988.

Pattern formation in the developing eye of *Drosophila melanogaster* is regulated by the homoeo-box gene, *rough*.

Nature. **334**: 151-154.

Sambrook, J., Fritsch, E.F., Maniatis, T., 1989.

Molecular cloning, a laboratory manual.

Cold Spring Harbor, New York: CSH Laboratory Press. Ed. 2

Saneto, R.P., DeVellis, J., 1985.

Characterization of cultured rat oligodendrocytes proliferating in a serum-free, chemically defined medium.

Proc. Natl. Acad. Sci. USA. **82**: 3509-3513.

Sasahara, M., Fries, J.W.U., Raines, E.W., Gown, A.M., Westrum, L.E., Frosch, M.P., Bonthron, D.T., Ross, R. and Collins, T., 1991.

PDGF B-chain in neurons of the central nervous system, posterior pituitary, and in a transgenic model.

Cell **64**: 217-227.

Schatteman, G.C., Morrison-Graham, K., Koppen, A.V., Weston, J.A., Bowen-Pope, D.F., 1992.

Regulation and role of PDGF receptor α-subunit expression during embryogenesis.

Development. **115**: 123-131.

Schlessinger, J., 1988.

Signal transduction by allosteric receptor oligomerization.

Trends in Biochem. **13**: 443-447.

Scott, M.P., Carroll, S.B., 1987.

The segmentation and homeotic gene network in early *drosophila* development.

Cell. **51**: 689-698.

Seydoux, G., Greenwald, I., 1989.

Cell autonomy of *lin-12* function in a cell fate decision in *C.elegans*

Cell. **57**: 1237-1245.

Simon, M.A., Bowtell, D.D.L., Rubin, G.M., 1989.

Structure and activity of the *sevenless* protein: A protein tyrosine kinase receptor required for photoreceptor development in *Drosophila*.

Proc. Natl. Acad. Sci. USA. **86**: 8333-8337.

Skoff, R.P., Price, D.L., Stocks, A., 1976a.

Electron microscopic autoradiographic studies of gliogenesis in rat optic nerve.

I. Cell proliferation

J. Comp. Neurol. **169**: 291-312

Skoff, R.P., Price, D.L., Stocks, A., 1976b.
Electron microscopic autoradiographic studies of gliogenesis in rat optic nerve. II. Time of origin.
J. Comp. Neurol. **169**: 313-333.

Slack, J.M.W., 1983.
From egg to embryo.
Camb. Univ. Press.

Slack, J.M.W., Darlington, B.G., Heath, J.K., Godsave, S.F., 1987.
Mesoderm induction in the early *Xenopus* embryos by heparin-binding growth factors.
Nature. **326**: 197-200.

Slack, J.M.W., Isaacs, H.V., 1989.
Presence of fibroblast growth factor in the early *Xenopus* embryo.
Development. **105**: 147-154.

Small, R.K., Riddle, P., Noble, M., 1987.
Evidence for migration of oligodendrocyte-type-2 astrocyte progenitor cells into the developing rat optic nerve.
Nature. **328**: 155-157

Smart, I., 1961.
The subependymal layer of the mouse brain and its cell production as shown by autoradiography after thymidine-H^3 injection.
J. Comp. Neurol. **116**: 325-348.

Smart, I., Leblond, C.P., 1961.

Evidence for division and transformation of neuroglial cells in the mouse brain, as derived from radioautography after injection of of thymidine-H^3

J. Comp. Neurol. **116**: 349-366.

Smith, J.C., Price, B.M., van Nimmen, K., Huylebroeck, D., 1990.

Identification of a potential *Xenopus* mesoderm-inducing factor as a homologue of activin-A.

Nature. **345**: 729-731

Smith, J.C., Yaqoob, M., Symes, K.,1988.

Purification, partial characterization and biological effects of the XTC mesoderm-inducing factor.

Development. **103**: 591-600.

Smith, J.C. 1987

A mesoderm-inducing factor is produced by a *Xenopus* cell line.

Development. **99**: 3-14.

Smits, A., Hermansson, M., Nistér, M., Karnushina, I., Heldin, C.-H., Westermark, B., Funa, K., 1989.

Rat brain capillary endothelial cells express functional PDGF-ß type receptors.

Growth Factors. **2**: 1-8

Smits, A., Kato, M., Westermark, B., Nistér, M., Heldin, C.-H., Funa, K., 1991.

Neurotrophic activity of PDGF: rat neuronal cells possess functional PDGF β-receptors and respond to PDGF.

Proc. Natl. Acad. Sci. USA. **88**: 8159-8163.

Specht, L.A., Pickel, V.M. Joh, T.H., Reis, D.J., 1981.
Light-microscopic immunocytochemical localization of tyrosine hydroxylase in prenatal rat brain. I. Early ontogeny.
J. Comp. Neurol. **199**: 233-253.

Sporn, M.B., Roberts, A.B., Wakefield, L.M., Assoian, R.K., 1986.
Transforming growth factor-ß: biological function and chemical structure.
Science. **233**: 532-534.

Stephenson, D.A., Mercola, M., Anderson, E., Wang, C., Stiles, C.D., Bowen-Pope, D.F., Chapman, V.M., 1991.
Platelet derived growth factor receptor α-subunit gene (*Pdgfra*) is deleted in the mouse patch (*Ph*) mutation.
Proc. Natl. Acad. Sci. USA. **88**: 6-10.

Sternberg, P.W., Horvitz, H.R., 1986
Pattern formation during vulval development in C. elegans.
Cell. **44**: 761-772.

Stroobant, P., Waterfield, M.D., 1984.
Purification and properties of porcine platelet-derived growth factor.
EMBO J. **3**: 2963-2967.

Sturrock, R.R., 1982.
Gliogenesis in the prenatal rabbit spinal cord.
J. Anat. **134**: 771-793.

Suaraez, I., Raff, M.C., 1989.
Subpial and perivascular astrocytes associated with nodes of Ranvier in rat optic nerve.
Eur. J. Neurosci. **1**: 172-180

Sulston, J.E., Horvitz, H.R., 1977.

Post-embryonic cell lineages of the nematode, *Caenorhabditis elegans.*

Dev. Biol. **56**: 110-156.

Sulston, J.E., Schierenberg, E., White, J.G., Thomson, J.N., 1983.

The embryonic cell lineage of the nematode *Caenorhabditis elegans.*

Dev. Biol. **100**: 64-119.

Sulston, J.E., White, J.G., 1980.

Regulation and cell autonomy during postembryonic development of *Caenorhabditis elegans.*

Dev. Biol. **78**: 577-5971.

Swan, D.C., McBride, O.W., Robbins, K.C., Keithly, D.A., Reddy, E.P., Aaronson, S.A., 1982.

Chromosonal mapping of the simian sarcoma virus onc gene analogue in human cells.

Proc. Natl. Acad. Sci. USA. **79**: 4691-4695.

Temple, S., Raff, M.C., 1986

Clonal analysis of oligodendrocyte development in culture: evidence for a developmental clock that counts cell division.

Cell. **44**: 773-779

Tseng, S.C.G., Savion, N., Stern, R., Gospodarowicz, D., 1982.

Fibroblast growth factor modulates synthesis of collagen in cultured vascular endothelial cells.

Eur. J. Biochem. **122**: 355-360.

Tomlinson, A., Bowtell, D.D.L., Hafen, E., Rubin, G.M., 1987.
Localization of the *sevenless* protein, a putative receptor for positional information, in the eye imaginal disc of Drosophila.
Cell. **51**: 143-150.

Tomlinson, A., Kimmei, B.E., Rubin, G.M., 1988.
rough, a Drosophila homeobox gene required in photoreceptors R2 and R5 for inductive interactions in the developing eye.
Cell. **55**: 771-784.

Trapp, B.D., Moench, T., Pulley, M., Barbosa, E., Tennekoon, G., Griffin, J., 1987.
Spatial segregation of mRNA encoding myelin-specific proteins.
Proc. Natl. Acad. Sci. USA. **88**: 7773-7777.

Turner, D.L., Cepko, C.L., 1987.
A common progenitor for neurons and glia persists in rat retina late in development.
Nature. **328**: 131-136.

Ullrich, A., Schlessinger, J., 1990.
Signal transduction by receptors with tyrosine kinase activity.
Cell. **61**: 203-212.

van den Eijnden-Van Raaij, A.J., van Zoelent, E.J., van Nimmen, K., Koster, C.H., Snoek, G.T., 1990.
Activin-like factor from a *Xenopus laevis* cell line responsible for mesoderm induction.
Nature. **345**: 732-734.

Vaughn, J.E., 1969.
An electron microscopic analysis of gliogenesis in rat optic nerves.
Z. Zellforsch. **94**: 293-324.

Vogelstein, B., Gillespie, D., 1979.
Preparative and analytical purification of DNA from agarose.
Proc. Natl. Acad. Sci. USA. **76**: 615-619.

Walicke, P.A., 1989.
Novel neurotrophic factors, receptors and oncogenes.
Ann. Rev. Neurosci. **12**: 103-126.

Wanaka, A., Milbrandt, J., Johnson, E.M., 1991.
Expression of FGF receptor gene in rat development
Development. **111**: 455-468.

Warf, B.C., Fok-Seang, J., Miller, R.H., 1991.
Evidence for the ventral origin of oligodendrocyte precursors in the rat spinal cord.
J. Neurosci. **11**: 2477-2488.

Waterfield, .M.D., Scrace, G.T., Whittle, N., Stroobant, P., Johnsson, A., Wasteson, A., Westermark, B., Heldin, C.H., Huang, J.S., Deuel, T.F., 1983.
Platelet-derived growth factor is structurally related to the putative transforming protein p28*sis* of simiam sarcoma virus.
Nature. **304**: 35-39.

Wenger, E.L., 1950.
An experimental analysis of relations between parts of the brachial spinal cord of the embryonic chick.
J. Exp. Zool. **114**: 51-81.

Wentworth, L.E., 1984.

The development of the cervical spinal cord of the mouse embryo.II. A golgi analysis of the sensory, commissural, and associated cell differentiation.

J. Comp. Neur. **222**: 96-115.

Werner, H., Woloschak, M., Adamo, M., Shen-Orr, Z., Roberts, C.T., LeRoith, D., 1989.

Developmental regulation of the rat insulin-like growth factor I receptor gene.

Proc. Natl. Acad. Sci. USA. **86**: 7451-7455.

Westermark, B., Heldin, C-H., 1989.

Growth factors and their receptors.

Current opinion in cell biol. **1**: 279-285.

Williams, D.E., Eisenman, J., Baird, A., Rauch, C., Ness, K.V., March, C.J., Park, L.S., Martin, U., Mochizuki, D.Y., Boswell, H.S., Burgess, G.S., Cosman, D., Lyman, S.D., 1990.

Identification of a ligand for the c-*kit* proto-oncogene.

Cell. **63**: 167-174.

Wolswijk, G., Noble, M., 1989

Identification of an adult-specific glial progenitor cell.

Development. **105**: 387-400

Wolswijk, G., Riddle, P., Noble, M., 1990

Co-existence of perinatal and adult forms of a glial cell during development of the rat optic nerve.

Development. **109**: 691-698

Wolswijk, G., Riddle, P., Noble, M., 1991.

Platelet-derived growth factor is mitogenic for O-2A^{adult} progenitors.

Glia. **4**: 495-503.

Yamada, T., Placzek, M., Tanaka, T., Dodd, J., Jessel, T.M., 1991.
Control of cell pattern in the developing nervous system: Polarizing activity of the floor plate and notochord.
Cell. **64**: 635-647.

Yarden, Y., Kuang, D.E., Yang-Feng, T., Coussens, L., Munomitsi, S., Dull, T.J., Chen, E., Schlessinger, J., France, U., Ullrich, A., 1987.
Human proto-oncogene *c-kit*: a new cell surface receptor tyrosine kinase for an unidentified ligand.
EMBO J. **6**: 3341-3351.

Yeh, H.-J., Ruit, K.G., Wang, Y.-X., Parks, W.C., Snider, W.D., Deuel, T.F., 1991.
PDGF A-chain gene is expressed by mammalian neurons during development and in maturity.
Cell **64**: 209-216.

Zsebo, K.M., Wypych, J., McNiece, I.K., Lu, H.S., Smith, K.A., Karkare, S.B., Sachdev, R.K., Yuschenkoff, V.N., Birkett, N.C., Williams, L.R., Satyagal, V.N., Tung, W,., Bosselman, R.A., Mendiaz, E.A., Langley, K.E., 1990a.
Identification, purification, and biological characterization of haematopoietic stem cell factor from buffalo rat liver-conditioned medium.
Cell. **63**: 195-201.

Zsebo, K.M., Williams, D.A., Geissler, E.N., Broudy, V.C., Martin, F.H., Atkins, H.L., Hsu, R.Y., Birkett, N.C., Okino, K.H., Murdock, D.C., Jacobsen, F.W., Langley, K.E., Smith, K.A., Takeishi, T., Cattanach, B.M., Galli, S.J., Suggs, S.V., 1990b.
Stem cell factor is encoded at the *Sl* locus of the mouse and is the ligand for the c-*kit* tyrosine kinase receptor.
Cell. **63**: 213-224.

Bondy, C.A., 1991.

Transient IGF-I gene expression during the maturation of funcionally related central projection neurons.

J. Neurosci. **11**: 3442-3445.

Choi, B.H., Kim, R.C., Lapham, L., 1983.

Do radial glia give rise to both astroglia and oligodendrocyte cells?

Dev. Brain Res. **8**: 119-130.

Choi, B.H., Kim, R.C., 1985.

Expression of glial fibrillary acidic protein by immature oligodendroglia and its implications.

J. Neuroimmunol. **8**: 215-235.

Clegg, C.H., Linkhart, T.A., Olwin, R.B., Hauschka, S.D., 1987.

Growth factor control of skeletal muscle differentiation: Commitment to terminal differentiation occurs in G1 phases and is repressed by fibroblast growth factor.

J. Cell Biol. **105**: 949-956.